Optimization of Inflow Performance for Underground Gas Storage

Diploma Thesis

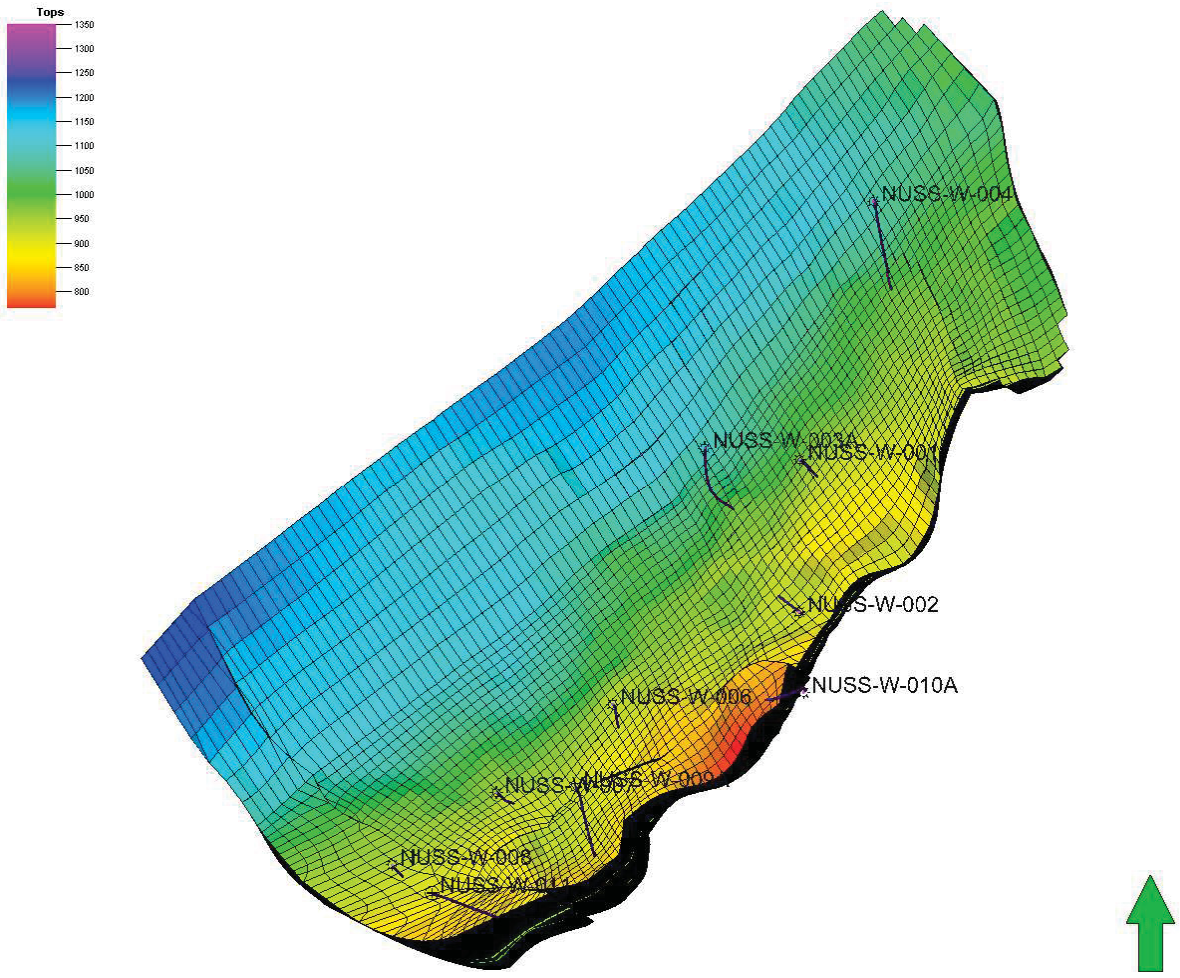

Alexander Gubik

Submitted to the

Department of Reservoir Engineering

University of Leoben, Austria

September 2009

I declare in the lieu of oath
that I did this thesis by myself
using only literature cited at
the end of this volume

_____

Alexander Gubik

Leoben, September 2009

Acknowledgement

I want to thank the employees of the Assets Gas, Oil and Midstream of Rohöl Aufsuchungs AG. With their open and helpful kind they contributed much to the success of this work.

Special thanks are entitled to my advisor Mr. Dipl. Ing. Bernhard Griess for his energizing ideas and his good support during the practical part of this thesis. Particularly I would like to thank Ao. Univ.-Prof. Mag. Dr. Clemens Brand for the support of programming.

I want to thank my advisor Univ.-Prof. Dipl. Geol. Ph. D. Stan Matthäi for taking over the support and revision of this work on part of university. He always supplied very prompt feedback to me.

Very special thanks go to my girlfriend Dipl. Ing. Eva Neumayer for supporting me very loyal, particularly in the final phase of this work.

Abstract

At present, Rohöl Aufsuchungs AG (RAG) is operating two underground gas storage facilities (UGS), in Upper Austria. Due to the high demand on these facilities RAG is planning to build additional UGS installations. Three potential sandstone reservoirs in the RAG concession area in the Molasse Basin are being investigated. The goal of this thesis is to calculate the working gas capacity for these three prospected UGS installations and to conduct sensitivity analysis on different well and reservoir parameters which have an impact on the underground gas storage performance. The results of this thesis research are compared with those of previous integrated reservoir and simulation studies. To achieve these objectives a method combining material balance with empirical deliverability equations and wellbore flow calculations is devised and used to calculate the working gas volume and the best-performing production profile for the three prospected gas storage installations, respectively. A newly implemented routine in Excel Visual Basic simplifies the input of different parameters, controlling the gas storage capacity. This program automates the calculation of well and reservoir capacity, facilitating a quick sensitivity analyses for any well and reservoir parameters. For material balance calculations the commercial material balance simulation program MBAL® and for well and inflow performance relationship calculations the commercial well modelling software PROSPER® are used.

The implemented method is applied to assess the turnover volume for each of the potential development scenarios preempting a full reservoir simulation study. As compared with the findings of a previous reservoir simulation study, my results do not deviate more than seven percent, but consistently indicate a reduced performance. To guarantee a minimum manifold pressure of 30 Bar during withdrawal, some cushion gas has to always remain within the reservoir. The amount needed depends on the number and performance of the underground gas storage wells. The parameter "skin" is used to quantify the predicted reservoir quality after drilling. A sensitivity analysis conducted with my model indicates a linear relationship between skin and the proportion of cushion gas present.

My recommendation for the development of the underground gas storage reservoir Zagling, is to use steeper well trajectories than those initially planned. Due to confidality reasons other findings of this work are restricted to the results chapter.

Kurzfassung

Derzeit betreibt die Rohöl Aufsuchungs AG (RAG) zwei unterirdische Gasspeicher in Oberösterreich. Aufgrund der hohen Nachfrage dieser Anlagen plant die RAG weitere Gasspeicheranlagen in diesem Gebiet. Drei potentielle Sandsteinlagerstätten der Molassezone innerhalb des RAG Konzessionsgebietes werden untersucht. Das Ziel dieser Arbeit ist es, das mögliche Arbeitsgasvolumen für diese drei geplanten Speicheranlagen zu berechnen und Sensitivitätsanalysen für verschiedene Sonden- und Lagerstättenparameter durchzuführen. Die Ergebnisse dieser Arbeit werden mit denen vorangegangener Lagerstättensimulationsstudien verglichen.

Um diese Ziele zu erreichen wurde eine Methode entworfen, welche den Ansatz der Materialbilanz mit empirischen Zuflussleistungsgleichungen und Sondenfließgleichungen kombiniert. Diese wurde anschließend dazu verwendet das Arbeitsgasvolumen der Lagerstätten zu errechnen und das beste Produktionsprofil zu ermitteln. Eine neue Prozedur in Excel Visual Basic vereinfacht die Eingabe von verschiedenen Parametern, welche die Größe der Speicherkapazität bestimmen. Dieses Programm automatisiert die Berechnung der Sonden- und Lagerstättenleistung und erleichtert somit Sensitivitätsanalysen für alle Einfluss nehmenden Parameter. Für Materialbilanzberechnungen wird das kommerzielle Materialbilanzsimulationspogramm MBAL® herangezogen und für die Berechnung des Sondenzuflusses wird die kommerzielle Sondenmodellierungssoftware PROSPER® verwendet.

Die implementierte Methode wird angewendet, um das Speichervolumen für jede der möglichen Entwicklungsszenarien abzuschätzen, ohne eine volle Lagerstättensimulationsstudie durchzuführen. Wie der Vergleich mit den Ergebnissen der vorangegangenen Studie zeigt, weichen meine Ergebnisse nicht mehr als sieben Prozent von dieser ab. Um einen minimalen Sondenkopfdruck von 30 bar während der Produktion zu gewährleisten, muss immer ein Gaspolster in der Lagerstätte verbleiben. Das benötigte Gasvolumen hängt von der Anzahl und der Zuflussleistung der Speicherbohrungen ab. Der Parameter "Skin" wird verwendet, um die vorhergesagte Qualität der Lagerstätte im Bereich der Bohrungen zu quantifizieren. Eine Sensitivitätsanalyse zeigt eine lineare Beziehung zwischen dem "Skin" und dem benötigten Gaspolster.

Meine Empfehlung für die Entwicklung der unterirdischen Speicherlagerstätte Zagling ist es, steiler zu bohren, als ursprünglich geplant. Aus Geheimhaltungsgründen sind alle weiteren Ergebnisse dieser Arbeit im Kapitel "Results" angeführt.

Contents

List of figures

List of tables

List of equations

Nomenclature

A	drainage area	[m²]
a	darcy Forchheimer coefficient	[-]
AOF	Absolute Open Flow potential ($P_{wf} \approx 0$)	[MSm³/d]
B	non-darcy Forchheimer coefficient	[-]
b	reservoir length in y- direction	[ft]
B_g	gas formation volume factor	[m³/Sm³]
B_{gi}	initial gas formation volume factor	[m³/Sm³]
B_w	Water formation volume factor	[m³/Sm³]
C	connectivity factor	[-]
c_f	rock compressibility	[Pa^{-1}], [Psi^{-1}]
c_g	isothermal gas compressibility	[Pa^{-1}], [Psi^{-1}]
C_H	Dietz shape factor	[-]
c_t	total system compressibility	[Pa^{-1}], [Psi^{-1}]
c_w	water compressibility (3.96 [Pa^{-1}])	[Pa^{-1}], [Psi^{-1}]
D	tubing diameter	[m], [in]
F	produced fluid volume	[MMSm³]
E_x	end point for the phase x	[fraction]
f	friction factor	[-]
F_r	total final field rate	[MSm³/d]
g	gravity constant	[m/s²]
g_c	gravity constant conversion factor	[-]
γ_g	Relative gas gravity (Air=1)	[-]
G	Initial gas in place	[MMSm³]
G_p	Gas produced	[MMSm³]
h	reservoir thickness	[m]
I_r	total initial field rate	[MSm³/d]
k	Permeability	[md];[m²]
k_r	relative permeability	[-]
k_{ri}; k_{rx}	phase relative permeability	[-]
k_x	horizontal permeability	[md];[m²]
k_z	vertical permeability	[md];[m²]
L	horizontal well length	[ft]
N_x	Corey exponent	[-]

n	Mole number	[-]
Φ	porosity	[fraction]
φ	inclination	[deg]
P	pressure	[Bara];[Pa]
$\overline{p}$	average reservoir pressure	[psia]
P_i	initial reservoir pressure	[Bara];[Pa]
P_{init}	Percent of the initial rate	[%]
P_{pc}	pseudo critical pressure	[Bara];[Pa]
P_{pr}	pseudo reduced pressure	[Bara];[Pa]
P_{wf}	well flowing pressure	[Bara];[Pa]
Q	production rate	[MSm³/day]
q_g	production rate	[sft³/d]
Q_{Field}	Production rate of the UGS field	[MSm³/day]
R	universal gas constant	[J/kg K], [psi ft³/lbm ℉R]
ρ	density	[kg/m³]
r_e	Radius of outer boundary	[ft]
r_w	well radius	[ft]
s	Skin factor	[-]
S_g	gas saturation	[fraction]
S_{mx}	phase maximum saturation	[fraction]
S_R	partial penetration skin	[fraction]
S_{rx}	phase residual saturation	[fraction]
S_{wc}	connate water saturation	[fraction]
S_w	water saturation	[fraction]
S_x	phase saturation	[fraction]
T	Temperature	[℃];[℉R];[K]
t_{DA}	Drainage shape factor	[-]
t	Production time of the field	[days]
t_{Ir}	Production time of initial field rate	[days]
t_{pss}	pseudo steady state time	[s]
TOV	turnover volume	[MMSm³]
v	velocity	[m/s]
V	volume	[Sm³];[Nm³]
V_a	Aquifer volume	[Sm³]
μ	viscosity	[cp];[Pa.s]
Z	Z-factor	[-]

1. Introduction

1.1. Historical Review

Long-term demand variations for natural gas caused by increased needs for space heating during cold weather, require large amounts of gas to be stored. These seasonal demand and supply variations can be satisfied effectively by underground natural gas storage (UGS), when such facilities exist close to the area where demand variations take place. In underground gas storage, the excess supply obtained during the summer season is injected into a depleted oil or gas field and it is produced again during peak load periods. Gas storage reservoirs became increasingly important in managing the gas supplies throughout central Europe. There is a big requirement of additional gas storage reservoirs managed in efficient ways. To convert producing fields into storage reservoirs or to upgrade existing storage fields in the most cost-effective way it is beneficial to determine the optimum combination of wells, cushion gas and compression facilities. Optimization of storage field design requires that many combinations of the afore mentioned flow system variables, together with their related costs, are studied and examined in a systematic fashion until the optimum development case is obtained. A survey of the petroleum literature found discussion of analytical and simulation-based methodologies for achieving these two desired outcomes.

Duane (1967) presented a graphical approach for optimizing gas storage field design. He developed this method to minimize the total field-development cost for a demanding peak-day rate and working gas capacity. To apply this method, a series of field-design optimization graphs for different compressor intake pressures has to be prepared. Each of the diagrams consists of a series of curves corresponding to different peak-day rates. Each curve shows the number of wells required to produce the given peak-day rate as a function of the gas inventory level. The trade-off between compression horsepower costs, cushion gas costs, and well can be investigated to determine the optimum design in terms of minimizing the field development cost. This method assumes that steady state flow will prevail throughout the reservoir.

Henderson et al. (1968) introduces a case study of storage-field design optimization with a single-phase, 2D numerical model of the reservoir. To reduce the number of wells necessary to meet the desired demand schedule they varied well schedules and well placement. For this, a trial-and-error method was used and it was stated that the results were preliminary. The outcome is the recommendation, that wells in the worst section of the field should be

used to meet the demand at the beginning of the production period. To meet the demand schedule additional wells should be added over time. Wells in the best part of the field should be held in reserve to meet the peak-day requirements. These producers should be connected at the end of the withdrawal period.

Van Horn et al. (1970) solved the gas-storage-design optimization problem with the help of a Fibonacci search algorithm. The investment requirements of a storage field are expressed in terms of cushion gas, number of wells, purification equipment, and compressor horsepower. The combination of these four variables that minimized investment costs were presented as the optimum design. A combination of an empirical backpressure equation with a simplified gas material-balance equation is used.

Tureyen et.al. (2000) introduces a field study of the Northern Marmara gas field located in the Thrace region of Turkey. The influences of well number, flowing wellhead pressures and skin factors on the working gas volume are studied. The approach is based on maximizing working gas volume for a particular configuration of reservoir, well and surface facilities. Reservoir performance is modelled by using material balance equations and the well inflow performances are predicted using a pseudo steady state gas deliverability equation. The findings are that the deliverability performance strongly affects the working gas volume and the number of wells operated. The results indicate the performance dependence on wellbore damage and hence the importance of well cleanup. This methodology is shown to be an effective way to forecast the production performance and to estimate the important design parameters of a prospected UGS facility.

Gouynes et al. (2000) presents a case study of an underground gas storage field design optimization with the help of a numerical model. Geologic modelling is integrated into a reservoir simulation package that incorporates modelling of subsurface, wellbore, and surface gathering system flows. The outcome is that the fully coupled reservoir characterization study is successful in improving overall field operation efficiencies.

McVay et al. (1994) prepared a systematic, simulation-based methodology to determine the maximum performance of a gas storage field with a minimum number of simulation runs. The procedure implies the solution of two major problems. Maximizing working gas volume and peak rates for a predefined configuration of reservoir, well and surface facilities, is the first problem. The second problem is to satisfy a specific production and injection schedule, which depends on peak rate requirements and working gas volume. This approach needs a preparation of a production and an injection performance curve. A specific number of

simulation runs is needed, to produce several graphs of average reservoir pressure plotted versus gas in place, production rate and injection rate. By combination of the different graphs the maximum working gas capacity and peak rates can be determined. By specifying the performance requirements first, this method can also be used to determine the optimum configuration of wells and surface facilities to satisfy a predefined working gas capacity. This technique assumes pseudo steady state conditions during the flow periods.

The historical review shows, that the problem of gas storage optimization exists since the 1960ies. In the early years the solution approaches were based on graphical or simple mathematical methodologies. After the implementation of personal computers, reservoir simulation studies were used to optimize the layout of gas storage facilities. For all these cases or methods mentioned above, the biggest issue during planning phase is the determination of the optimum number and position of the storage wells in relation with the desired working gas capacity.

Due to the depositional systems in the molasse basin, which are governed by small turbidity currents and axial deep marine channels, reservoir thickness and quality can be strongly fluctuating within short intervals. This may lead to a big uncertainty of different reservoir parameters, mainly, if there are just one or two existing production wells penetrating the main gas bearing layers. With little information about the prospected gas reservoirs, the issue of gas storage optimization becomes more and more challenging. To assess the range of probable development situations, some sensitivity analyses on major parameters should be done. The methodology of material balance simulation holds the advantage of few geological input factors and allows simple parameter change, which is beneficial for sensitivity analyses.

1.2. Claim of this thesis

The goal of this thesis is to calculate the working gas volume for three prospected UGS installations and to conduct sensitivity analyses on different well and reservoir parameters, which have an impact on the underground gas storage performance. To achieve these objectives a solution method, based on the combination of material balance simulation, analytical or empirical deliverability equations and wellbore flow calculations, is devised.

The prospected underground gas storage facilities should satisfy the following demands:

- The working gas capacity (turnover volume) should be maximized.
- The working gas volume has to be producible within 100 days.

- The initial field production rate has to be

$$I_r = \frac{TOV}{80} \quad (1)$$

- The initial rate has to be sustainable for 40 days. For the remaining 60 days the production profile of the field can be freely chosen.
- The manifold pressure of the field must not fall below 30 Bara, because of compressor limitations.

1. Claims for UGS Zagling:

- Determination of the turn over volume
- Determination of the best-performing production schedule
- Sensitivity analyses on the parameter “skin factor”
- Comparison of two development scenarios
    - Scenario 1: originally planned trajectories with more inclination and more reservoir contact
    - Scenario 2: alternatively planned trajectories with less inclination, less reservoir contact and shorter well path.
- Comparison with the results of a previous reservoir simulation study, using the commercial reservoir simulation software ECLIPSE 100®

2. Claims for UGS Berndorf

- Determination of the turn over volume
- Determination of the best-performing production schedule
- Sensitivity analyses on the parameter “skin factor”, assuming reduced reservoir contact of the UGS wells caused by minor and uncertain reservoir thickness and quality
- Comparison of two development scenarios
    - Scenario 1: originally planned completion size, 7 inch

- Scenario 2: alternatively planned completion size, 5.5 inch

- Comparison with the results of a previous reservoir simulation study, using the commercial reservoir simulation software ECLIPSE 100®

3. Claims for UGS Nußdorf

- Determination of the turn over volume
- Determination of the best-performing production schedule

The performance requirements for gas injection are not investigated and are not part of this study.

1.3. Agenda

The historical review shows, that the problem of gas storage optimization is well known since the 1960ies. Many different solution approaches were devised since the construction of the first underground gas storage facilities, but due to the general dissimilarity of gas reservoirs, every method has its own disadvantages when applied to miscellaneous gas fields.

The claim of this thesis is to calculate the turnover volume for three prospected UGS installations, to conduct sensitivity analyses on different well and reservoir parameters, which have an impact on the underground gas storage performance and to verify several development scenarios. The results of this thesis are compared with those of previous integrated reservoir simulation studies.

The historical background of the gas reservoirs Zagling, Berndorf and Nußdorf shows the reasons for strong heterogeneity and limited information within the fields. Previous integrated reservoir simulation studies were carried out on the commercial simulation software ECLIPSE100®.

In the methodology chapter all used models and calculation approaches are shown and declared, except the multi-lateral model used in the commercial well simulation software PROSPER®. This is an in house developed model of the company PETROLEUM EXPERTS®, which is not released for publication.

In the chapter UGS reservoir Zagling, the specific gas bearing layers are described and some basic field data is stated. PROSPER® models of the existing production well and of the prospected gas storage wells are described. An MBAL® prediction model is generated and linked with the result data of the PROSPER® well models. The influence of the parameter "skin" on the storage capacity is investigated and the effect of well trajectories with less inclination is examined.

The general situation of the field Berndorf is explained and some basic reservoir data is stated. Well models of the prospected gas storage wells are described. An MBAL® model is generated and linked with the calculated vertical lift performance and inflow performance data of the PROSPER® well models. The influence of the horizontal well length on the storage capacity is examined and the effect of a smaller completion size is investigated.

All results of the calculated scenarios are listed in the result section.

In the discussion section the results and the model performance are reviewed. The advantages, limitations and possible model-specific options are mentioned.

1.4. Background

In Upper Austria Rohöl Aufsuchungs AG (RAG) is already operating two underground gas storage facilities. Due to the high demand on these facilities RAG is planning to build additional UGS installations. Three potential UGS sandstone reservoirs, located in the molasse basin are investigated.

In many gas reservoirs in the molasse zone reservoir quality and thickness are strongly alterating within short intervals. This effect is caused by the dominating depositional systems, which are governed by small turbidity currents and axial deep marine channels. In the gas fields Zagling and Berndorf just one well is delivering log and core data for the porosity/permeability correlation. This leads to an additional uncertainty of many reservoir parameters.

In September 2005 a feasibility study was undertaken by Schlumberger Data and Consulting Services (DCS), to assess the gas storage potential of the gas fields Zagling, Berndorf and Nußdorf. In May 2007, another, more detailed study was performed by HOT Engineering, including a complete revision of the seismic interpretation and reservoir characterization. A static 3D model was created and a dynamic simulation in ECLIPSE100® was carried out.

The ECLIPSE100® simulation models are using 100m x 100m x 1m and 50m x 50m x 1m grid cells. The usage of such grid dimensions leads to very high grid aspect ratios (GAR). ECLIPSE100® uses the Peaceman formula for anisotropic reservoirs to predict well productivity (Schlumberger, 2004). However, since the early 1990ies it is known that this formula leads to a very strong over-prediction of the well performance for horizontal wells in coarse, non uniform grids, especially for GARs greater than 3 (D. K. Babu, 1991), (Jing Wan, 2000). In the projected gas storage reservoirs most of the prospected storage wells are highly deviated or horizontal.

2. Methodology

2.1. Governing equations

Material balance equation for gas reservoirs

The material balance is based on the principle of the conservation of mass.

$$G_p = G * \left[(B_g - B_{gi}) + \left(B_{gi} * \frac{S_w * c_w + c_f}{1 - S_{wc}}\right) * (P_i - P)\right] + B_w * \left(W_e - W_p\right) \quad (2)$$

The material balance simulator MBAL® uses a conceptual model of the reservoir to predict the reservoir behaviour based on the effects of reservoir fluids production and gas or water injection. The material balance equation is zero- dimensional, meaning, that it is based on a tank model and does not take into account the geometry of the reservoir, the drainage areas, the position and orientation of the wells (Petroleum Experts Ltd., 2005).

The material balance approach can be used to

- Quantify different parameters of a reservoir, such as hydrocarbons in place
- Determine the presence, the type and the size of an aquifer
- Estimate the gas/water contacts.
- Predict the reservoir pressure for a given production or injection schedule
- Predict the reservoir performance and manifold back pressures for a given production schedule.
- Predict the reservoir performance and well production for a given manifold pressure schedule.

Throughout the reservoir the following assumptions apply:

- Homogeneous pore volume
- Constant temperature
- Initial Uniform pressure distribution
- Uniform hydro carbon saturation distribution
- The black oil model (two phase flow) is used for fluid behaviour calculation

Inflow performance equations

The inflow performance relationships for the prospected gas storage wells and the production wells are calculated with the well modelling software PROSPER®. This software can compute a wide assortment of IPR models as well as vertical lift performance models.

Forchheimer inflow model

To conduct a simulation run and furthermore to predict the gas storage potential of a reservoir, the material balance model needs “gas producers” with defined IPR curves. The planned wells are allocated to the proper reservoir compartments and the related IPR is defined by the Forchheimer equation (Economides, et al., 1994; Petroleum Experts Ltd., 2005).

$$P_r^{\,2} - P_{wf}^{\,2} = a * Q + B * Q^2 \tag{3}$$

Multi-lateral inflow model

The multi-lateral IPR is a unique, in house developed model of PETROLEUM EXPERTS®, which allows simulating very complex completions, like in highly deviated wells. The model accounts for the pressure drop in the wellbore, the effect of the position of the perforated interval within the reservoir and the interference effect of one set of perforations on the other in the same reservoir. When using the multi-lateral model, the program calculates the potential of each layer based on the geometry of the well and includes the effect of pressure drop in the completion on the inflow. Basically the model calculates the skin due to the deviation and partial penetration, and with the skin it calculates the rate produced along the perforated completion using a point source solution technique. This is based on the work done by Heber Cinco-Ley (1975), modified for three dimensions. The calculated fluxes are used to get the first estimate of pressure profile along the completion. The completion pressure drop is converted into a skin value, then this skin is used to estimate fluxes along the completion. Once these fluxes are reworked, the process is carried out iteratively until the calculation converges. The end of iteration thus yields fluxes, pressure profile and the apparent skin of the completion. This means that the multi-lateral IPR model takes in consideration the well deviation and also the position of the perforations with respect to the formation and with respect to each other. The multi-lateral IPR model is a method based on the combination of several techniques and a lot of original work was done by PETROLEUM EXPERTS®. Therefore the model is not released for publication.

The references about the methodologies used in the multi-lateral IPR model are Gringarten (1973), Muskat (1973) and Cinco - Ley (1975).

In each point source the inflow is locally determined using the pseudo steady state solution for gas inflow determined by Russel and Goodrich, published in Fundamentals of Reservoir Engineering (Dake, 1978), Chapter 8, Gas well testing.

$$\overline{P}^2 - {P_{wf}}^2 = \frac{1422 * q_g * \mu * Z * T}{k * h} * \left(\ln \frac{r_e}{r_w} - \frac{3}{4} + s \right) \quad (4)$$

The multi-lateral model differs between individual layers and calculates an individual IPR for each horizon, which are added together to produce a cumulative IPR of the well. However, applying the model to horizontal wells leads to highly over predicted well inflow performances.

Babu – Odeh inflow model

For the Babu - Odeh (1989) horizontal well model, rearranged for gas by Kamkom (2006), PROSPER® offers the possibility to set blank and perforated interval zones within the completion. In perforated zones it is possible to set local permeability and skin factor, but the calculation result is an inflow performance for the whole well.

$$q_g = \frac{b * \sqrt{k_y * k_z} * \left(\overline{P}^2 - {P_{wf}}^2 \right)}{1424 * \overline{Z} * \overline{\mu}_g * T \left[\ln \left(\frac{A^{0.5}}{r_w} \right) + \ln C_H - 0.75 + s_R \right]} \quad (5)$$

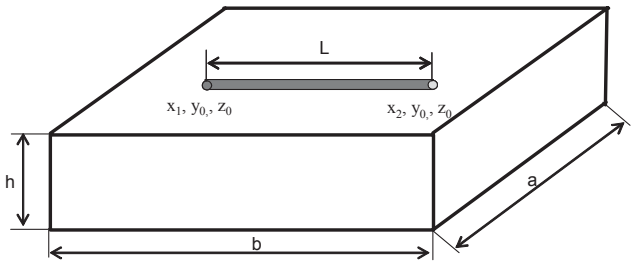

Figure 2.1: Drainage area and position of a horizontal well in a box shaped reservoir, defining the parameters of the Babu-Odeh model.

Tubing outflow equation

The mechanical energy balance equation for pipeline flow of a compressible single phase fluid in consideration of elevation, acceleration and friction, published in Petroleum Production Systems (Economides, et al., 1994) is used to calculate the pressure drop in the

well. Due to the fact that gas storage wells are assumed to be dry gas producers, which are designed to handle high gas rates, the friction term has the highest impact on pressure losses within the wells. The tubing roughness is supposed to be 0.015mm (stainless steel).

$$\frac{Z*R*T}{28.97*\gamma_g*P}dP + \left\{\frac{g*\sin\varphi}{g_c} + \frac{32*f}{\pi^2*g_c*D^5} * \left[\left(\frac{T}{T_{sc}}\right) * \left(\frac{P_{sc}}{P}\right) * q * Z\right]^2\right\} dL = 0 \quad (6)$$

The VLP curves are calculated by using the Petroleum Experts 2 model in PROSPER®. To solve Equation 6 this model uses the Gould et. al. (1974) flow map for dry gas and the Duns and Ros (1963) correlation for mist flow (Petroleum Experts Ltd., 2005). To calculate a VLP curve of the well, the model needs a description of deviation survey, the installed completion and the temperature profile. In all calculated wells the selected bottom node is located at reservoir top. The VLP curves were exported and loaded into the MBAL® models manually.

2.2. Specific equations

Tank connection in MBAL®

Normally a material balance is calculated from a single tank, but the material balance simulator MBAL® offers the option to construct multi-tank models. The different tanks are connected together, to form one communicating reservoir. This gives the opportunity to picture several reservoir compartments, which are showing restricted communication. The fluxes between individual tanks are calculated by a connectivity equation, where the empirical constant C describes the quality of the connection between two reservoir compartments (Petroleum Experts Ltd., 2005).

$$Q_{(t)} = C * \sum_{i=1}^{i} \frac{k_{r,i}}{\mu_i} * \Delta P \quad (7)$$

Relative Permeability

Each tank has its own relative permeability curves described by Corey functions. The functions are published by Li et. al. (2002) and are mentioned in the MBAL® technical description (Petroleum Experts Ltd., 2005). Corey exponents determine the curvature of relative permeability curves. An exponent of 1 would result in a straight line, higher numbers increase the curvature. The Corey exponents can be modified within the MBAL® models.

$$k_{rx(Sw)} = E_x * \left(\frac{S_x - S_{rx}}{S_{mx} - S_{rx}}\right)^{nx} \quad (8)$$

For flux calculation between the tanks, the relative permeability of the flux source tank is used.

Formation volume factor

The black oil model is based on two phase flow. The thermodynamic behaviour of the gas phase is expressed by the gas formation volume factor, which depends on pressure and temperature difference between reservoir and normal conditions published in Introduction to Petroleum Reservoir Engineering (Zolotukhin, et al., 2000).

$$B_g = \left(\frac{P}{Z*T}\right)_{normal} * \left(\frac{Z*T}{P}\right)_{reservoir} \quad (9)$$

Formation compressibility model

Additionally to the produced fluids, the rock extension is taken into consideration, which is calculated by the following correlation (Petroleum Experts Ltd., 2005).

$$C_f = 2.6 * 10^{-6} + (0.3 - \phi) * 2.415 * 7.8 * 10^{-5} \quad (10)$$

Fetkovich Aquifer model

The Fetkovich influx model for linear aquifers is used to simulate the water influx for the UGS reservoir Nußdorf. The model is described in the MBAL® user manual (Petroleum Experts Ltd., 2005).

$$\frac{dW_e}{dt} = J * (P_i - P) \quad (11)$$

$$J = \frac{0.00708 * k_a * h * w_r}{\mu_w * L_a} \quad (12)$$

Correction of the multi-lateral model

The multi-lateral model calculates separate IPRs of individual layers and a total IPR of the simulated UGS well. The IPR curve of every layer is described by 20 pairs of values (pressure and related inflow rate). One of these is the absolute open flow potential, where p_{wf} is equal to the atmospheric pressure. The IPR, calculated by the horizontal well model of Babu – Odeh consists of analogical values. Now the calculated AOF of the horizontal well model is used to correct all layer IPRs. Subscript number 1 stands for multi-lateral model and subscript number 2 identifies values of the Babu-Odeh model.

$$\text{corr. } \text{IPR}_{\text{layer}} = \frac{\text{AOF}_1}{\text{AOF}_2} * \text{ IPR}_{\text{layer}} \tag{13}$$

Numerical approximation

The IPR curves calculated by PROSPER®, applying the Babu - Odeh or the multi - lateral model are automatically recalculated into Forchheimer coefficients (Petroleum Experts Ltd., 2005) by numerical approximation. This is done by applying the least squares method (Bartsch, 1999). Twenty rate and pressure points of the IPR curves are taken to form an over determined equation system with two unknowns (Forchheimer coefficients a, B). The Visual Basic Excel routine creates normal equations, which are solved with the help of Cramer's rule.

2.3. Pseudo steady state conditions

Earlougher (1977) has shown, that the travel time of the pressure wave to the reservoir boundaries is given by

$$t_{p_{ss}} = \frac{\phi * \mu * c_t * A}{k} * t_{DA} \tag{14}$$

The total gas compressibility is given by

$$c_g = \frac{1}{P} - \frac{1}{Z * P_{pc}} * \left(\frac{\partial Z}{P_{pr}}\right)_T \tag{15}$$

$$c_t = S_g * c_g \tag{16}$$

The travel time of the wave is calculated with 5 different permeabilities and the following parameters.

parameter	value	unit
μ	1.50E-05	[Pa*s]
c_g	6.77701E-08	[1/Pa]
A	48000	[m²]
S_g	0.8	[fraction]
t_{DA}	0.8	
c_t	5.4216E-08	[1/Pa]
ϕ	0.15	[fraction]

Table 2.1: parameters for pseudo steady state time calculation

Due to the parallel well pattern of the storage wells, the drainage shape is assumed to be a 1x4 rectangle in all prospected UGS fields, which sets the value for t_{DA} to 0.8.

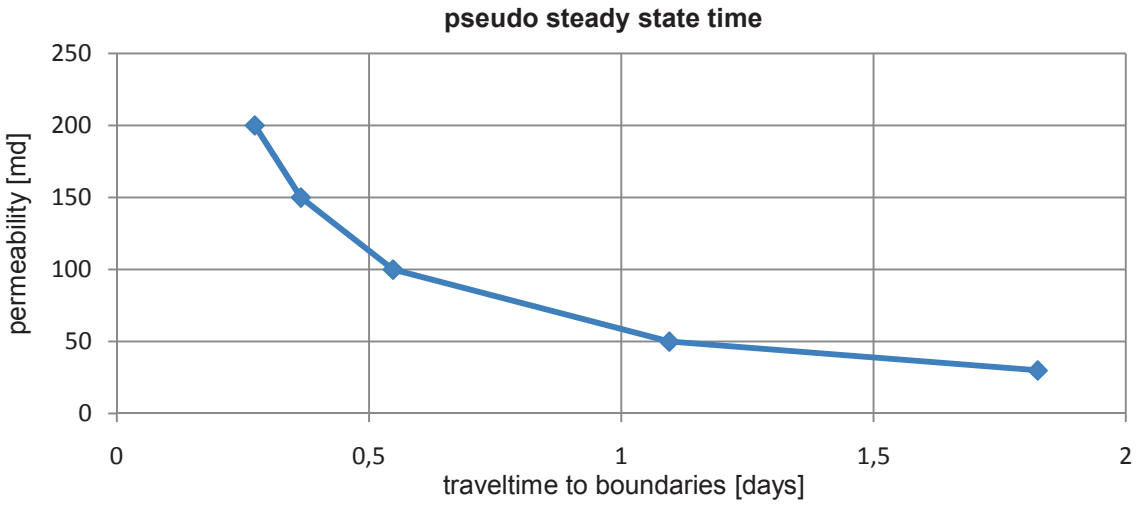

Figure 2.2: Dependence of the pressure wave travel time on reservoir quality. Several wave travel times are calculated related to different permeability values.

The permeability is strongly altering between the three reservoirs. However, even with a permeability of 30 md, the travel time to the reservoir boundaries is not higher than 1.83 days, which is 1.83 percent of the designed 100 days production schedule. Therefore the transient flow period is neglected and pseudo steady state conditions are assumed for all calculations.

2.4. Requirements for the UGS installations

Every gas storage facility has to achieve special performance requirements.

- The turnover volume has to be producible within 100 days.
- For the first 40 days a total field production rate of working gas volume divided by 80 must be achieved (Equation 1)
- To optimize the performance of the particular gas reservoir the profile can be selected individually during the remaining days of production.
- A manifold pressure of 30 Bar must be guaranteed during production
- The turnover volume should be maximized

The turn over volume is calculated by the following equation, which assumes a linear, daily reduction of the field rate after $t > t_{lr}$.

$$TOV = I_r * t_{Ir} + (100 - t_{Ir}) * \left(\frac{I_r - F_r}{2}\right) + F_r \quad (17)$$

The production rate for the last day of the production schedule is calculated as a per cent portion of the initial rate.

$$F_r = I_r * \frac{P_{init}}{100} \quad (18)$$

Production profiles

The production profiles are illustrated either rate versus time or rate versus cumulative production. For each reservoir three different production profiles are analyzed.

The rate profile of the field after passing the initial field rate production period (t_{Ir}) is defined as

$$Q_{Field(t)} = I_r - \frac{I_r - F_r}{100 - t_{Ir}} * (t - 100 + t_{Ir}) \quad (19)$$

The initial rate and the production profile are directly dependent on the reservoir turn over volume, which is being calculated during the prediction runs. On the other hand, the optimum production profile affects the amount of turn over volume available for production. To overcome this related argument problem, an iterative solution approach is selected.

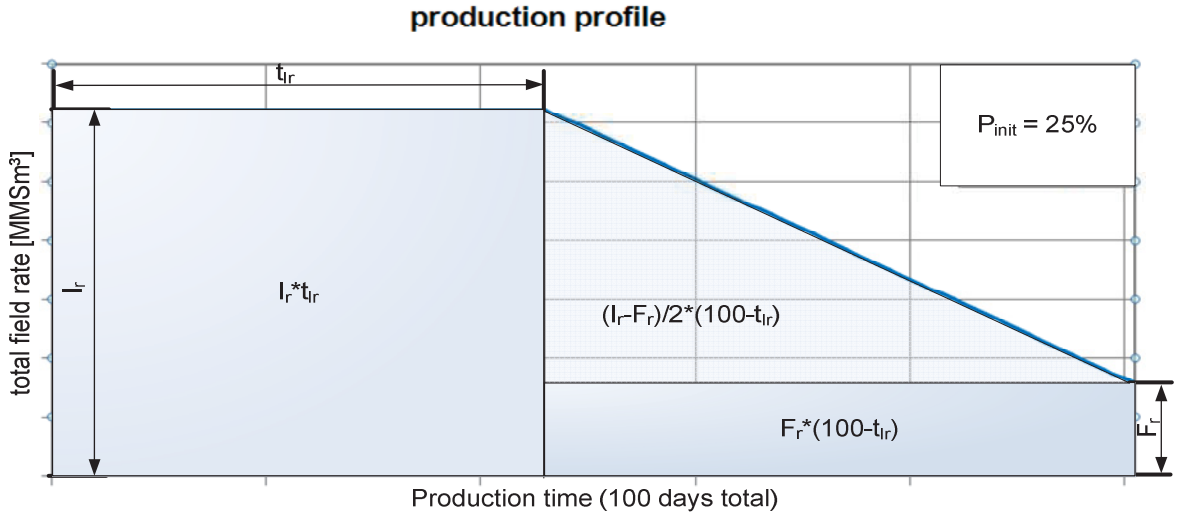

Figure 2.3: Turn over volume of a 100 days production profile of an UGS field. The surface area equals the prospected turn over volume. Specific terms of Fehler! Verweisquelle konnte nicht gefunden werden. **are allocated to their sphere of action. Total field rate plotted versus production time.**

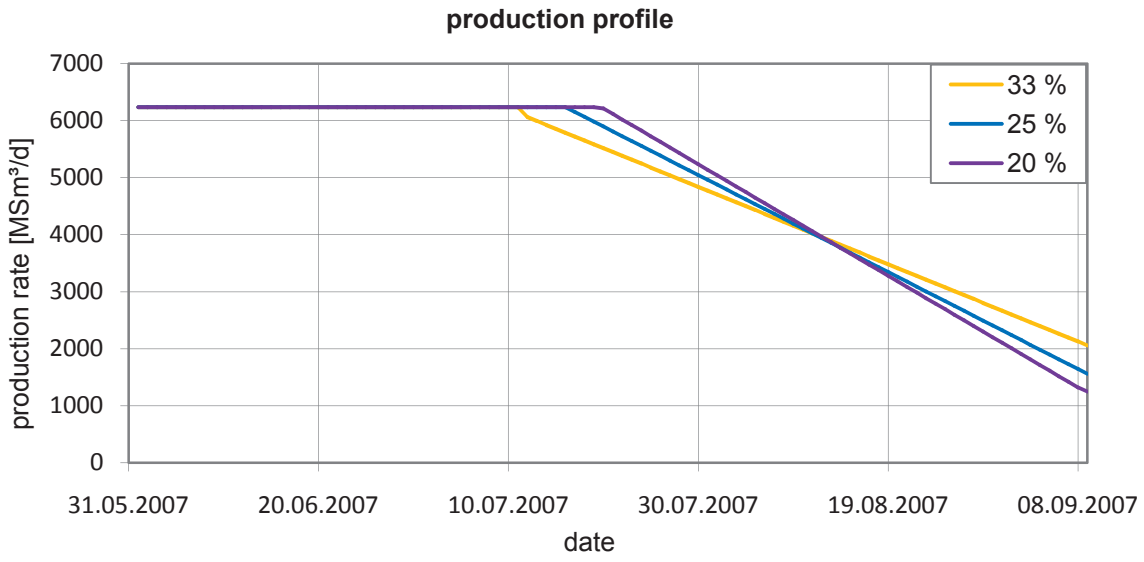

Figure 2.4: Example for three different production profiles during a 100 days production schedule of a UGS field. The total field production rate is plotted versus time. The production schedules are labeled with their desired value of P_{init}.

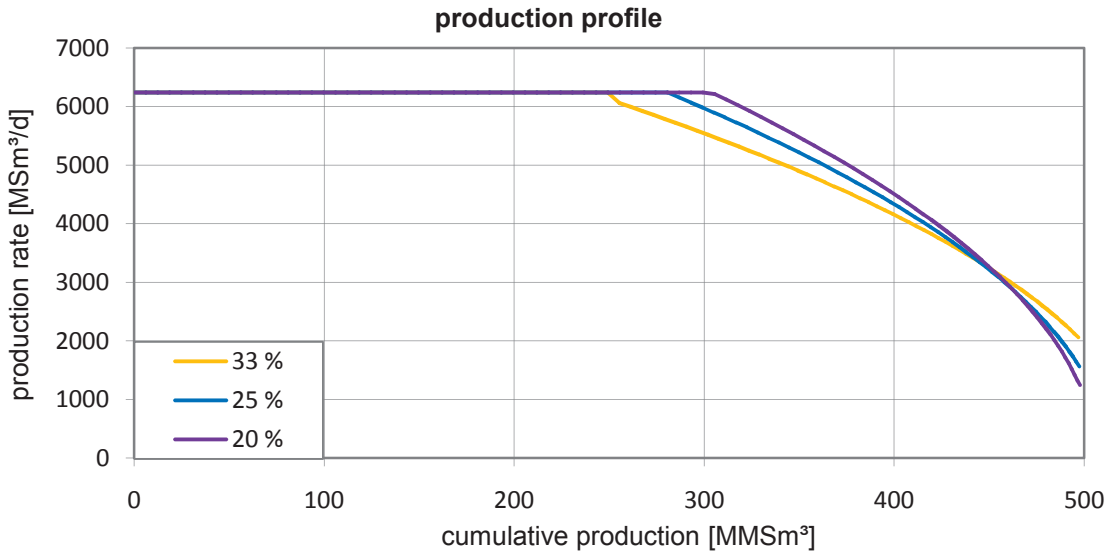

Figure 2.5: Example for three different production profiles during 100 days production of the entire working gas capacity of a UGS field. The total production rate is plotted versus the cumulative produced volume. The production schedules are labeled with their desired value of P_{init}.

The influences of production profiles with a final rate of 20, 25 and 33 percent are being investigated for all UGS reservoirs.

Beside the production rate, the manifold pressure is the other important performance parameter. Due to compressor and delivery requirements a wellhead pressure of at least 30 Bar must be guaranteed during production in all three gas reservoirs.

2.5. Reference Conditions

Gas volumes reported by RAG are based on Normal Cubic Meter (Nm3) with reference conditions of 0 degree Celsius and 1 atmosphere of absolute pressure. ECLIPSE100® simulator uses Standard Cubic meter (Sm^3) with a reference temperature of 60 degree Fahrenheit as standard condition, which cannot be changed. For better comparability all MBAL® and PROSPER® models were set up with Standard Cubic meters.
The universal gas law for ideal gases $P \cdot V = n \cdot R \cdot T$ can be re-arranged as

$$\frac{P}{n*R} = \left(\frac{T}{V}\right)_{normal} = \left(\frac{T}{V}\right)_{standard} \quad (20)$$

Inserting absolute Temperature is leading to

$$V[Sm^3] = 1.056949 * V[Nm^3] \quad (21)$$

2.6. Constructive situation

Preparing models of production wells and prospected UGS wells in PROSPER®

To calculate Inflow Performance Relationship (IPR) and Vertical Lift Performance (VLP) curves of the UGS and production wells, the commercial well simulation software PROSPER® is used.

First models of existing production wells are prepared with the help of geological information of resistivity and gamma ray logs, completion and production test data. The logging data was used to detect the thickness, porosity and saturation of the different gas bearing layers. With the completion and production test data the different perforated and productive zones are determined and allocated to the identified horizons. Afterwards the inflow performance relationship of every single layer is matched with the production test data. The production history and the IPRs of the productive layers are integrated manually into the material balance simulation models, to reproduce past production performance.

Secondly, models of the UGS wells are prepared. As mentioned in chapter 1.4, two detailed reservoir simulation studies, including a complete revision of the seismic interpretation and reservoir characterization, on the reservoirs have been performed. These existing reservoir models are now used for well planning purposes. To get appropriate permeability data for the

prospected UGS wells, artificial permeability well logs are created out of the existing static 3D reservoir models. In Excel the average permeability of the layers is calculated, open perforation intervals are assigned and the production intervals are allocated to the appropriate layers. In all three investigated reservoirs more than one gas bearing layer exists. Due to this fact it is necessary to build multi-lateral inflow performance models, where a separate IPR for each layer is calculated. The individual IPRs are assigned to the associated reservoir compartments in MBAL®. The configuration of the downhole equipment is specified by RAG and is listed for every UGS well in the appropriate appendices.

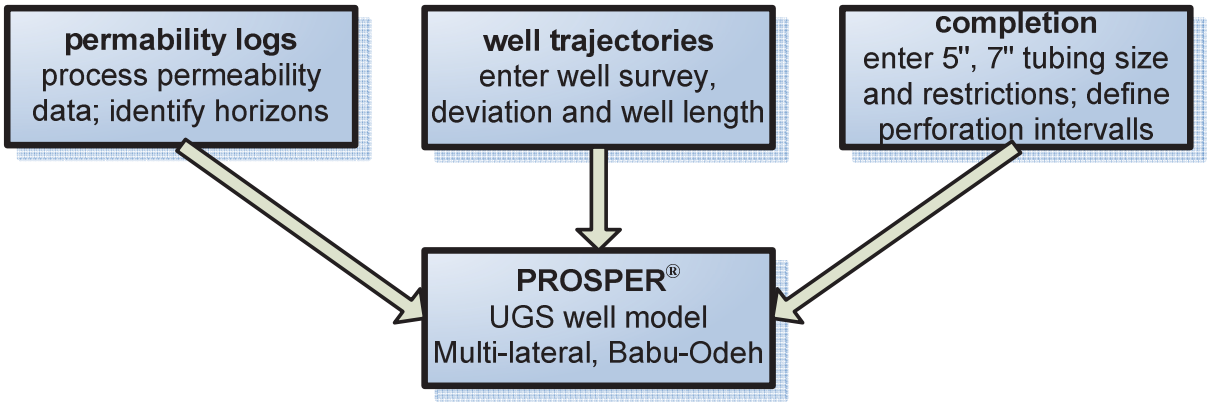

Figure 2.6 Flowchart explaining the construction of the PROSPER® UGS well models

Preparing the material balance models

The material balance simulation software MBAL® is used to create multi-tank models of the reservoirs. For construction of the multi-tank models it is essential to know how many different tanks are needed to get a realistic picture of the reservoir behaviour.

To construct the model, regarding amount of tanks and layer cross flow, the following criteria are decisive:

- As first criteria, the amount of different horizons is important. The individual layers are identified by log and pressure data of the production wells. A number of tanks, representing the amount of layers are generated. Information of the cross flow between these horizons is derived from geological findings or from production and pressure data observation.

- As second criteria it is important how many production wells are existing and how many UGS wells are planned. Every UGS well and every production well requires a

tank within every layer, which it is intersecting. The production history of a well is loaded in every tank, which is originated by the intersection of a production well with a reservoir layer. In case of several productive layers, the production history is split by assigned allocation factors, accounting for permeability data and perforation history. The gas volumes of the tanks are dependent on the geometry and porosity of the particular reservoir compartments.

- As third criteria it is necessary to get a history match for the constructed models. In some reservoirs in Upper Austria tight rocks are leading to a late production period, which cannot account much for the working gas capacity of the underground gas storage. However, these late pressure points have to be history matched and the small volumes should be taken into consideration. As a consequence additional tanks with a poor connection are added to simulate that kind of behaviour.

MBAL® needs information about the following reservoir parameters for every tank:

- fluid temperature
- original gas in place
- initial pressure
- porosity
- connate water saturation
- relative permeability
- viscosity function
- connectivity factor C (if connected to another tank)

The initial pressure for all connected tanks has to be equal. Therefore the measured pressure history of the different gas bearing horizons is recalculated to a reference depth.

To come up with any results for the prospected development scenarios, it is important to calibrate the material balance models with historical production and pressure data. All generated MBAL® models are able to reproduce past reservoir performance accurately, before they are used to predict future performance. The performed history matches are explained in the particular reservoir chapters. During history matching, monthly average historical gas production rates are entered into the model and static pressures are computed. They have to reproduce measured values in the past.

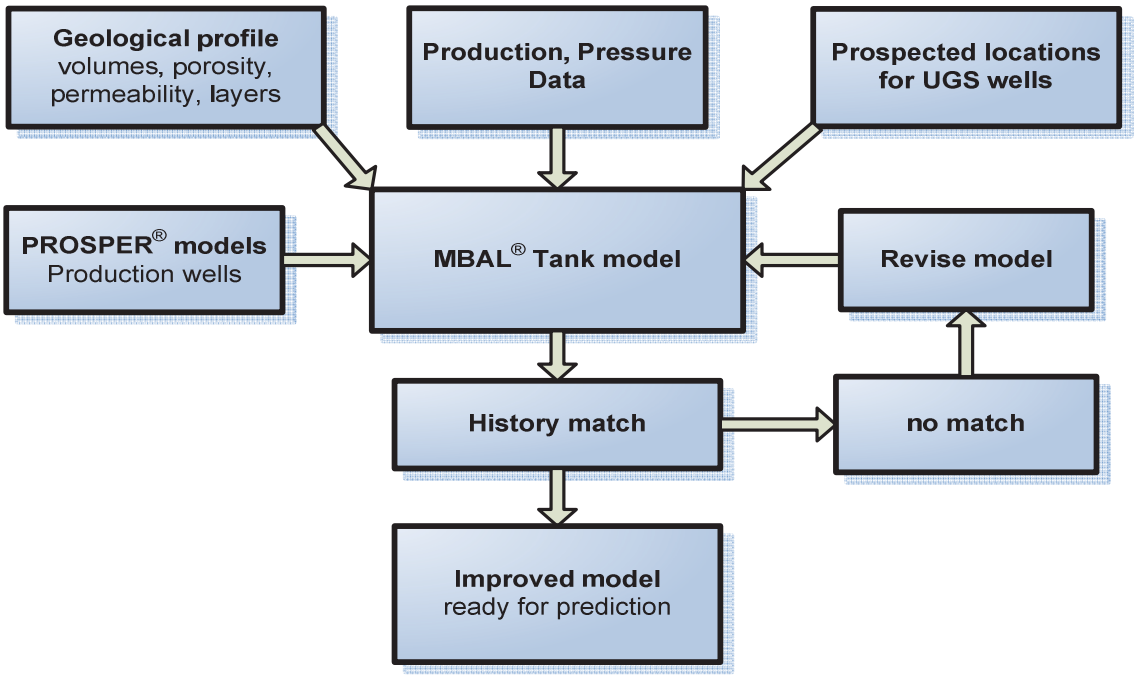

Figure 2.7 Flowchart explaining the workflow of the prepared MBAL prediction models

2.7. Conceptual model setup

Excel Visual Basic routine

The manual exchange of data between the well modelling software PROSPER® and the material balance simulator MBAL® is time consuming and not very practical. To predict the reservoir performance of several different production and development scenarios a big amount of time would be consumed by converting and exchanging data between PROSPER® and MBAL®. To accelerate the data exchange between the programs a Visual Basic routine is written, automating the data exchange.

After construction of the PROSPER® well models and preparation of the MBAL® prediction model, an Excel Visual Basic routine is implemented to automate the calculation processes for sensitivity evaluation. To connect the well modelling software PROSPER® with the material balance simulator MBAL® the routine uses the OPENSERVER® commands of MBAL® and PROSPER®. The OPENSERVER® feature is a built in open source command interface of both commercial simulation programs. It allows the software to be directly assessed and driven by external routines.

It is not possible to enter in MBAL® ending conditions like target pressure or target rate for a prediction run. To find the optimal production profile some iteration runs are necessary. The implemented Excel Visual Basic routine automates the data loading process of the

parameters. Just the production profile has to be chosen or changed by the user to meet the requirements of the underground gas storage facilities. The advantage of this approach is that the production profile can be handled like a sensitivity parameter. For better understanding of the reservoirs three profiles were simulated for every UGS field.

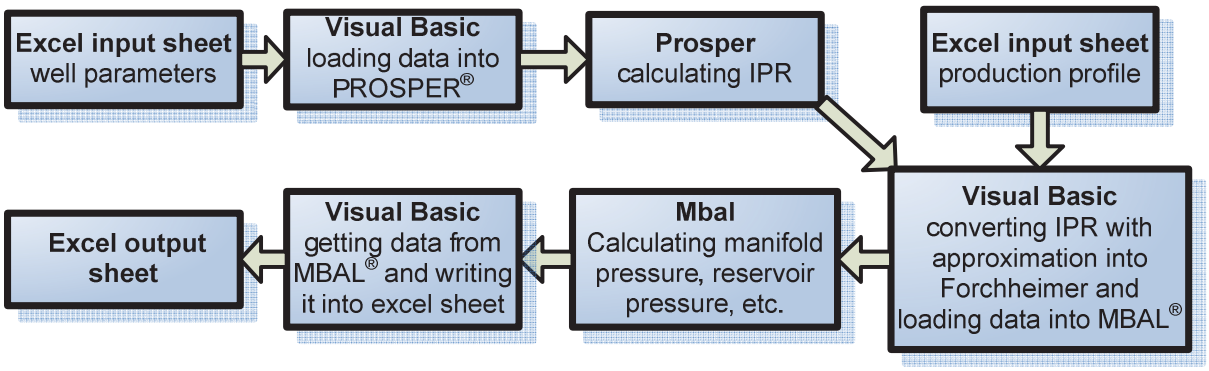

Figure 2.8: The labelled boxes show the workflow of the implemented Excel Visual Basic routine. The parameters are entered into an input sheet.

Excel input sheet

To facilitate the change of well and reservoir parameters an input template in Excel is created, including the following model parameters. The routine uses commands of the OPENSERVER® library to start calculation runs in PROSPER® and MBAL®.

Well parameters for PROSPER® IPR calculation:

- skin factor
- permeability
- layer height
- reservoir pressure
- effective well length

Reservoir parameters for MBAL® prediction model:

- production profile and TOV

Excel output sheet

The Visual Basic routine gets the calculated values of the 100 day prediction run and displays them in an Excel worksheet.

The following parameters are listed per day:

Field results:

- Average reservoir pressure [Bara]
- Total gas rate [MSm³/d]
- Manifold pressure [Bar]

Well results:

- Bottom hole flowing pressure [Bara]
- pressure drop tubing [Bar]
- well gas rate [MSm³/d]

Calculation of the UGS IPRs

Applying the multi-lateral well model to horizontal wells leads to highly over predicted well inflow performances. Thus in highly deviated wells the multi-lateral model is just used to get separate IPRs for the different gas bearing layers and then they are corrected by the absolute open flow potential (AOF) of the Babu - Odeh model. This means for every prospected horizontal UGS well both models are applied.

As mentioned before, the multi-lateral model calculates separate IPRs of the different layers and a total IPR of the simulated UGS well. The calculated AOF of the horizontal well model is used to correct all layer IPRs.

With the described approach it is possible to use the multi-lateral model for splitting the IPRs, to allocate them to different reservoir zones and to get appropriate inflow values by using the horizontal well model for correction.

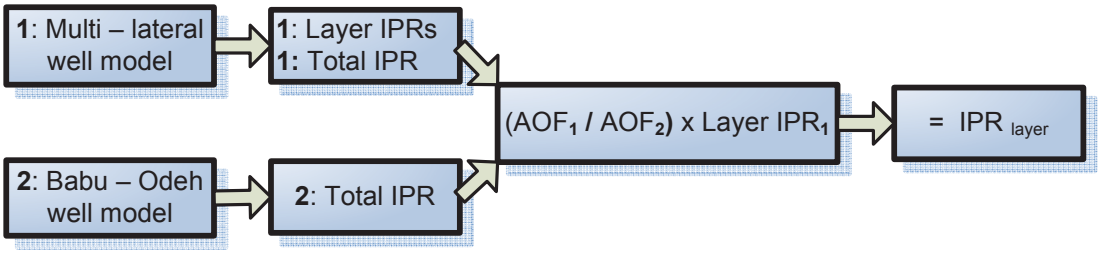

Figure 2.9: Explanation of the used method to correct the over-predicted layer IPRs of the multi - lateral model. The results of this model are labelled with subscript one and the results of the Babu – Odeh horizontal well model are labelled with the subscript two.

Prediction in MBAL®

After calibrating the models by history matching, prediction runs in MBAL® are carried out to assess the influence of reservoir parameters on storage capacity or to calculate the turnover volume. The PROSPER® IPR models are recalculated optionally if a well inflow parameter is changed. The workflow and the applied equations of the particular calculation steps is explained in Figure 2.10.

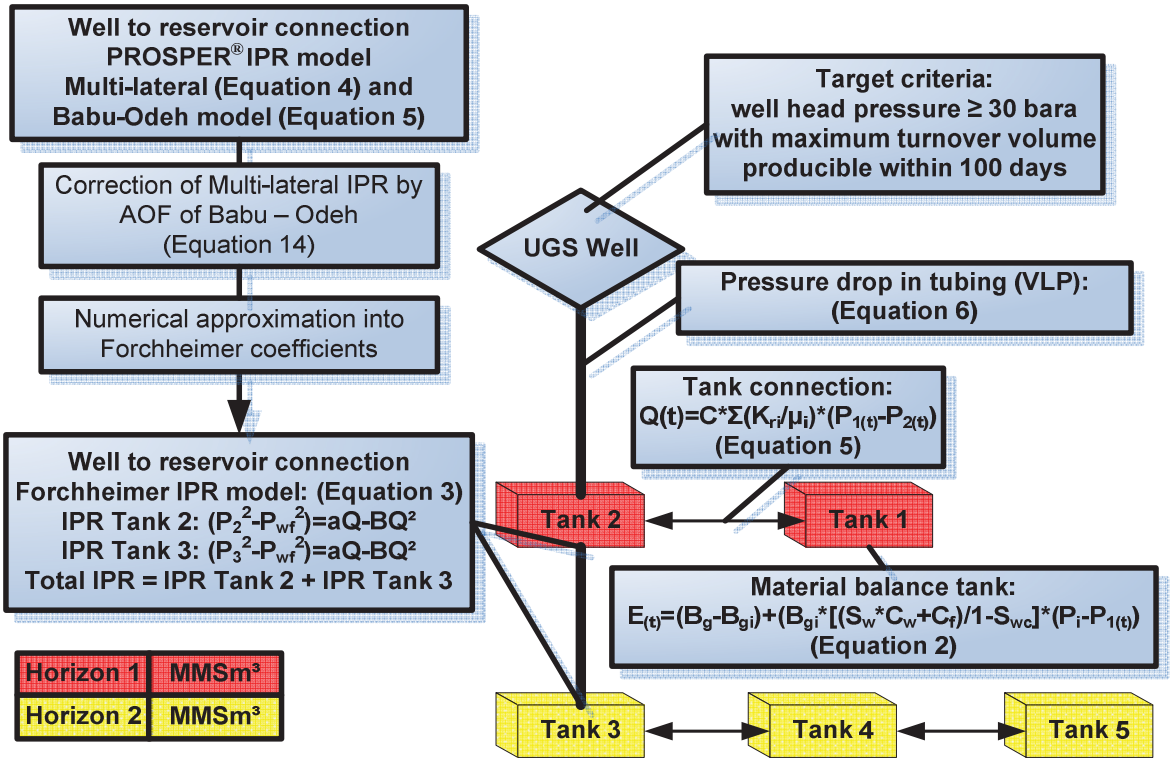

Figure 2.10: Example of the devised model. Two layers of a reservoir are represented by 2 or 3 Tanks, respectively. There is no communication between the horizons. An UGS well penetrates both layers. The annotations state the applied equations in every part of the model.

3. Underground Gas Storage Zagling

The gas field Zagling is located between Strasswalchen and Frankenmarkt in the most northeast part of Salzburg. It lies in the Austrian portion of the molasse basin and borders in the shingled Puchkirchener Series in the south. The Molasse basin is a classical asymmetric foredeep, filled predominantly by Cenozoic clastics, reaching a thickness of up to 4500 m in front of the Alps. While the northern margin of the Molasse basin was mainly formed by a gently dipping mud-pone slope, the southern margin was steep and tectonically active.
Parts of foreland deposits were incorporated in the emerging mountain front and form a pile of thrust sheets (Molasse imbricates).
While in the west, in Bavaria, level-marine delta sediments were deposited, it came in the Austrian part of the molasse basin to deep-marine depositions from Eocene till the Miocene. Sands and shaly marls of the Rupel as well as the lower and the upper Puchkirchener series and the deeper Haller series alternate each other. They were mainly deposited as a result of turbidity currents. The latest sediments exist particularly from deltaic depositions of the Haller series and fluviatile depositions of the Innviertler series. The horizon OPS-A2Z50 / 1 of Zagling consist of local turbiditic depositions at the southern border of the shingled molasse zone. The transport distances of the secondarily deposited sediments were very low. The reservoir is approximately 6 km ² large and has a maximum thickness of more than 90 m.
The reservoir sands can be correlated with the sediment layers of the A2 layers of the upper Puchkirchener series. (Rohöl Aufsuchungs AG, 2007)

In the area of Zagling four wells have been drilled: ZAG-001, ZAG-002, EGG-001 with the distractions EGG-001A and EGG-001B, as well as WEIS-001. ZAG-001 was the only economically successful well in the area of the reservoir. The gas field Zagling, horizon OPS-A2Z50 / 1, was found in 2004 by the well Zagling 1 (ZAG-001), which intersects 45.9 m of gas-leading sandstones in the prospected storage area. In the same year the well Zagling 2 (ZAG-002) was drilled about 1.8 km to the east of the first well. Only low net gas sand thicknesses were found. The wells EGG-001,-001A and-001B, to the east of ZAG-002 were drilled in a similar geological situation, they also proved no gas discovery. The well Weissenkirchen 1 (WEIS-001), drilled in 1991, shows only distal rest sand thickness, silts and shaly marls, far below the gas water contact in ZAG-001.

The cumulative production to the end of May 2007 was 373 Mio VNm³. Water production was small and probably consists only of condensation water. The production history of the field Zagling and the trajectory of ZAG-001 are listed in Appendix A.

All production originates from perforations of the upper A2Z50 sands. At first it was not for sure, if the A2Z50-a and A2Z50-b sands are in communication with the lower gas bearing layers. In August 2007 the lower sands have been perforated, showing a risen GWC and pressures according to the upper sands. This means the shaly layers at the base of the upper and middle sands are not sealing. Nevertheless, for modelling purposes the A2Z50 sand is split up into 5 different layers, named a - e. The gas-water contact was found at 840 m-SS, which is at 1414 m TVD at ZAG-001. ZAG-002, also drilled in 2004, did not encounter reservoir quality sands in the A2Z50 formation.

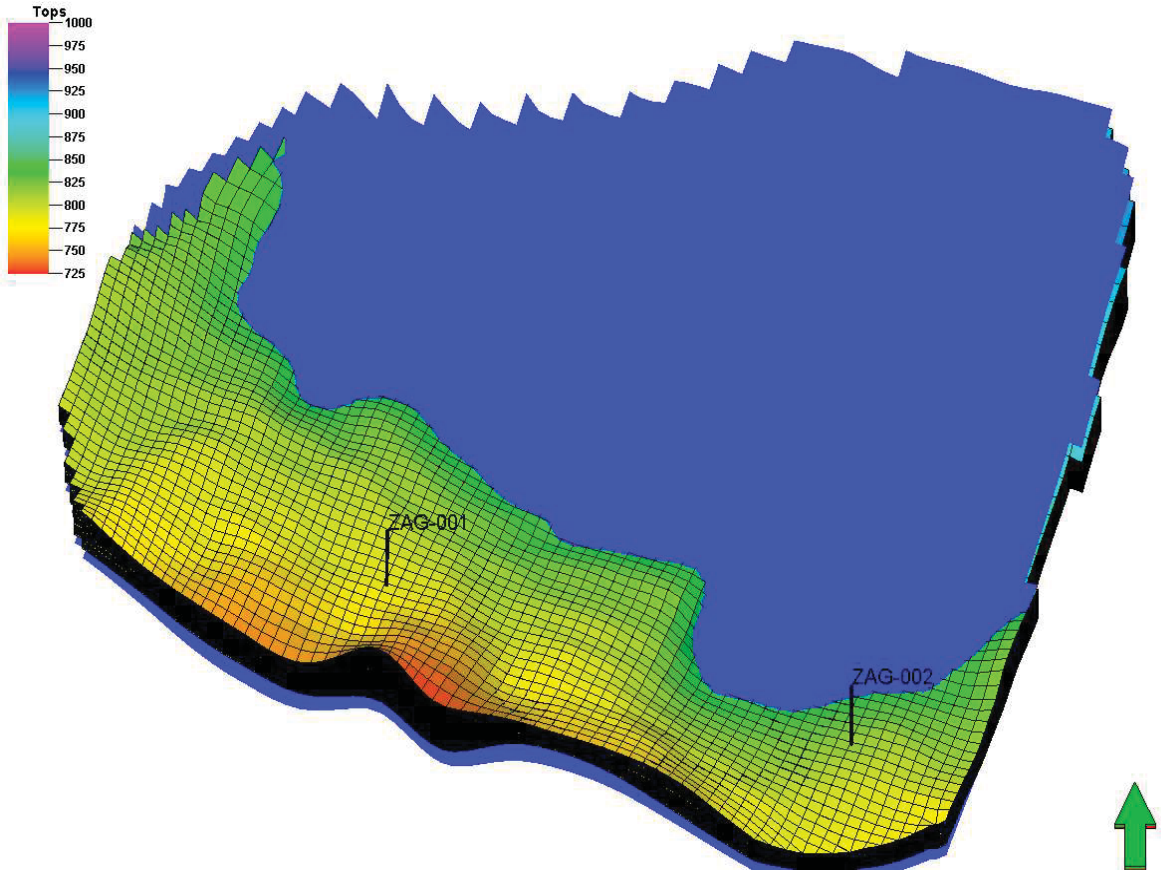

Figure 3.1: The reservoir top of Zagling and the wells ZAG-001 and ZAG-002. The depth is measured in m-SS and the gas-water contact was found at 840 m-SS at ZAG-001.

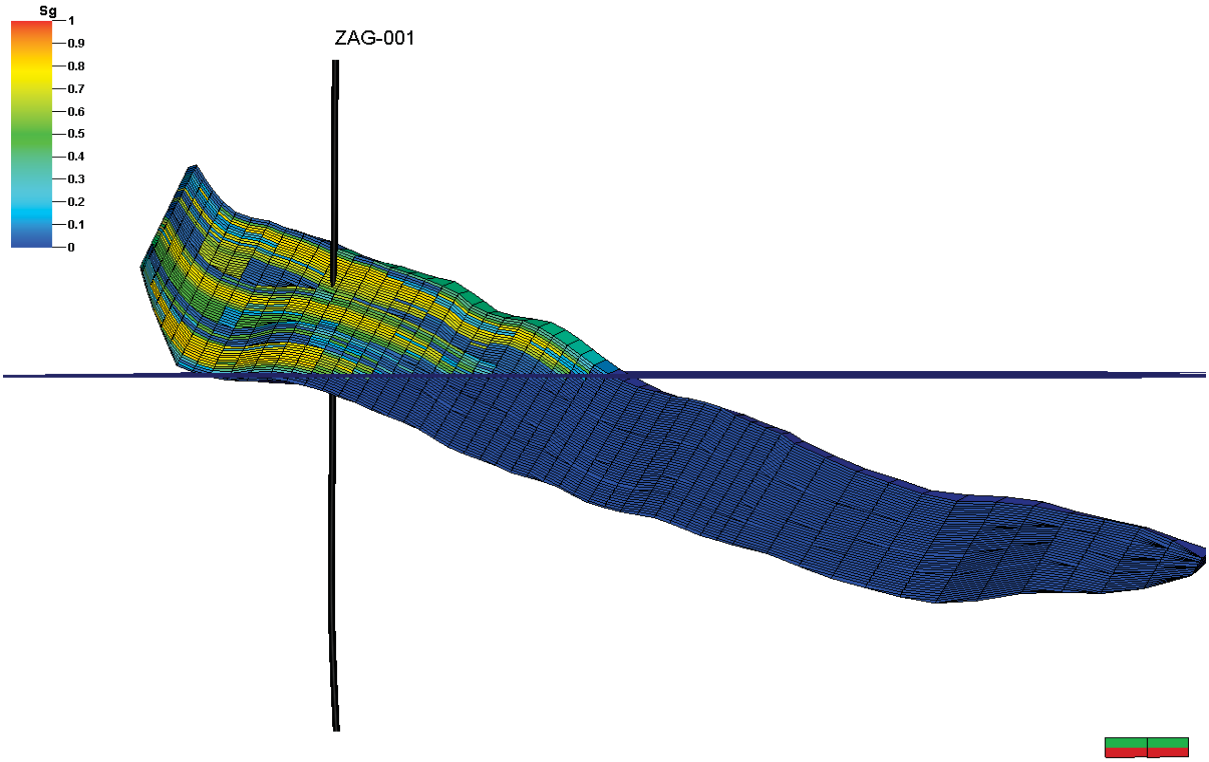

Figure 3.2: An intersection of the reservoir Zagling at ZAG-001 plotted with the gas saturation Sg. The gas-water contact is at 840 m-SS.

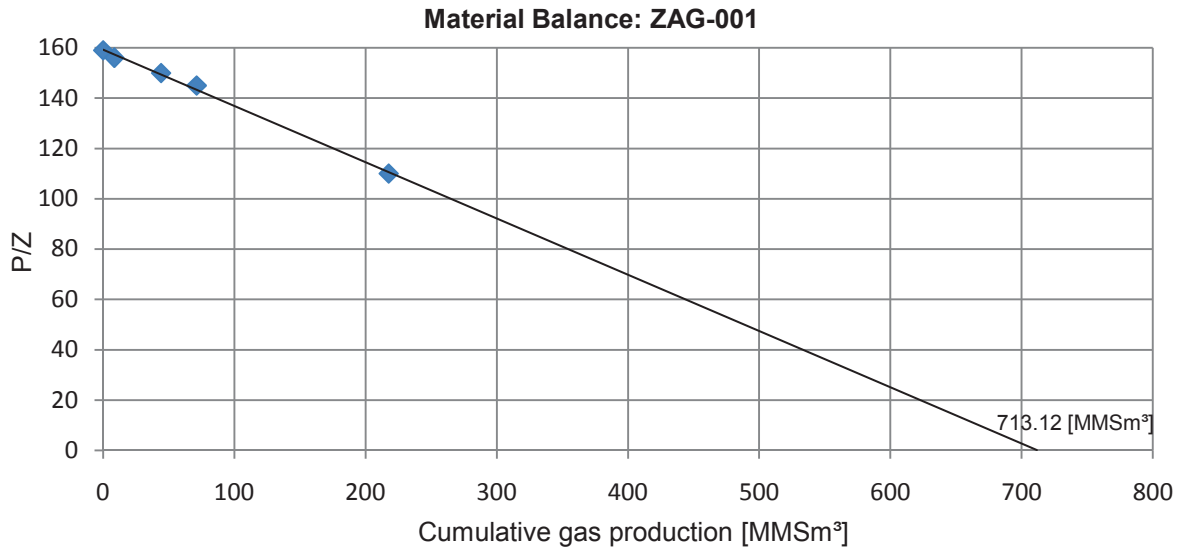

Figure 3.3: The material balance (P/Z plot) indicates depletion drive and shows initial gas in place of 713 million Sm³ (676 MMNm³)

3.1. PVT and Fluid properties

The initial reservoir pressure was measured in September 2004 at 1340.2 m MD at ZAG-001 with 135.2 Bara. The pressure of 135.4 Bara, used in the MBAL® models was calculated at

the reference depth of 781 m-SS. Reservoir temperature is about 44 degree Celsius. The gas composition was measured in March 2007.

C1	Mol.-%	98.9935
C2	Mol.-%	0.3131
C3	Mol.-%	0.1404
iC4	Mol.-%	0.0235
nC4	Mol.-%	0.0377
iC5	Mol.-%	0.0075
nC5	Mol.-%	0.0228
C6+	Mol.-%	0.0561
		100.0000
c_g [1/Pa]		6.78 E-08
B_g [m³/Sm³Pa]		1.16*10^5
Density [kg/m3]		0.7279
Density air=1		0.57

Table 3.1: Fluid composition measured at ZAG-001 on 27.03.2007 (HOT Engineering, 2007)

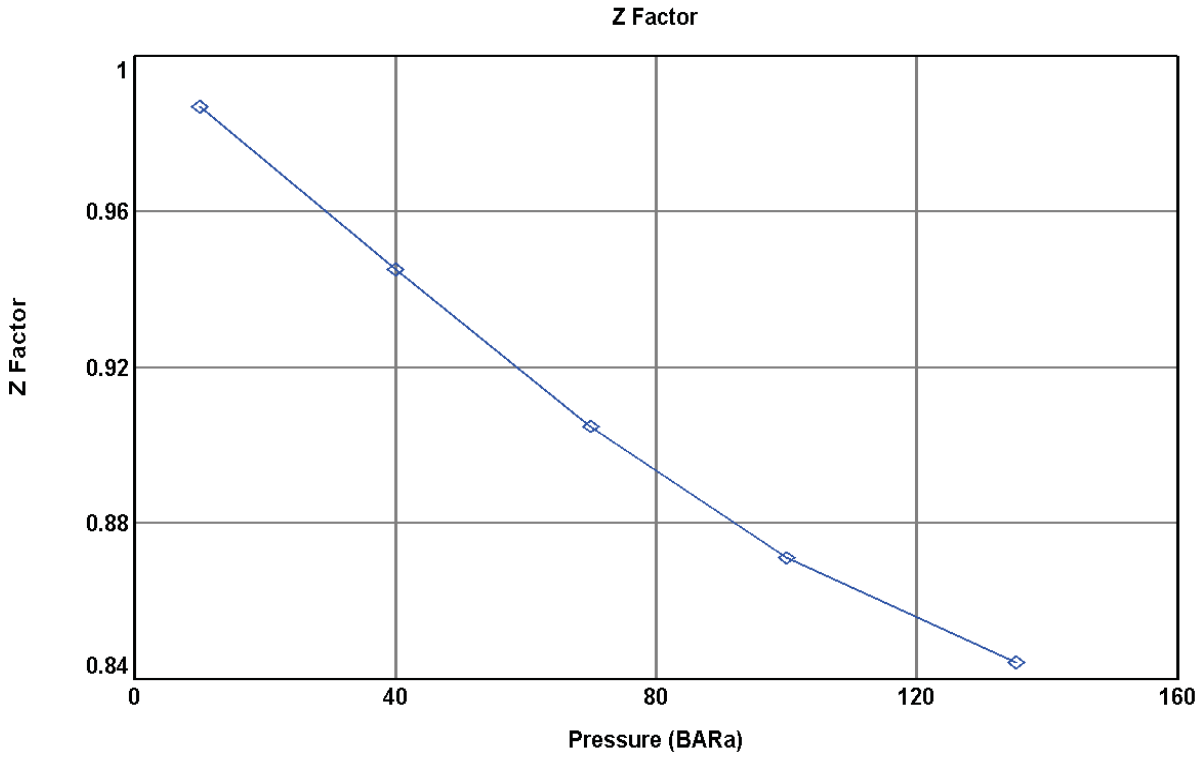

Figure 3.4: Z-factor versus pressure correlation of the Zagling gas.

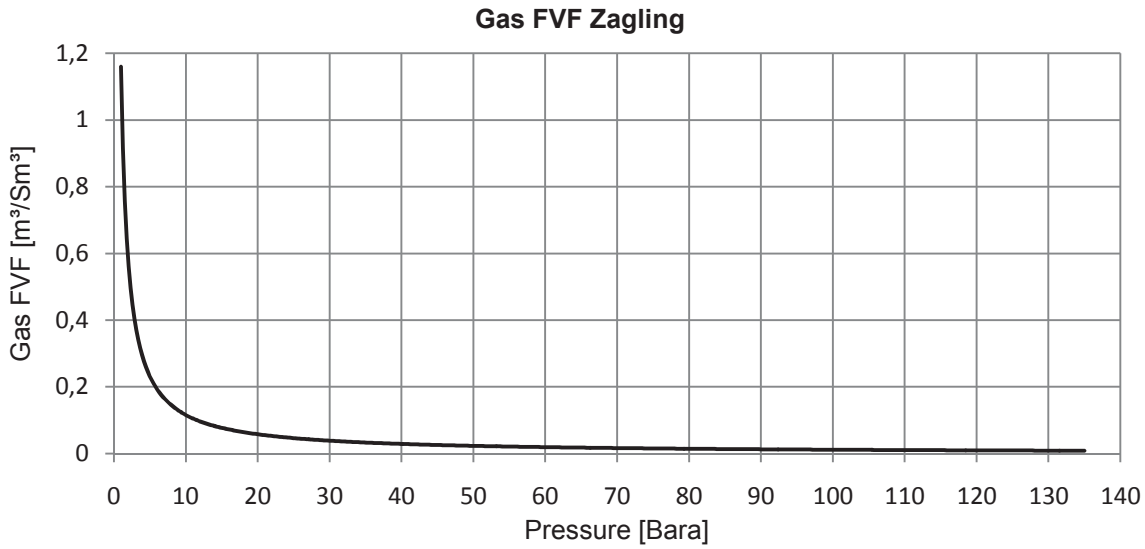

Figure 3.5: Correlation of formation volume factor (B_g) versus pressure for Zagling reservoir.

The formation water salinity is about 15000 ppm. Due to the volumetric decline of the reservoir no aquifer model was implemented into the material balance model. For gas viscosity calculation the correlation after Lee at al was used.

3.2. Relative permeability

The residual gas saturation was set to 30%. In a gas-water reservoir, the water is always the strongly wetting phase and the maximum water relative permeability must be small. Material balance plots to date (Figure 3.3:) do not indicate pressure support by aquifer influx. The water production in ZAG-001 seems to be condensation water only.

	residual saturation	end point	exponent
	faction	faction	
krw	0.3	0.5	2
krg	0.3	1	4

Table 3.2: The table shows the relative permeability data for the Zagling MBAL® model.

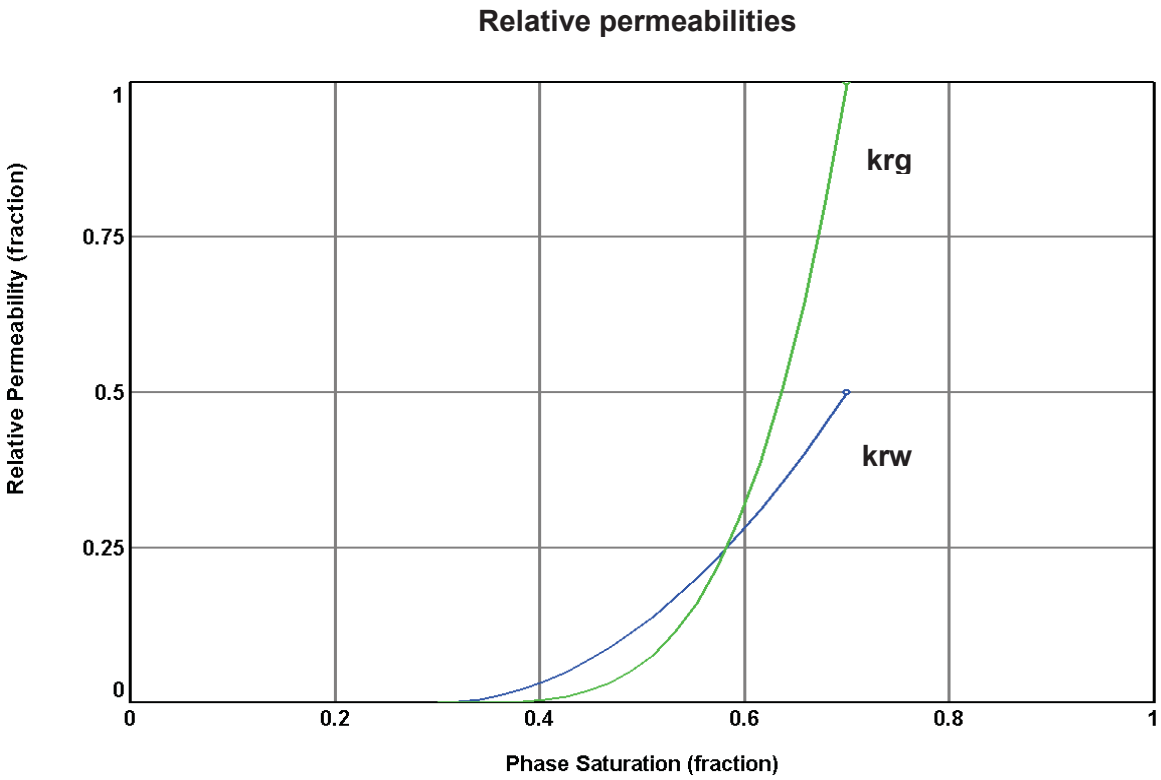

Figure 3.6: The blue curve describes the relative permeability of water dependent on the water saturation. The green curve characterizes the relative permeability of the gas phase plotted versus gas saturation. Relative permeability curves of the MBAL® Zagling reservoir model.

3.3. Inflow Performance Relationship for ZAG-001

The test data of the production test in May 2005 was used to create multi-lateral inflow model and to compare them with the test data. A good interpretation of skin and permeability of this test exists. At this time the reservoir pressure was at 133 Bara.

rate	BHFP
[Sm³/d]	[bara]
253180	131.9
379769	131.4
506359	130.8
632949	130

Table 3.3: production test data of ZAG-001, May 2005

The multi-lateral model has the additional advantage of separated IPR calculation for each reservoir layer.

The production well ZAG-001 was drilled nearly vertical (Appendix A) and the prospected UGS wells ZASP 1 – ZASP 4 have a maximum inclination of 50°. The production well and

the planned UGS wells perforate more than one gas bearing layer. The OPENSERVER® commands support the program based exchange of IPR data between the PROSPER® multi-lateral model and MBAL®. Due to that reasons the multi-lateral model was selected to calculate the inflow performance relationships for the MBAL® prediction runs.

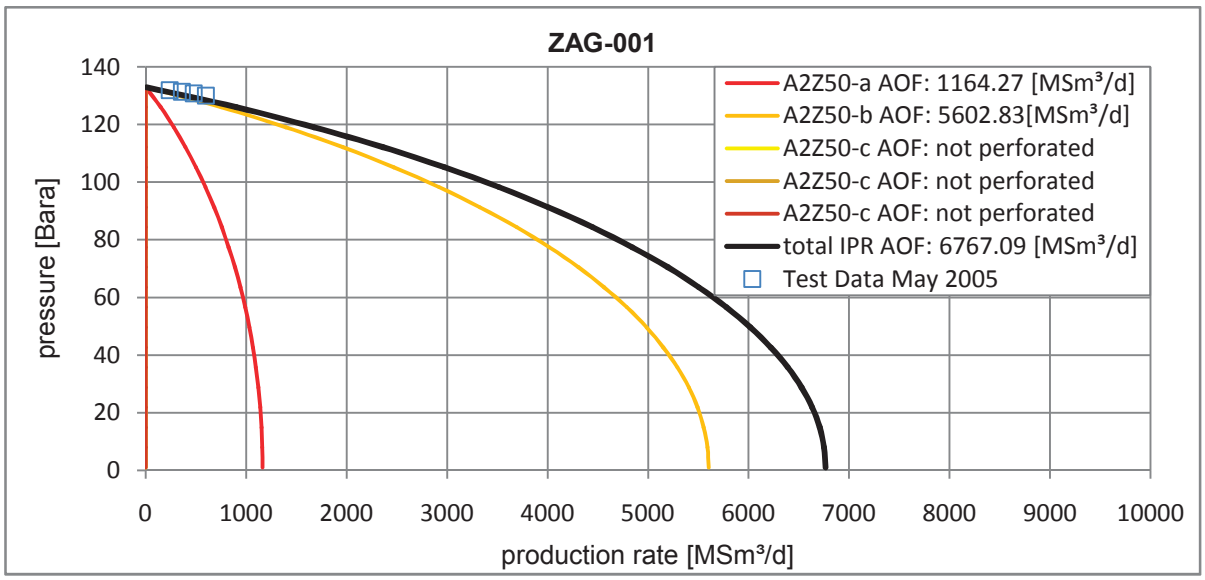

Figure 3.7: Calculated IPR of the multi-lateral model for the produced gas layers of well ZAG-001.

For every layer an individual IPR is calculated. In the specific case of ZAG-001 only layer 1 and layer 2 are perforated. The overall IPR of the well consists of layer 1 and layer 2. The data of the production test, performed in May 2005 (Table 3.3), is used to match the curve of ZAG-001. In the right upper corner the AOF of the well and of the produced layers are shown.

3.4. Zagling MBAL® multi-tank model history match

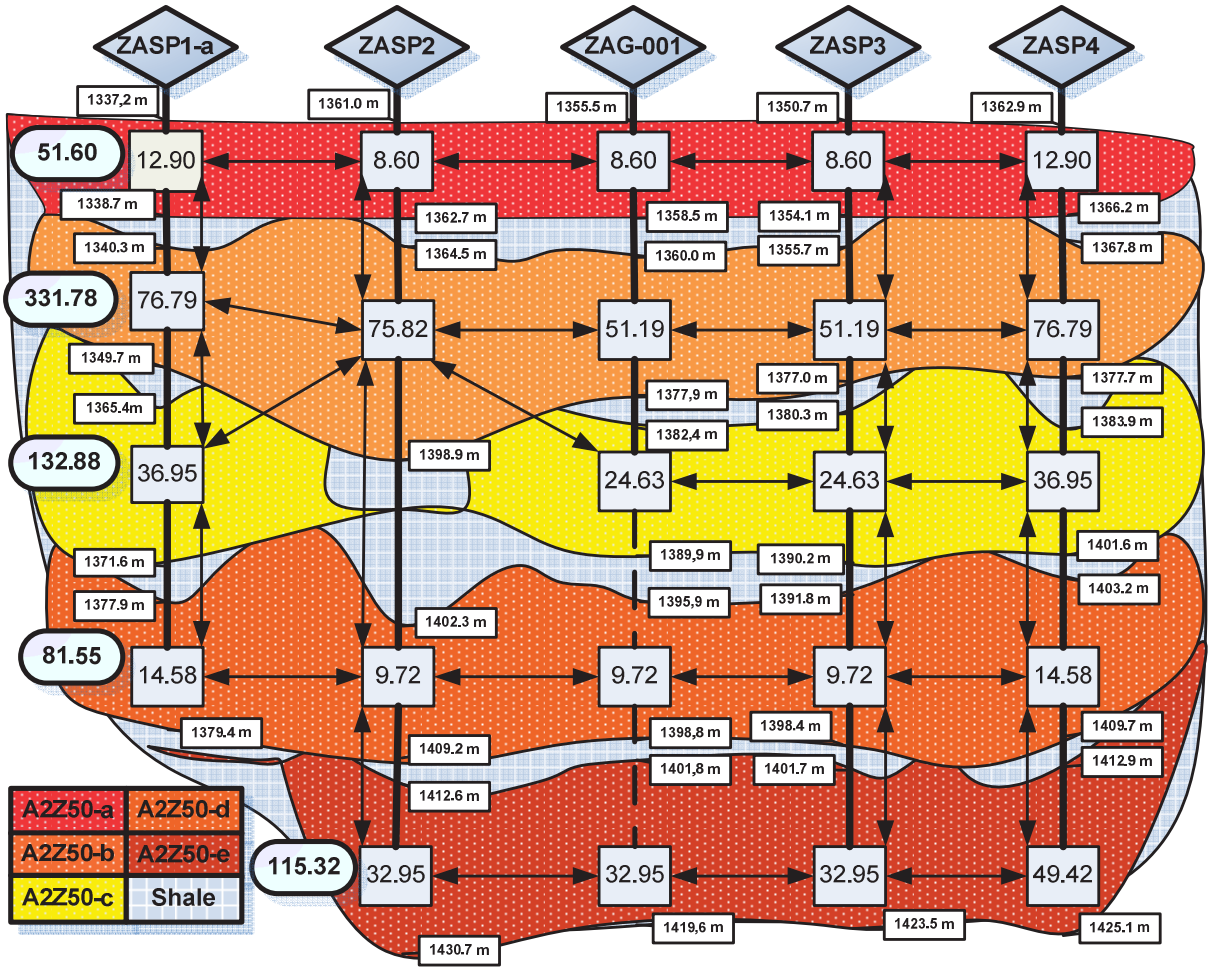

Figure 3.8: The multi-tank system of the reservoir Zagling created in MBAL®. Every tank is filled with a part of the initial volume of 676 MMNm³. The LOG data of ZAG-001 shows a seperation of the different layers (A2Z50-a – A2Z50-e), therefore the tanks are not vertically connected in that area. After testing, the sands A2Z50-c – A2Z50-e were showing pressures accoording to the produced layers. Therefore the tanks are vertically connected throughout the rest of the reservoir.

To model the different reservoir layers and their connection with the UGS wells a multi-tank model in MBAL® is prepared. The issue is to get a history matched model, which is further used to predict the turn over volume (TOV) and the rates of the four UGS wells. The tank volume distribution (Appendix A) was assessed with the help of parameters like layer thickness, distance to gas water contact (GWC) and drainage radius of the wells. History matching starts in September 2004 and ends in July 2007.

The IPR multi-lateral model (Figure 3.7) and a calculated VLP for the production well ZAG-001 are implemented into the MBAL® model, to get a match for the cumulative production over time (Figure A.4, Figure A.5). This was done to check the accuracy of the compounded system. The prediction run starts in September 2004 and ends in May 2007.

3.5. Zagling UGS Wells

To get appropriate permeability data for the prospected UGS wells, artificial logs are created out of the PETREL® static reservoir model. To save investment costs, the question of shorter wells with less inclination is coming up during the planning process. Thus the influence of less perforation and well length on the UGS performance is being investigated. Therefore more than one well trajectory is created for the UGS wells ZASP2, ZASP3 and ZASP4. To investigate the influence of inclination, no new log files are created for the alternative trajectories, because the intersected reservoir areas remain the same. The alternative well path data is entered into the PROSPER® multi-lateral models and the perforation length is adjusted. Permeability data remains the same, just the reservoir contact length is changed. Afterwards the well IPRs and VLPs are calculated in PROSPER® and the results are loaded into the MBAL® model.

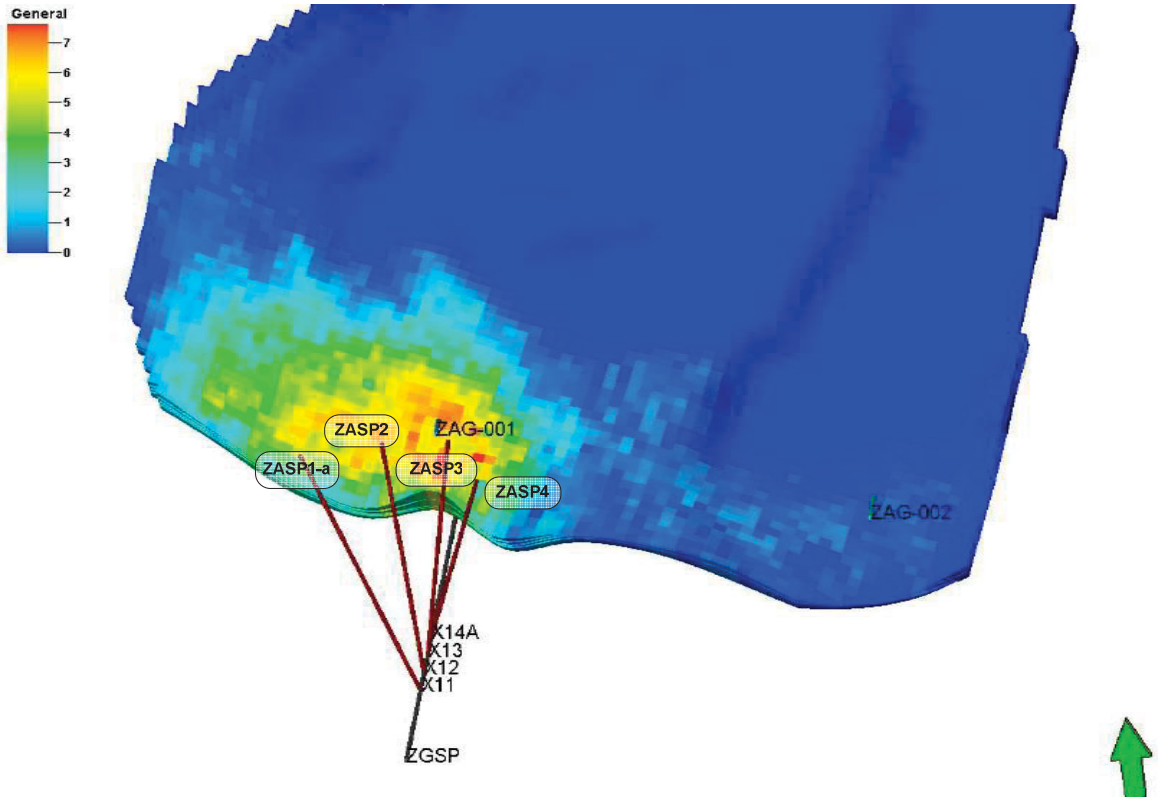

Figure 3.9: Trajectories of four prospected UGS wells intersecting Zagling reservoir. The initial gas saturation is highest around ZAG-001.

The well paths, which are planned first, are labelled with “original” trajectory. The wells planned in second order will be marked as “alternative” trajectories.
The alternative well paths spare about 50 to 100 m for each well. The kick off point is chosen at 300 m TVD. At well ZASP2 and ZASP3 the inclination within the reservoir area changes from about 45° (original) to 24° (alternative). At ZASP4 an inclination with 43° is chosen for the alternative well path.

The well ZASP1-a was originally planned to be drilled in the far western area of the Zagling reservoir, but after a few inflow performance relationship calculations it was decided to change the trajectory, to get a better inflow performance for that UGS well. The new well is named ZASP1, which is planned to end near the production well ZAG-001, to reach the known good reservoir quality in that area. Therefore for ZASP1-a and ZASP1 no alternative well paths are beeing investigated. For the UGS well ZASP1 the permeability data of ZAG-001 is used for IPR calculation. For all Zagling UGS wells a 7 inch completion is selected (Appendix A).

UGS well ZASP 1-a

For the planned trajectory of well ZASP1-a an artificial log is created out of PETREL®, which is fully listed in Appendix A.

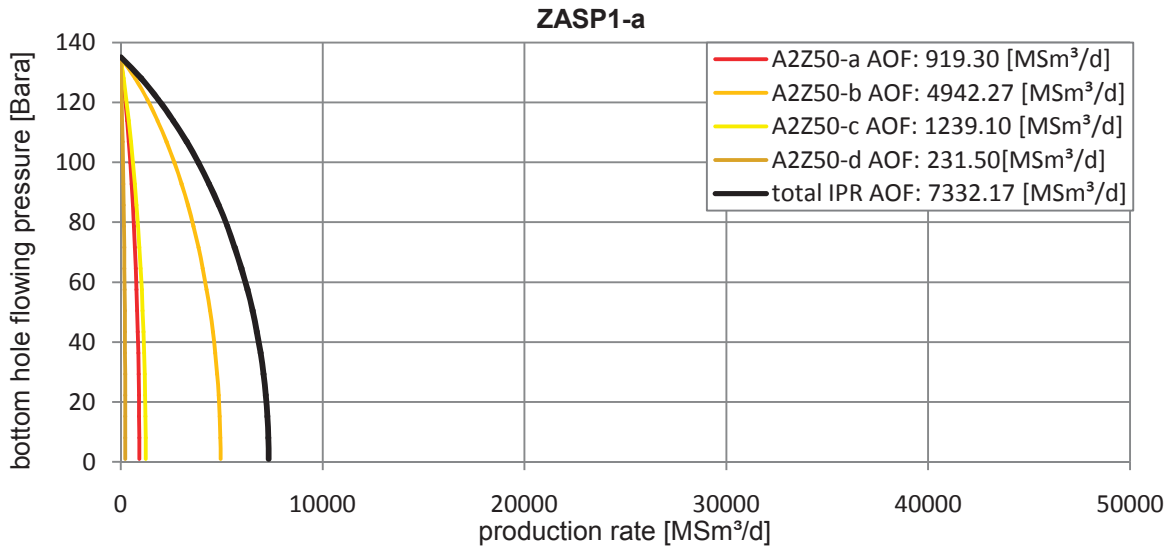

Figure 3.10: Inflow Performance Relationship of the PROSPER® multi-lateral model for well ZASP1-a plotted bottom hole flowing pressure versus production rate at initial reservoir pressure.

tank		TVD	perforation MD	average permeability
		[m]	[m]	[mD]
SP1A2Z50-a	Top	1337.22	1556.50	200.19
	Base	1338.79	1559.50	
SP1A2Z50-b	Top	1340.36	1561.50	189.05
	Base	1349.77	1576.00	
SP1A2Z50-c	Top	1365.41	1600.00	54.30
	Base	1371.66	1610.00	
SP1A2Z50-d	Top	1377.90	1619.00	42.10
	Base	1379.46	1621.50	

Table 3.4: abstract of artificial log, ZASP1-a

The inflow performance of this UGS well is reduced in comparison to the other planned wells. The problem is not the permeability, but the less encountered thickness.

UGS Well ZASP 1

This well is not pictured in Figure 3.9. ZASP1 is prospected to be drilled in the near northwest area of ZAG-001 to encounter higher reservoir thickness. The encountered permeability data and thicknesses of ZAG-001 are used. The trajectory data is mentioned in Appendix A.

tank		TVD	Perforation MD	average permeability
		[m]	[m]	[mD]
ZA1A2Z50-a	Top	1351,07	1441.00	175.02
	Base	1355,15	1445,50	
ZA1A2Z50-b	Top	1356,06	1446,50	191.43
	Base	1373,31	1465,50	
ZA1A2Z50-c	Top	1377,85	1470,50	313.75
	Base	1386,93	1480,50	
ZA1A2Z50-d	Top	1391,47	1485,50	142.96
	Base	1395,1	1489,50	

Table 3.5: Permeabilities and perforations of ZASP1

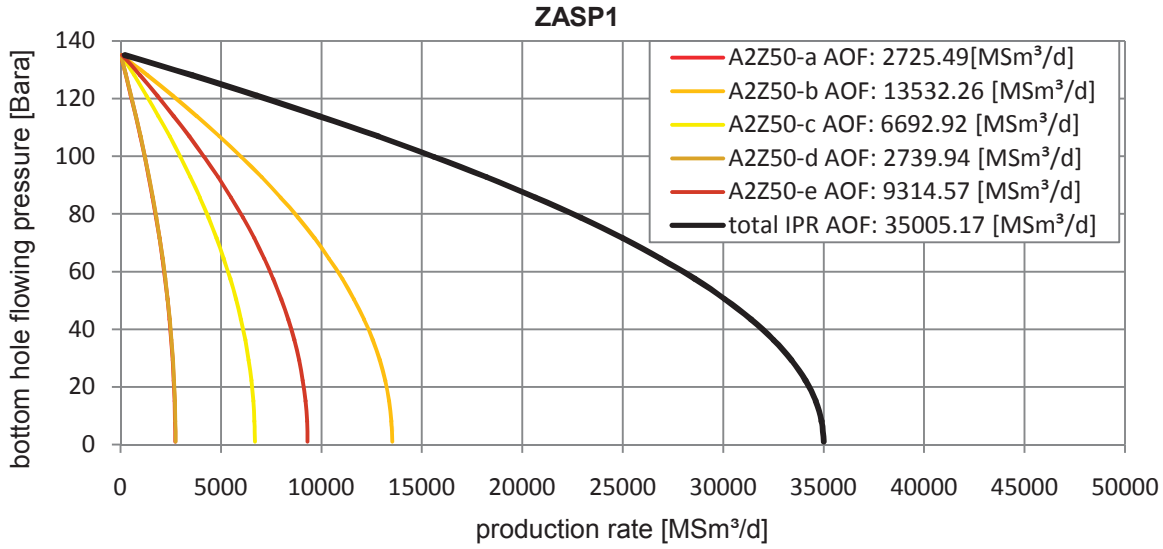

Figure 3.11: Inflow Performance Relationship of the PROSPER® multi-lateral model for well ZASP1, plotted bottom hole flowing pressure versus production rate at initial reservoir pressure.

UGS Well ZASP 2

Two different trajectories are planned for the well ZASP 2 (Appendix A), but just for the original trajectory an artificial log is created out of PETREL®. The alternative well path data is entered into the PROSPER® multi-lateral model and the perforation length is adjusted. The complete artificial log data is headed in Appendix A.

tank		TVD	perforation MD	average permeability
		[m]	[m]	[mD]
SP2A2Z50-a	Top	1361.04	1525.50	236.70
	Base	1362.77	1529.00	
SP2A2Z50-b	Top	1364.51	1531.00	279.12
	Base	1398.93	1586.00	
SP2A2Z50-d	Top	1402.36	1591.00	86.86
	Base	1409.20	1602.00	
SP2A2Z50-e	Top	1412.63	1607.50	138.53
	Base	1430.71	1636.50	

Table 3.6: abstract of artificial log, original trajectory, ZASP2

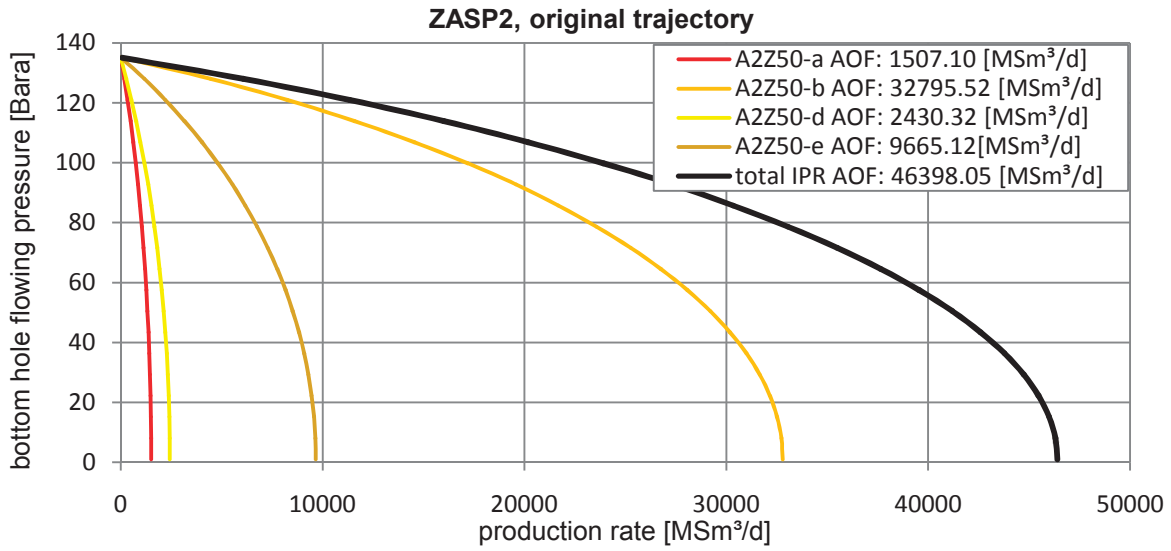

Figure 3.12: Inflow Performance Relationship of the PROSPER® multi-lateral model for the original trajectory of well ZASP2 plotted bottom hole flowing pressure versus production rate at initial reservoir pressure.

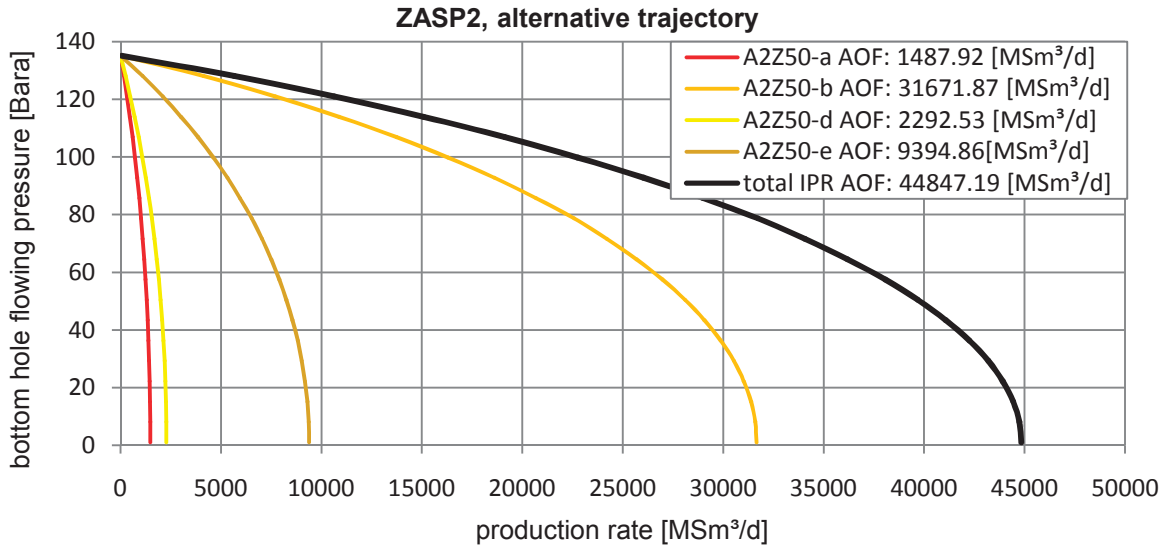

Figure 3.13: Inflow Performance Relationship of the PROSPER® multi-lateral model for the alternative trajectory of well ZASP2, plotted bottom hole flowing pressure versus production rate at initial reservoir pressure.

UGS Well ZASP 3

The different trajectories, which are planned for the well ZASP 3, are headed in Appendix A and, just for the original trajectory an artificial log has been created out of PETREL®. The complete artificial log data is listed in Appendix A.

tank		TVD	perforation MD	average permeability
		[m]	[m]	[mD]
SP3A2Z50-a	Top	1350.78	1486.00	72.19
	Base	1354.06	1491.00	
SP3A2Z50-b	Top	1355.70	1493.00	161.26
	Base	1377.04	1523.00	
SP3A2Z50-c	Top	1380.32	1527.50	169.99
	Base	1390.17	1541.50	
SP3A2Z50-d	Top	1391.81	1543.50	103.82
	Base	1398.38	1553.00	
SP3A2Z50-e	Top	1401.66	1557.00	200.64
	Base	1423.51	1588.00	

Table 3.7: abstract of artificial log, original trajectory, ZASP3

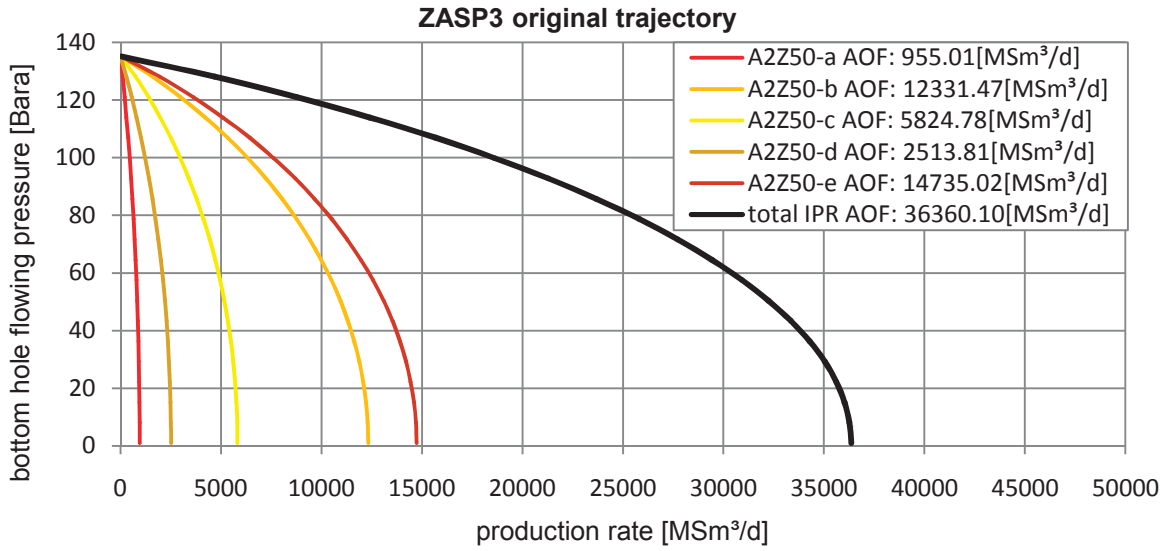

Figure 3.14: Inflow Performance Relationship of the PROSPER® multi-lateral model for the original trajectory of well ZASP3, plotted bottom hole flowing pressure versus production rate at initial reservoir pressure.

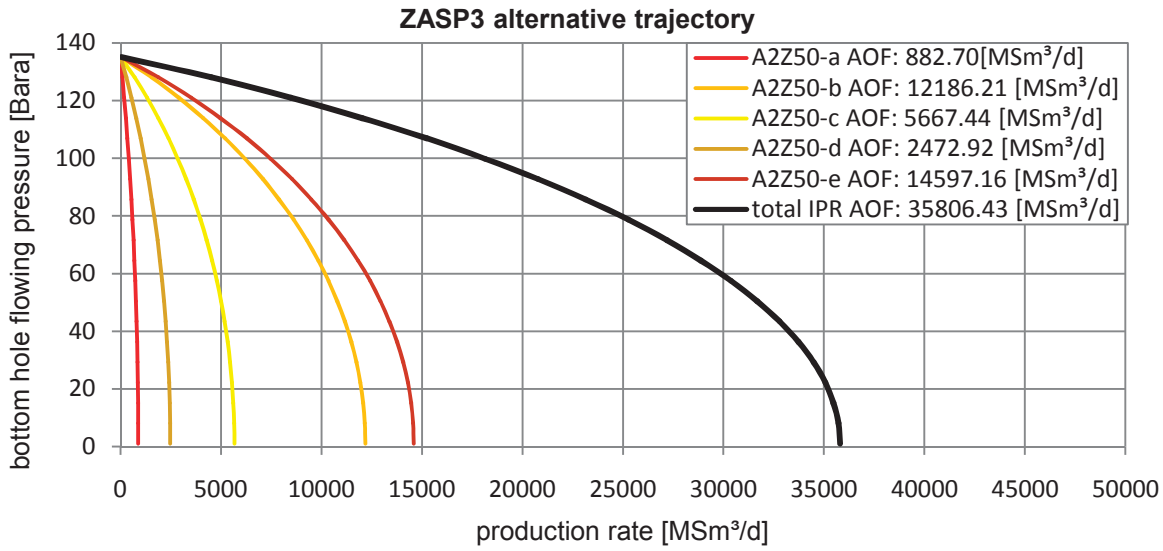

Figure 3.15: Inflow Performance Relationship of the PROSPER® multi-lateral model for the alternative trajectory of well ZASP3, plotted bottom hole flowing pressure versus production rate at initial reservoir pressure.

UGS Well ZASP 4

For the original trajectory of well ZASP 4 artificial log data is generated. The complete artificial log data is headed in Appendix A.

tank		TVD	perforation MD	average permeability
		[m]	[m]	[mD]
SP4A2Z50-a	Top	1362.93	1711.00	110.62
	Base	1366.15	1716.50	
SP4A2Z50-b	Top	1367.76	1718.50	260.14
	Base	1377.73	1734.00	
SP4A2Z50-c	Top	1383.87	1744.00	215.64
	Base	1401.60	1772.50	
SP4A2Z50-d	Top	1403.21	1774.50	38.40
	Base	1409.67	1785.00	
SP4A2Z50-e	Top	1412.89	1790.00	142.43
	Base	1425.05	1809.50	

Table 3.8: abstract of artificial log, original trajectory, ZASP4

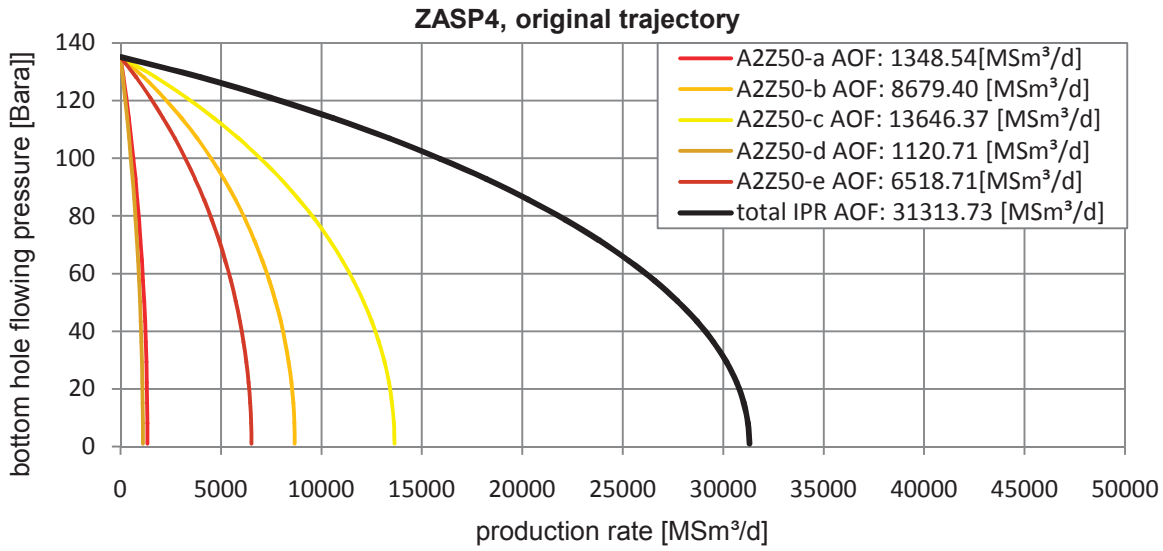

Figure 3.16: Inflow Performance Relationship of the PROSPER® multi-lateral model for the original trajectory of well ZASP4, plotted bottom hole flowing pressure versus production rate at initial reservoir pressure.

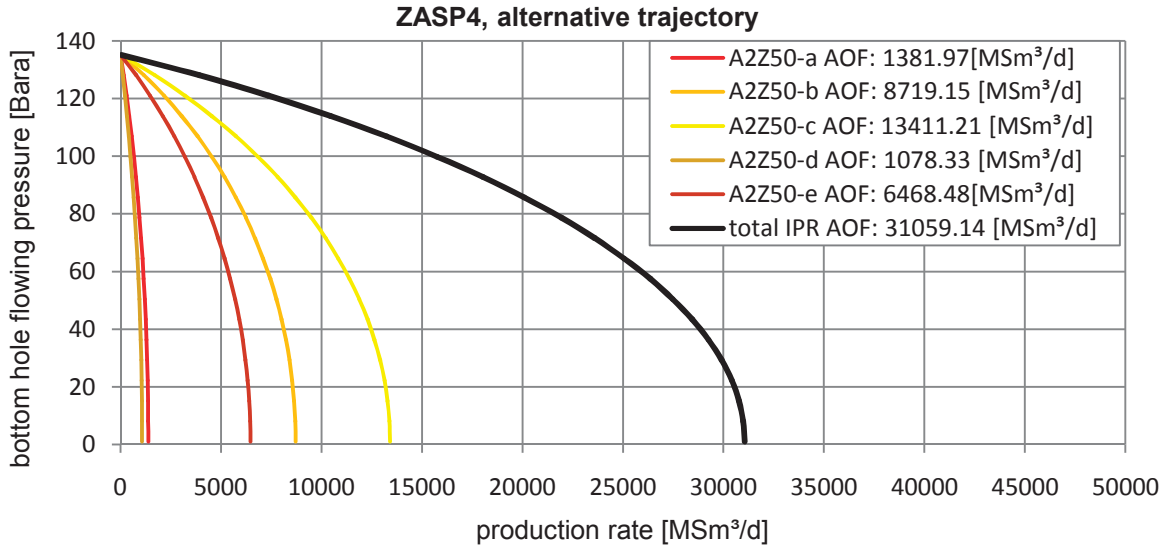

Figure 3.17: Inflow Performance Relationship of the PROSPER® multi-lateral model for the alternative trajectory of well ZASP4, plotted bottom hole flowing pressure versus production rate at initial reservoir pressure.

3.6. Zagling MBAL® multi-tank prediction model

After the successful history match of the Zagling multi-tank model, the four UGS wells are implemented into MBAL®. With the help of the OPENSERVER® commands it is possible to investigate the influence of the alternative well paths, different skin effects and several production profiles on reservoir performance. The prediction runs are carried out for a 100 days production schedule. The entire turnover volume (TOV) has to be producible within these 100 days. Due to compressor limitations the manifold pressure must not fall below 30 Bar during production. The production profiles are defined by Equation 19. Therefore the initial rates and further the production profiles depend directly on the reservoir turnover volume, which has to be calculated during the prediction runs. After 40 days of production, the initial total field production rate can be changed. This gives the opportunity for selecting the best possible production profile to optimize reservoir performance and turnover volume.
Three different production profiles with various end rates have been selected. The end rate is defined in percentage of the initial rate.

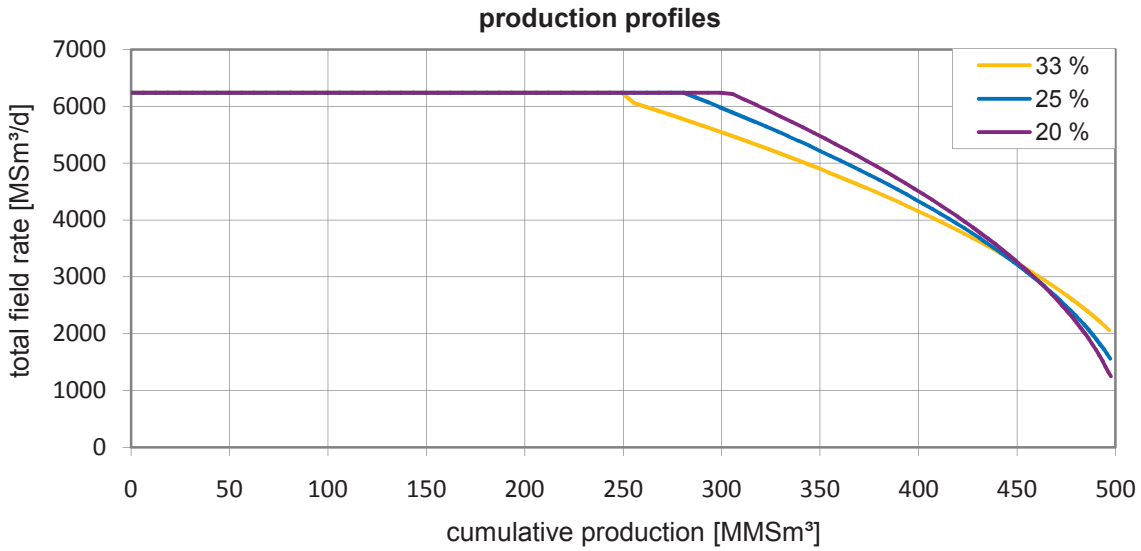

Figure 3.18: Three production profiles with an initial rate of 6218.37 MSm³/d, but different values of P_{init}. They are plotted field production rate versus cumulative production.

The following scenarios have been calculated for both trajectories (original and alternative) for the UGS wells Zagling:

- Skin 0
- Skin12
- Skin30
- Skin40

4. Underground Gas Storage Berndorf

The Berndorf reservoir is the top of the frontal fold of the Berndorf imbricate and forms a westward tilted fold anticline. The Berndorf sands extend over 4.1 km²; are located in about 1270 m-MD with a gross thickness close to 30 m. The reservoir sands are an allochthonous part of the Upper Puchkirchen Formation and are interpreted as debris flow deposits grading upward into turbidites. The Lauterbach sands onlap the Berndorf sands and extend over 1.4 km². They comprise two coarsening upward cycles with a gross thickness of about 30 m. Gas field Berndorf was found by BERN-001, which was drilled in 1989. The well started production in January 1990 from the "Untere Puchkirchner Serie-Schuppe" (UPS). Cumulative production to March 2007 was slightly more than 200 million Nm³. The Water production was small and consists probably only of condensation water. The production history of the field Berndorf is listed in Appendix B. Initial reservoir pressure was 136.1 Bara, measured at the reference depth of 760 m-ss. Reservoir temperature is about 43℃. Until 1998 the pressure had declined below 20 Bara. Since 1999 production was intermittent and the pressure remained in the 15-20 bar range. No gas – water contact was encountered (Rohöl Aufsuchungs AG, 2009).

If only early pressure data is considered, the material balance P/z plot (Figure 4.3) indicates a depletion drive reservoir with a gas initial in place of about 180 million Nm³, but the cumulative production was slightly over 200 million Nm³. The very small water production indicates no significant water influx. It is most probable that gas from tight rock is feeding the higher permeability reservoir layers. The total volume available for gas storage seems to be close to 180 million Nm³. (HOT Engineering, 2007)

The production well LAUT-004 was drilled in May 2006. Initial pressures showed significant depletion in the A2 L55-60 sands. Several different pressure levels are present, which are indicating poor vertical communication through the shale layers. The most likely reason for the partial depletion is communication with BERN-001. The shale layers, separating the three Berndorf sands are clearly visible (Figure 4.2).

Three major faults exist in Berndorf (Figure 4.9) and it is not proven yet if they are sealing or not. Sealing faults would lead to a compartmentalization of the reservoir, limiting the north-south transmissibility. Non sealing faults would indicate a communication between the three Berndorf layers.

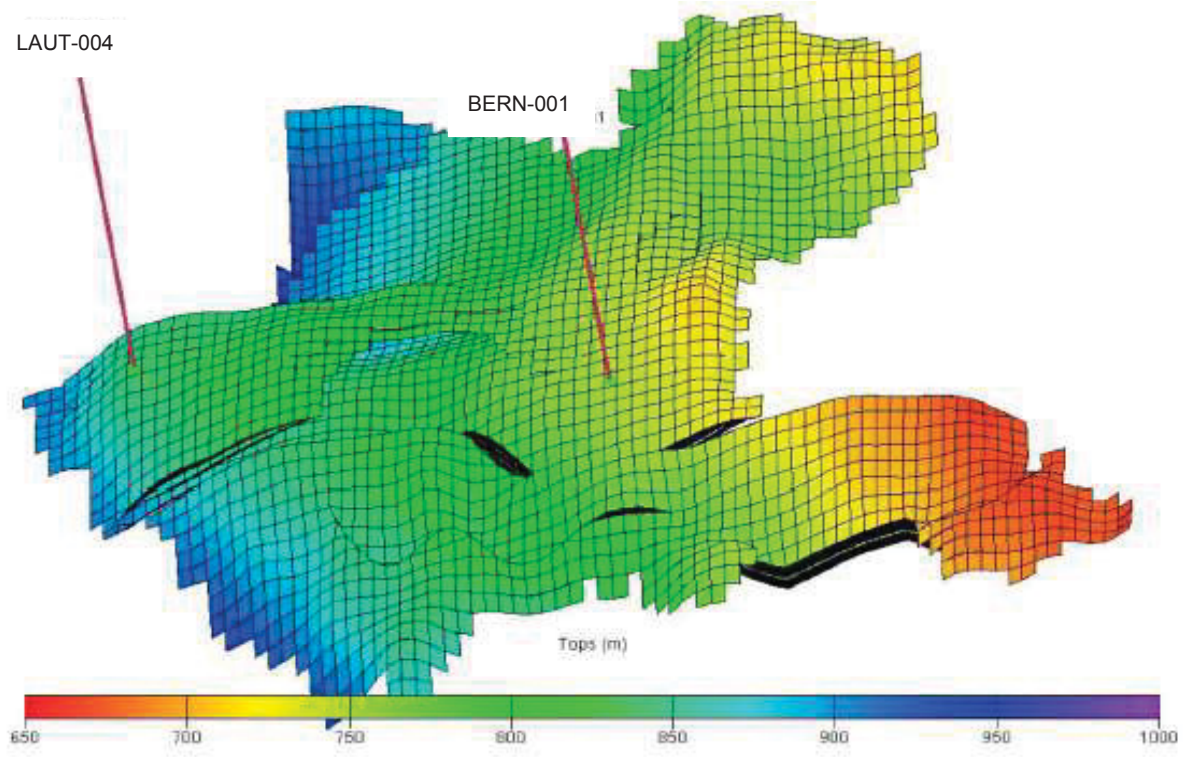

Figure 4.1: The wells BERN-001 and LAUT-004 are intersecting the geological structure of UGS Berndorf .ECLIPSE100® flow simulation grid, Top view [mSS], (HOT Engineering, 2007)

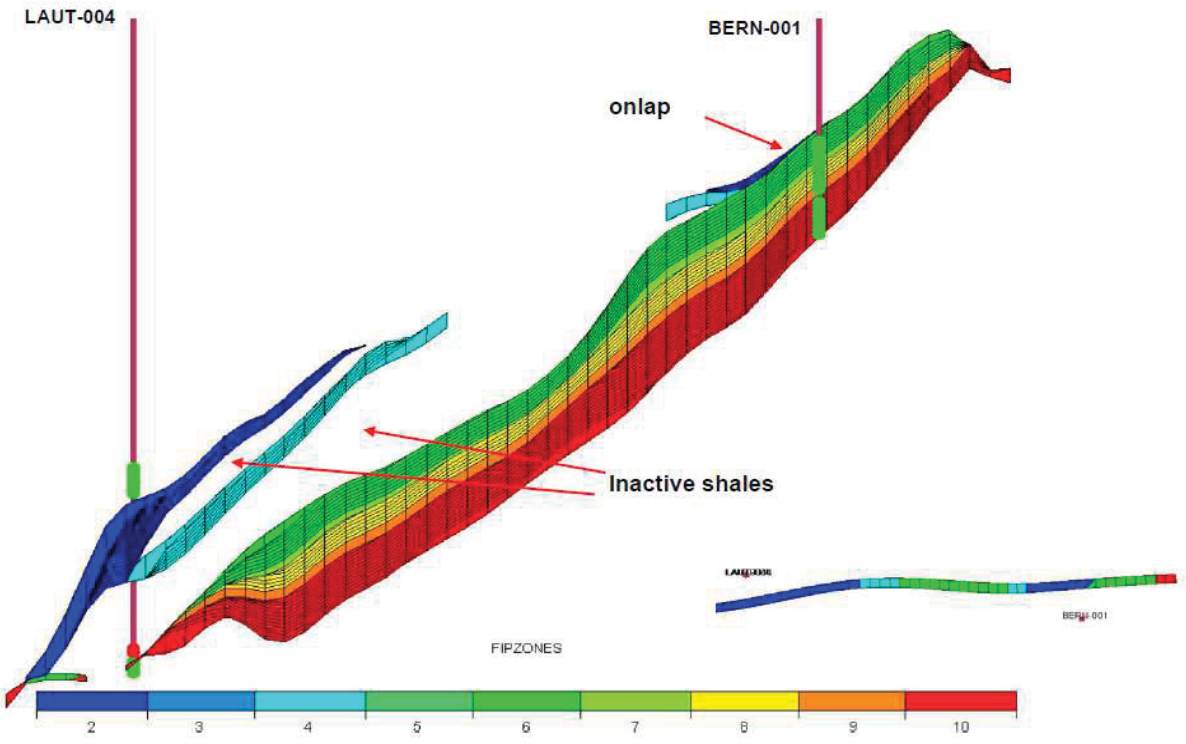

Figure 4.2: Between the communicating reservoirs Berndorf and Lauterbach inactive shale layers are deposited. The A2 L55-60 sands are deposited above the Berndorf layers. Cross section ECLIPSE simulation grid, classification of Reservoir Zones (HOT Engineering, 2007)

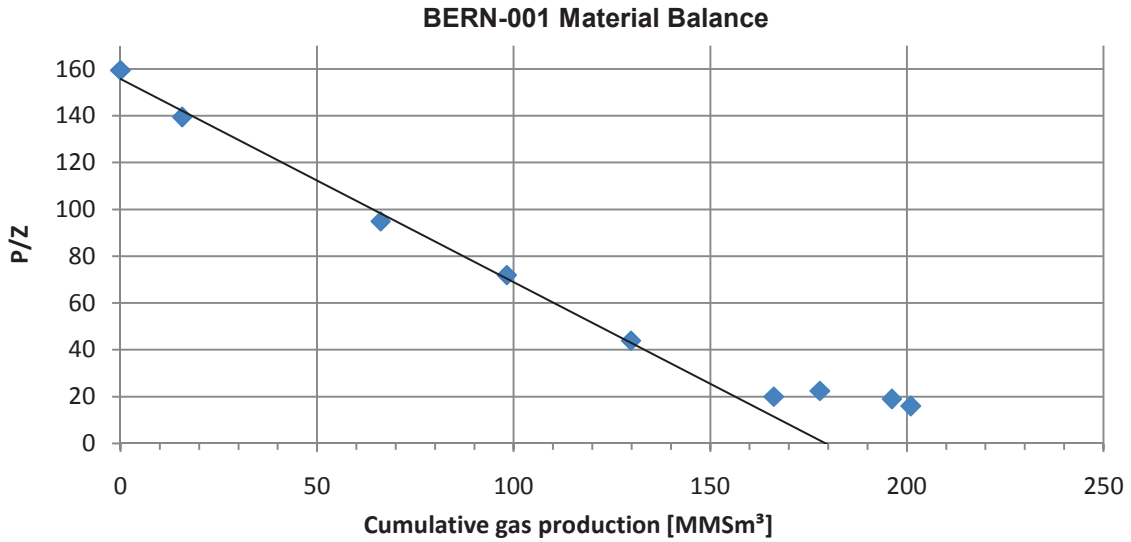

Figure 4.3: The P/Z values of the measured reservoir pressures plotted versus cumulative production of Berndorf are showing a gas initial in place of 180 million Nm³ in the Berndorf sands.

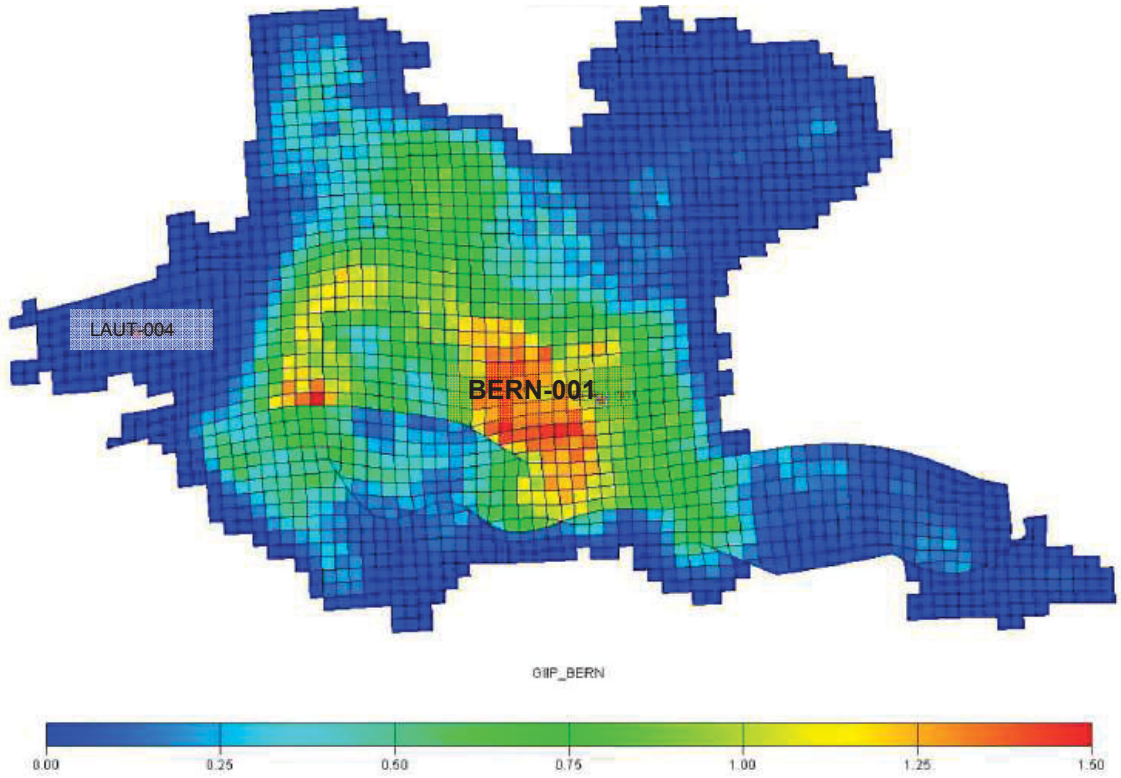

Figure 4.4: The well BERN-001 is intersecting the Berndorf reservoir aside the area with the best initial gas in place distribution [rm3/m2]. (HOT Engineering, 2007)

4.1. PVT and Fluid properties

The gas properties for use in the material balance simulation model were computed based on a gas gravity of 0.56, reservoir temperature of 43 ℃, N2 of 0.35 Vol.% and CO2 of 0.06 Vol. % (measured on Dec.12.,1994). In PROSPER® and MBAL® the viscosity correlation after Lee et al is used. Formation water salinity is about 15000 ppm.

Gas Analyses Berndorf										
Datum		15.10.1989	22.06.1993	14.06.1994	12.12.1994	28.03.2007				
Intervall	m	1286-1294	1273.3-1296.0							
Formation		UPS Schuppe								
		OHT						Minimum	**Average**	Maximum
CO_2	Vol. %	0,03	0,05	0,06	0,06	0,03		0,03	**0,07**	0,16
N_2	Vol. %	0,32	0,37	0,35	0,36	0,32		0,32	**0,36**	0,39
C1	Vol. %	99,32	99,24	99,25	99,23	99,32		99,09	**99,23**	99,32
C2	Vol. %	0,20	0,23	0,23	0,23	0,20		0,20	**0,22**	0,23
C3	Vol. %	0,05	0,05	0,05	0,05	0,05		0,05	**0,05**	0,05
iC4	Vol. %	0,02	0,02	0,02	0,02	0,02		0,02	**0,02**	0,02
nC4	Vol. %	0,01	0,01	0,01	0,01	0,01		0,01	**0,01**	0,01
iC5	Vol. %	0,01	0,01	0,01	0,01	0,01		0,01	**0,01**	0,01
nC5	Vol. %	Trace	Trace	Trace	Trace	Trace				
C6+	Vol. %	0,04	0,02	0,02	0,03	0,04		0,02	**0,03**	0,04
		100,00	100,00	100,00	100,00	100,00		100,00	**100,00**	100,00
c_g	[1/Pa]								**6.45 E-08**	
B_g	[m³/Sm³Pa]								**1.105 E05**	
Density	[kg/m³]	0,72	0,72	0,72	0,72	0,73		0,72	**0,72**	0,73
Density	Air=1	0,56	0,56	0,56	0,56	0,56		0,56	**0,56**	0,56

Table 4.1: Gas composition and properties measured at BERN-001 since production. (HOT Engineering, 2007)

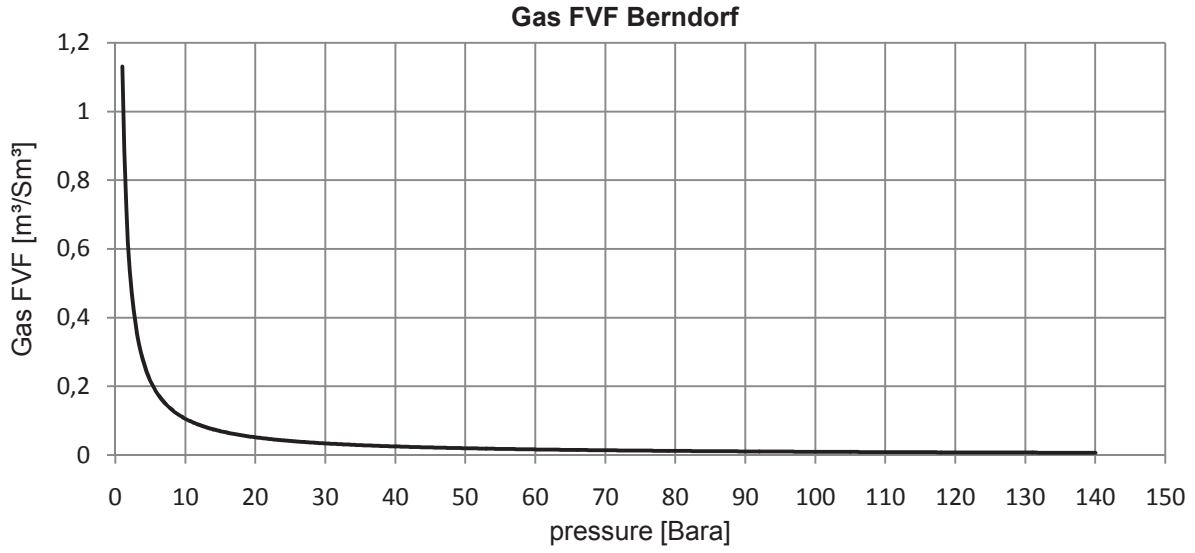

Figure 4.5 Gas formation volume factor plotted versus pressure

4.2. Relative permeability

The residual gas saturation was set to 30%. Material balance plots to date (Figure 4.3: The P/Z values of the measured reservoir pressures plotted versus cumulative production of Berndorf) do not indicate pressure support by aquifer influx. The water production in BERN-001 seems to be condensation water only.

	residual saturation	end point	exponent
	faction	faction	
krw	0.3	0.5	2
krg	0.3	1	4

Table 4.2: Relative permeability data, Berndorf

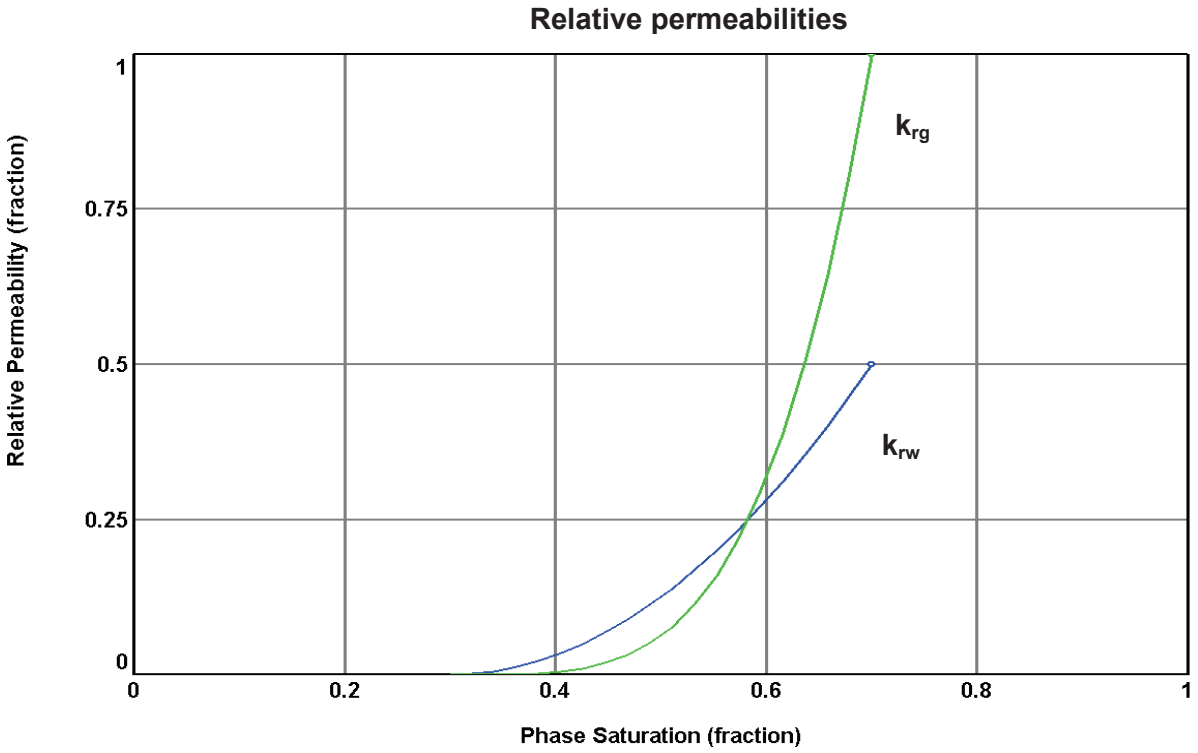

Figure 4.6: Relative permeability curves of the MBAL® Berndorf reservoir model. The blue curve describes the relative permeability of water dependent on the water saturation. The green curve characterizes the relative permeability of the gas phase plotted versus gas saturation.

4.3. Inflow Performance Relationship for BERN-001

The production well BERN-001 encounters three gas bearing layers of the Berndorf reservoir. A multi-lateral IPR model is created in PROSPER® and matched with the production test data of January 1990.

Rate	BHFP
[Sm³/d]	[Bara]
80180	131.81
107731	130.77
156786	128.4

Table 4.3: Production test data of BERN-001, January 1990

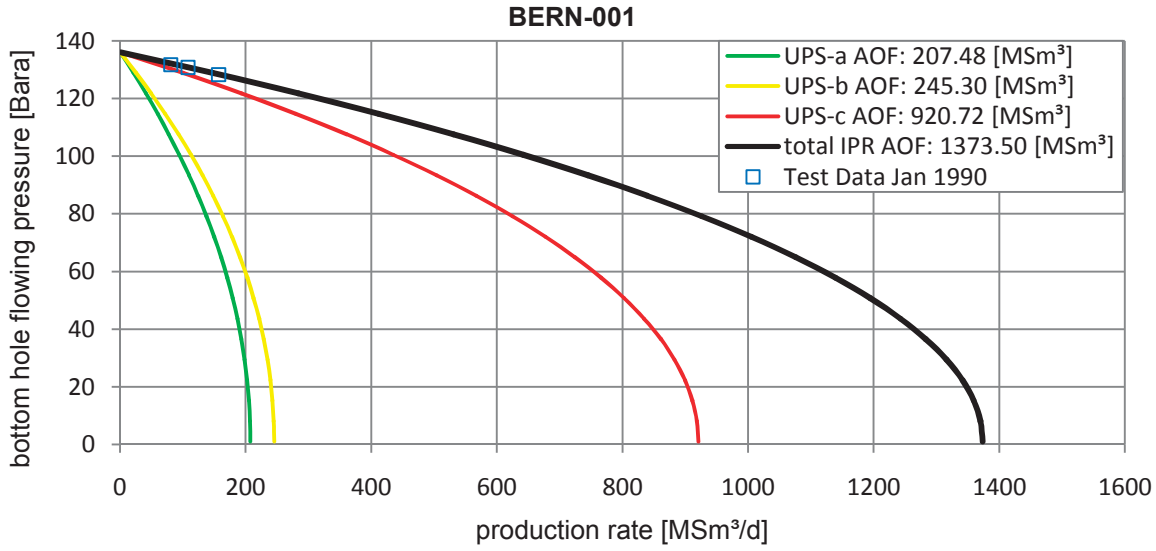

Figure 4.7: Calculated IPR of the PROSPER® multi-lateral model for all three gas bearing layers of well BERN-001. The production test data of Table 4.3: Production test data of BERN-001, January 1990Table 4.3 is used to match the curve.

tank		TVD	Perforation MD	average permeability
		[m]	[m]	[mD]
BE-001UPS-a	Top	1273.05	1273.05	15
	Base	1278.24	1278.24	
BE-001UPS -b	Top	1280.24	1280.24	22
	Base	1285.23	1285.23	
BE-001UPS -c	Top	1286.73	1286.73	38
	Base	1295.72	1295.72	

Table 4.4: Permeabilities and perforations of BERN-001

The deviation of BERN-001 is insignificant, the well path is supposed to be vertical.
The comingled production of BERN-001 is split up with the help of allocation factors, based on the permeability data listed in Table 4.4.

tank		TVD	Perforation MD	average permeability
		[m]	[m]	[mD]
BE-001UPS-a	Top	1273.05	1273.05	15
	Base	1278.24	1278.24	
BE-001UPS -b	Top	1280.24	1280.24	22
	Base	1285.23	1285.23	
BE-001UPS -c	Top	1286.73	1286.73	38
	Base	1295.72	1295.72	

Table 4.4. The production and pressure history is listed in Appendix B.

4.4. Berndorf MBAL® multi-tank model history match

For simulation purposes the Berndorf reservoir is split up into three non-connected layers (UPS-a, UPS-b, UPS-c), but it is most probable, that the gas sands are connected with each other. Regrettably it was not possible to set up a model, which simulates the connection between the three Berndorf layers, so the solution is to come up with a slightly simpler MBAL® material balance model. During history matching monthly average historical gas production rates are entered into the model, flowing and static pressures are computed and have to reproduce measured pressures. The model contains a total gas volume of 256 million standard cubic meters.

Due to the tight gas sands, located in the north and south of that field and the connection to the field Lauterbach, the model has to be very complex and is difficult to match. The tight sands and the connected gas field to the west cause a very untypical behaviour for the depletion drive reservoir in the years after 1998. The main problem is to assess the volume and transmissibility of the tight reservoir areas, which are delivering gas to the more permeable zones. The outer zones are represented by the additional tanks on the upper and lower end of Figure 4.8 and contain a total volume of about 60 million Sm^3. The pressure points of Lauterbach are also matched. Communication between Berndorf and Lauterbach sands exists either along a major fault north of LAUT-004 or due to on-lap deposited sands, connecting both reservoirs with each other. Based on formation tester data there are at least 4 layers with different pressures in LAUT-004, but due to their less size they are comingled

together into the tanks A2L55-60 and A2L55-65. The history match shows a gas flux from Lauterbach to Berndorf of about 11 million Sm³.

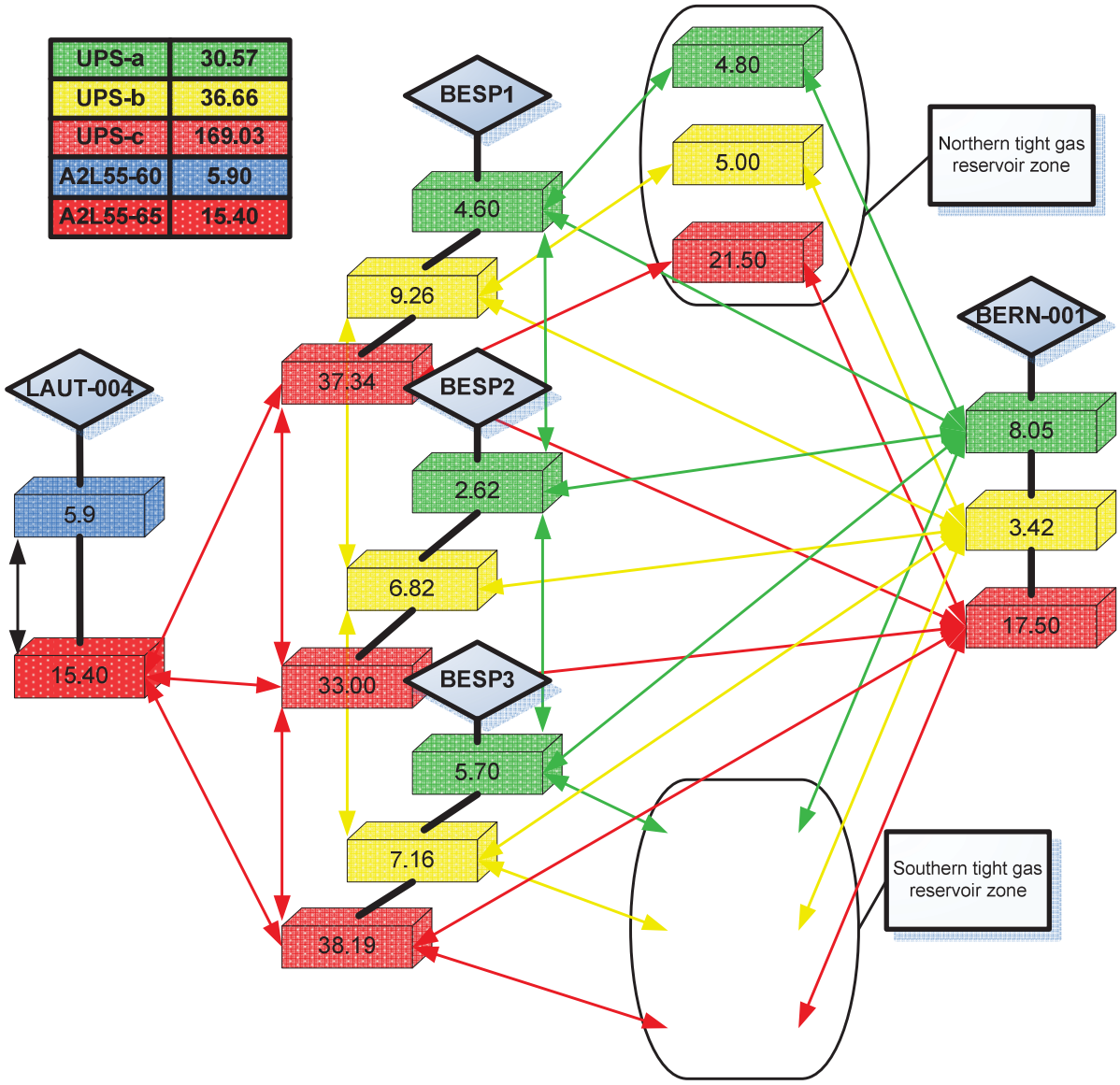

Figure 4.8: Set up multi-tank system in MBAL® representing all reservoir layers of Berndorf and Lauterbach. A colour code helps to identify the 5 different horizons. All equally coloured connections are indicating only communication within the dedicated layers.

The Berndorf tanks contain a total volume of 236.26 million Sm³. For the well BERN-001 also a prediction over production period is carried out. Unfortunately it is not possible to match the production for the lower two sands in BERN-001 exactly (Figure B.8, Figure B.9). The volume distribution of the Berndorf MBAL® model is listed in Appendix B.

4.5. Berndorf UGS Wells

To get appropriate permeability data for the prospected horizontal UGS wells BESP1 – BESP3, artificial logs are created out of the PETREL® static reservoir model. The planned wells perforate all three UPS layers. Therefore IPR curves are calculated for each layer to operate the MBAL® prediction model. Unfortunately the PROSPER® multi-lateral model is not applicable for highly deviated wells. For that reason the Babu-Odeh model is used to get proper inflow values and the multilateral-model is used to split up the IPRs in the appropriate relationship. Afterwards the results are loaded into the MBAL® model.

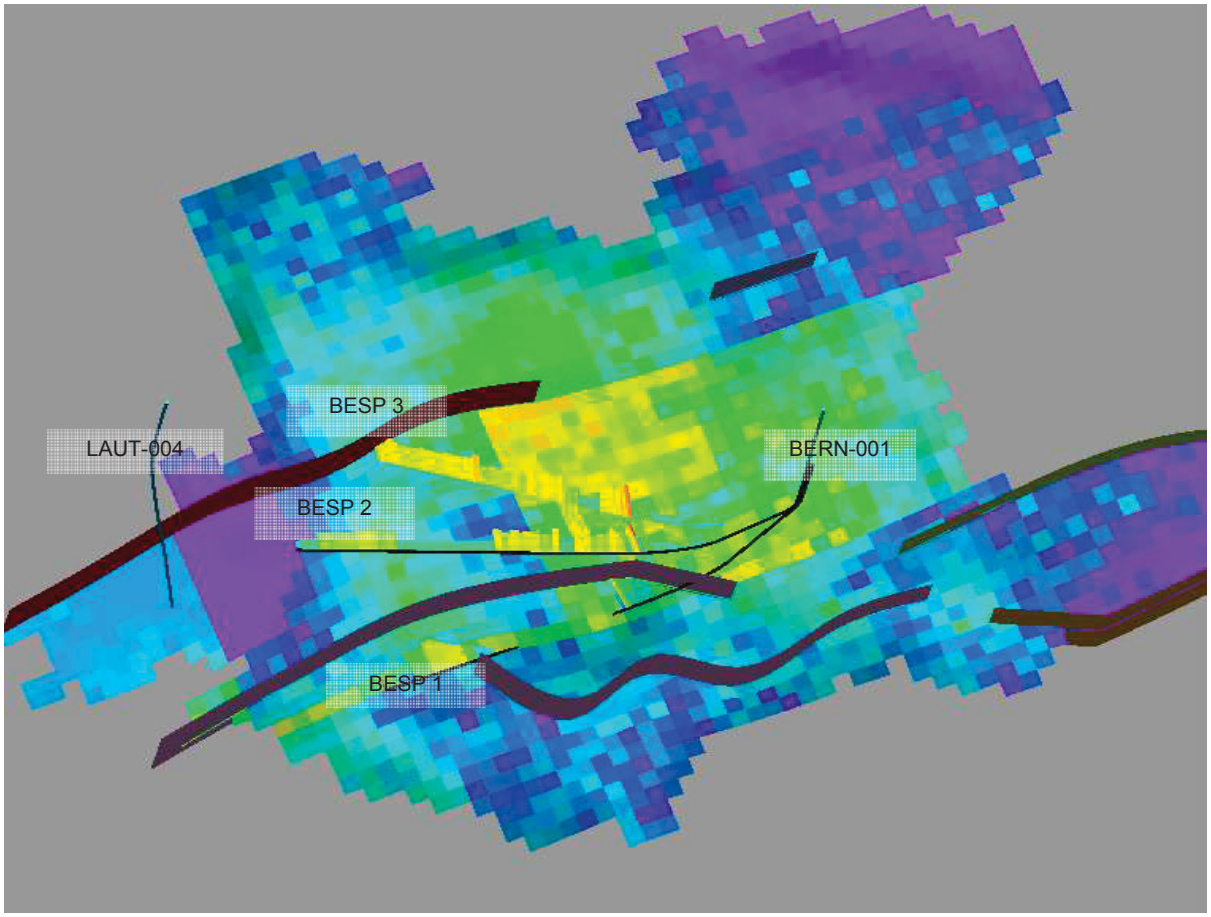

Figure 4.9: The three prospected horizontal UGS wells are drilled towards the lauterbach reservoir, which is in communication with Berndorf reservoir. Several normal faults strike in NE-SW direction. BESP1 is planned to intersect a normal fault to reach the reservoir compartment located between two normal faults.

To save investment costs the questions of a smaller tubing size and shorter wells are coming up. Therefore all Berndorf simulation runs are carried out for a 7 inch and a 5.5 inch completion. To assess the influence of well length on Berndorf UGS performance a new parameter called “effective well length” is introduced. This factor, which is multiplied with the

perforation length of the artificial logs (Appendix B), reduces the well length within the permeable zones. It ranges between 0 and 1. Due to the uncertainty of the reservoir parameters between the well LAUT-004 and BERN-001 (distance 1.2 km) it can be possible that the real reservoir is not very similar to the model.

The Berndorf reservoir is very similar to the UGS Puchkirchen sands. The experience of drilled skin factors in Puchkirchen averages about factor 10. For the calculation of the Babu-Odeh IPR models in PROSPER® the ratio of vertical to horizontal permeability was set onto 0.001.

UGS Well BESP 1

The UGS well BESP 1 is planned to drain the area between two faults in the southern part of the reservoir. The faults cannot yet be identified as sealing or not, but in the case of compartmentalization, this zone would be rather isolated. The artificial log data, the completion data and the well path are shown in Appendix B.

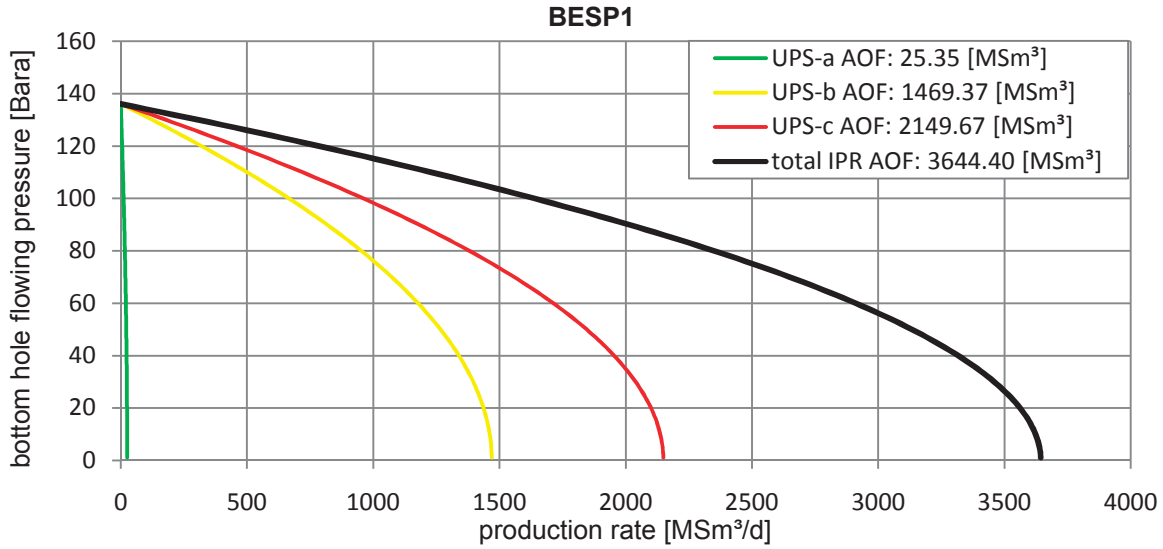

Figure 4.10: IPRs of well BESP1, calculated with multi-lateral and Babu-Odeh inflow model

UGS Well BESP 2

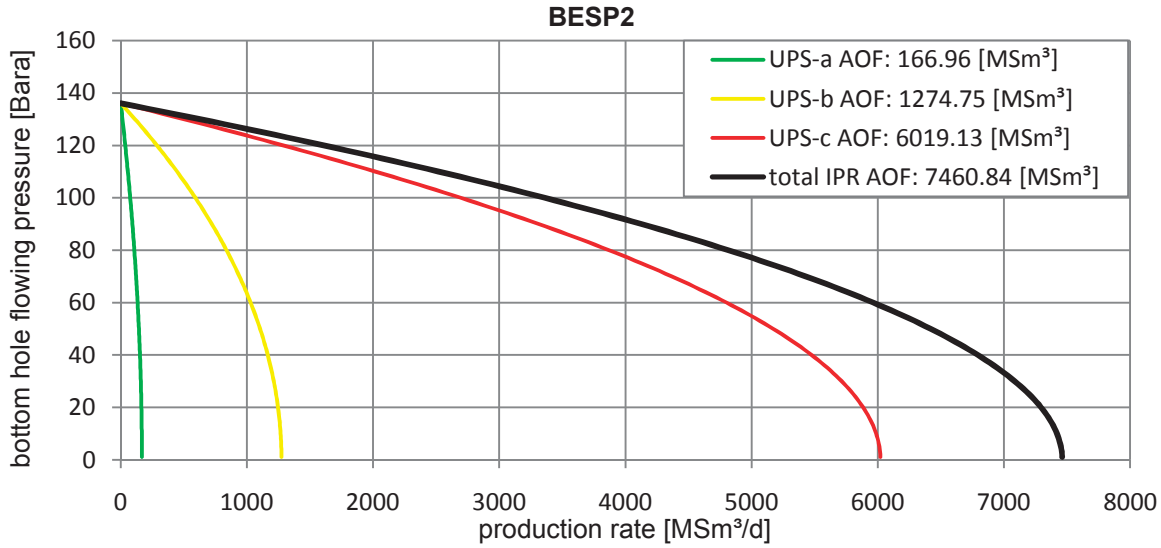

Figure 4.11: IPRs of well BESP2, calculated with multi-lateral and Babu-Odeh inflow model

BESP 2 is planned to penetrate the reservoir within the zone of the highest initial gas distribution (Figure 4.4, Figure 4.9). The well heel is supposed to be in the area of BERN-001. Permeability and completion data are listed in Appendix B.

UGS Well BESP 3

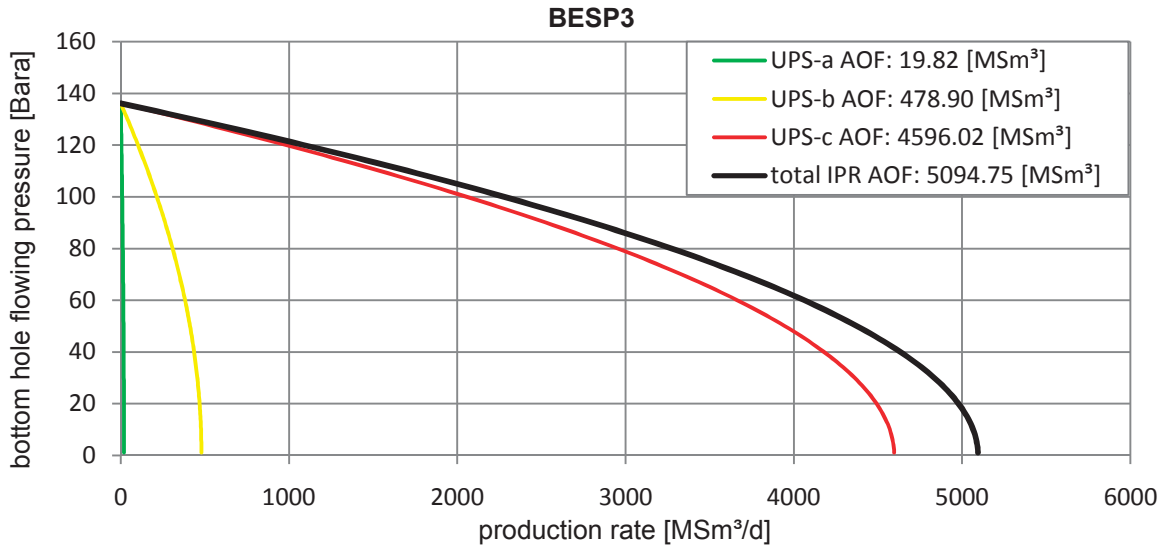

Figure 4.12: IPRs of well BESP3, calculated with multi-lateral and Babu-Odeh inflow model

The well BESP 3 is planned to penetrate the reservoir northern of BESP 2 to intersect the zone of the highest initial gas distribution (Figure 4.4, Figure 4.9). The well heel is supposed to be in the area of BERN-001. Permeability and completion data are listed in Appendix B.

4.6. Berndorf MBAL multi-tank Prediction Model

After the successful history match of the Berndorf multi-tank model, the three UGS wells are implemented into MBAL®. With the help of the OPENSERVER® commands it is possible to investigate the influence of the reduced well length, different skin effects and several production profiles on reservoir performance.

Three different production profiles with various end rates are selected.

The following scenarios have been calculated for UGS Berndorf:

- 5.5 inch completion size
  - Skin 0
  - Skin10
  - Skin20

- 7 inch completion size
  - Skin 0
  - Skin10
  - Skin20

5. Underground Gas Storage Nußdorf

During the late Oligocene, stronger tectonic activities in the south caused a rise of the alpine hinterland. This rise caused intensified erosion and thus an increased sediment entry into the neighbouring deep-marine sediment basins. In the area of Nußdorf reservoir, the deposit of these sediments took place in form of turbidites and mass streams, stretched out in SE – NW direction. Analyses of 3D-seismic data and their attributes show several delivery areas along the southeast delimitation of the reservoir. The increased tectonic activity caused not only the rise of the hinterland, but re-activated also the thrust of the sheds underneath the basin. Thus, the front of these deposits was gradually shifted and became unstable. Those slope sediments were then deposited into the basin. These mass movements were released by tectonic events. This process was repeated several times in the area of Nußdorf reservoir. The basin was finally tilted into NW direction caused by tectonic thrust from downside and from the hinterland.

The raw material of the debris streams came from sand-rich helvetian sheds. The deposit of this material took place along the whole front of the sheds. In the case of reservoir Nußdorf this happened from SE direction. The mass movements (turbidites and debris flow) consist mainly of central to coarse-grained sandstones with partially large clastic material of clay marl and carbonates. Since the grains and the clastic material show a bad roundness degree, the origin of the material must be very close. Both events, the deposit of the turbidites and the debris stream along the SE front of the sheds, took place temporally close to each other. Therefore a mixture from both deposit forms was found in the cores of the wells Nußdorf west 1, -4, -6, -7, -8 and 9. However, the petro physical parameters in the two deposit mechanisms are very similar. The entire gas field of Nußdorf possesses a SW-NE longitudinal extension of approximately 7 km and a maximum width of about 1.6 km. The net sand thicknesses ranges between 20 m and 60 m. Altogether 4 superimposed gas bearing horizons with partial limited vertical communication are interpreted with the help of LOG and production data (A3N08/1; A3N10/1, A3N20-30/1; A3N40/1). The most important gas bearing horizon is, due to its high amount of initial gas volume, the horizon A3N20-30/1. Pressure measurements confirm vertical communication between the small horizons of the A3N20-30/1 layer package. In the gas field Nußdorf altogether ten wells were drilled. All prospected storage horizons were encountered in different attitudes.

Gas field Nußdorf was found in the year 2000 by the well NUSS-W-001, which intersected 37.5 m of gas bearing sandstone. In the same year the well NUSS-W-002 was drilled about 950 m south of the first well. A net gas sand thickness of 23.7 m was encountered. In the following years eight additional wells were drilled to produce the different gas bearing layers of Nußdorf reservoir.

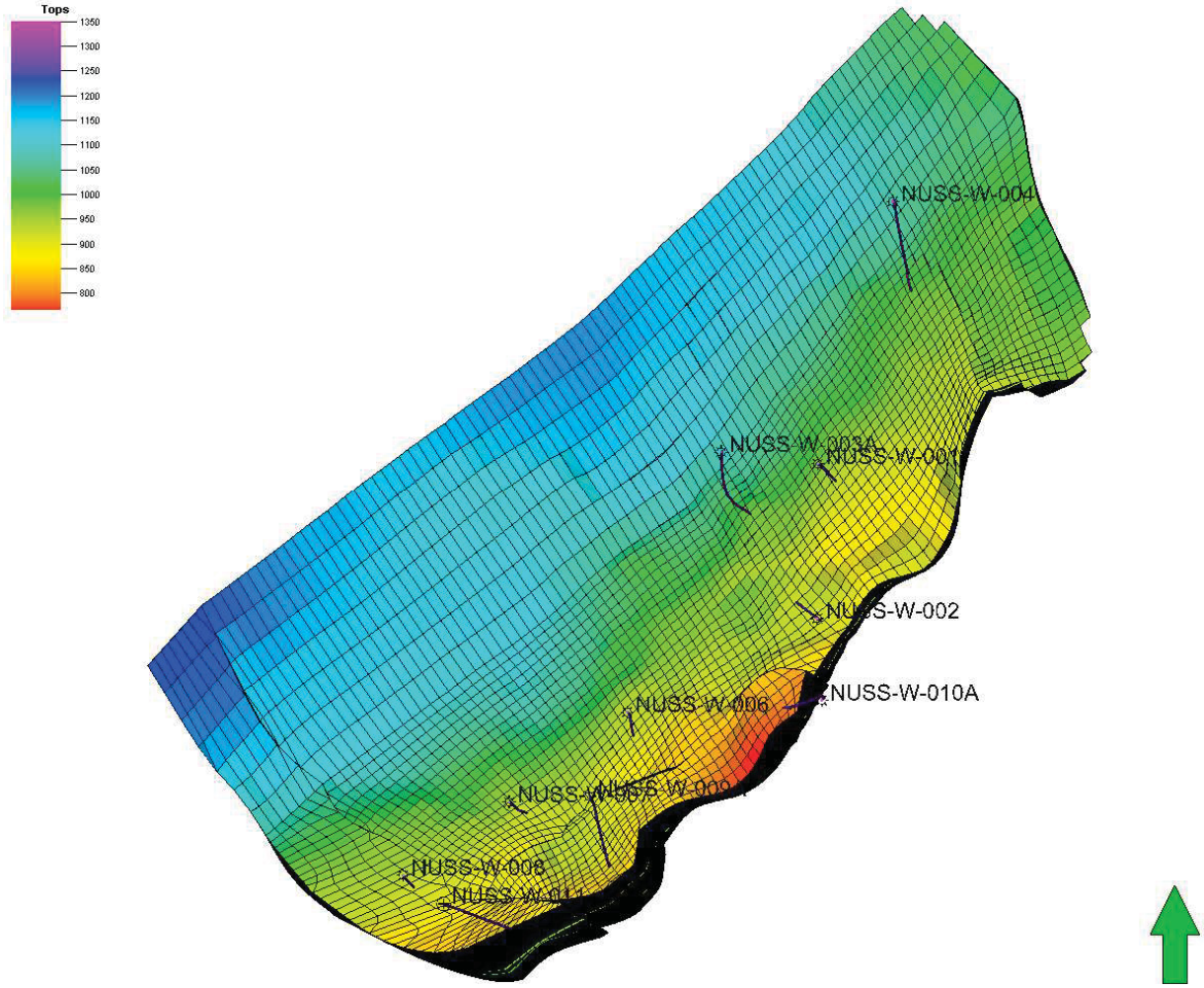

Figure 5.1: The simulation grid of the field Nußdorf is viewed from south direction showing the reservoir top in m-SS.

Altogether from the first drilled well in the year 2000 to the end of the year 2007, natural gas in the amount of 913 million normal cubic meters was produced. The reservoir pressure was lowered from initially 152 Bara to approximately 32 Bara in the north and to 80 Bara in the southern range. The pressure development during production indicates an expansion regime, without clear influence of aquifer. In the lowest gas bearing horizon A3N40/1 water influx was determined during production, indicating aquifer drive mechanism. This horizon is isolated from the upper reservoir thus this horizon is excluded from storage activity. (Rohöl Aufsuchungs AG, 2009)

Figure 5.2: Ten production wells and six prospected storage wells are intersecting Nußdorf reservoir. The storage wells are planned to be drilled from two cluster well sites.

5.1. PVT and Fluid properties

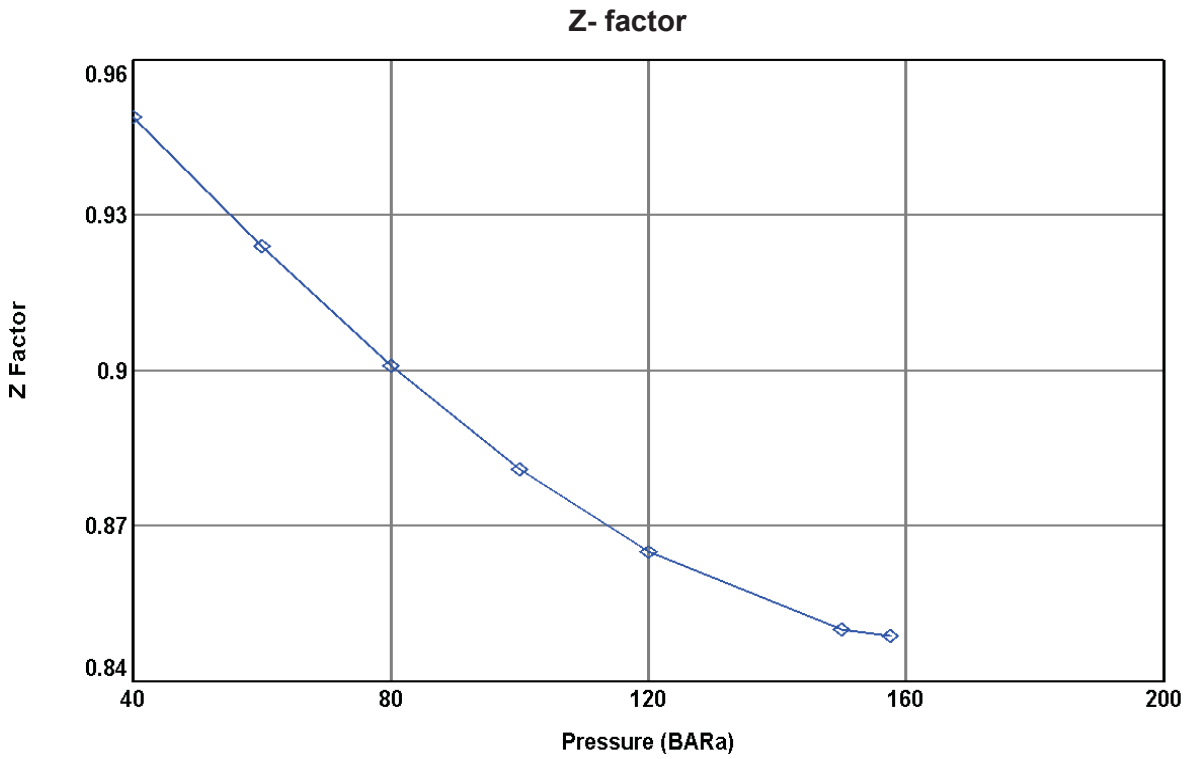

Figure 5.3: Z-factor plotted versus pressure

The gas properties for use in the material balance simulation model were computed based on a gas gravity of 0.5626, reservoir temperature of 48 ℃, N2 of 0.830 Mole % and CO2 of 0.130 Mole %. In PROSPER and MBAL the viscosity correlation after Lee et al is used. Formation water salinity is about 15000 ppm.

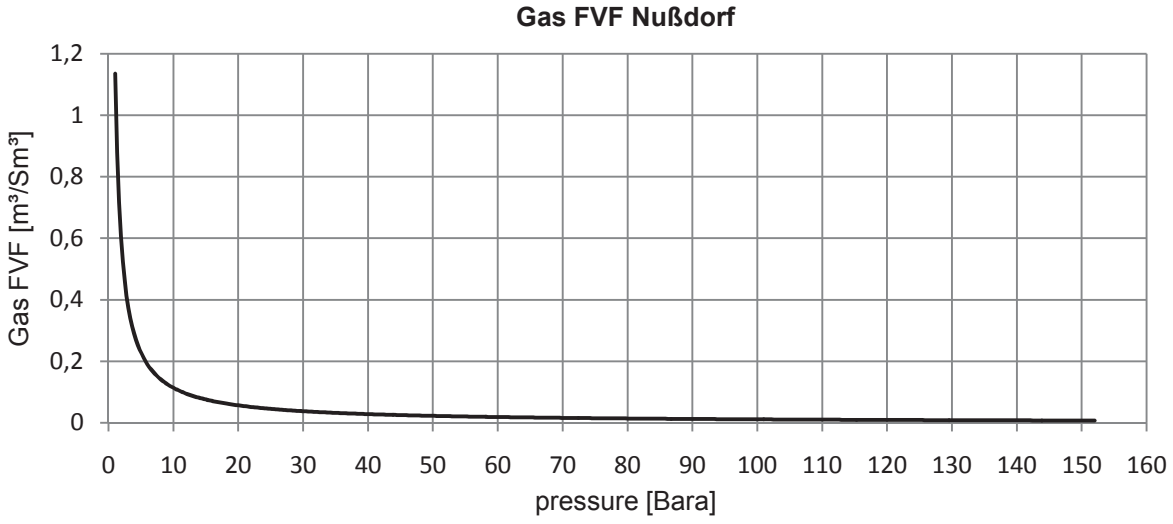

Figure 5.4: Gas formation volume factor plotted versus pressure

5.2. Relative permeability

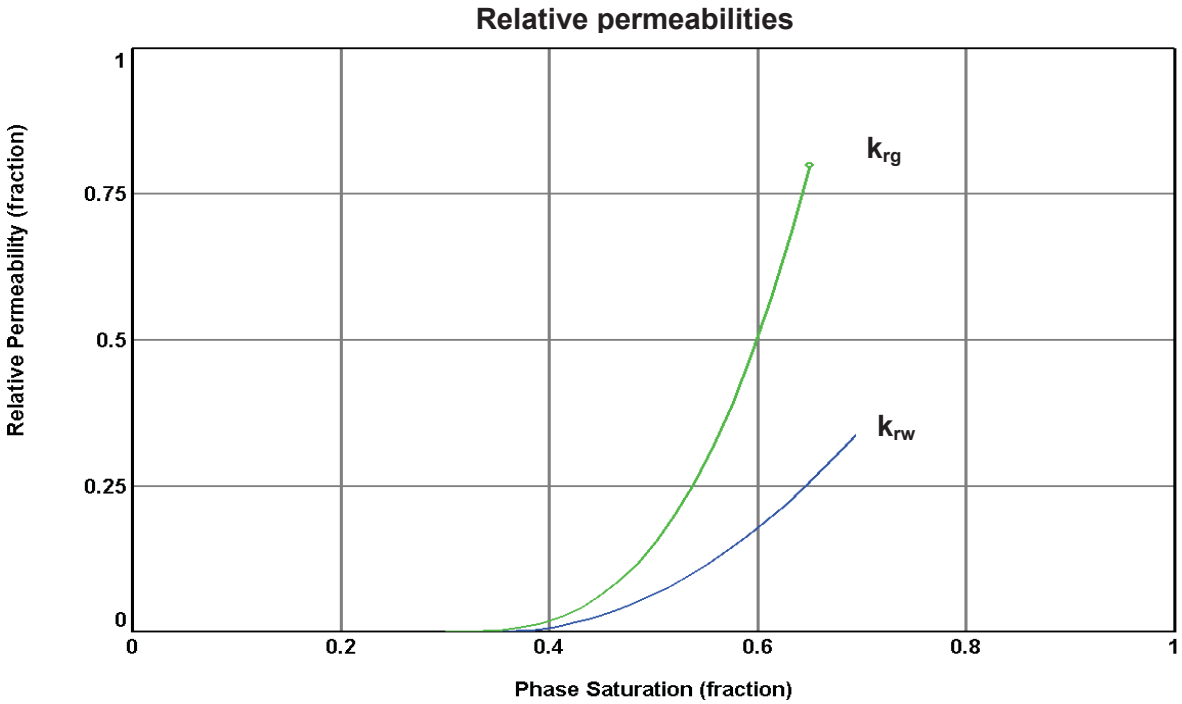

Figure 5.5: Relative permeability curves of the MBAL® Nußdorf reservoir model. The blue curve describes the relative permeability of water dependent on the water saturation. The green curve characterizes the relative permeability of the gas phase plotted versus gas saturation.

5.3. Nußdorf MBAL multi-tank model history match

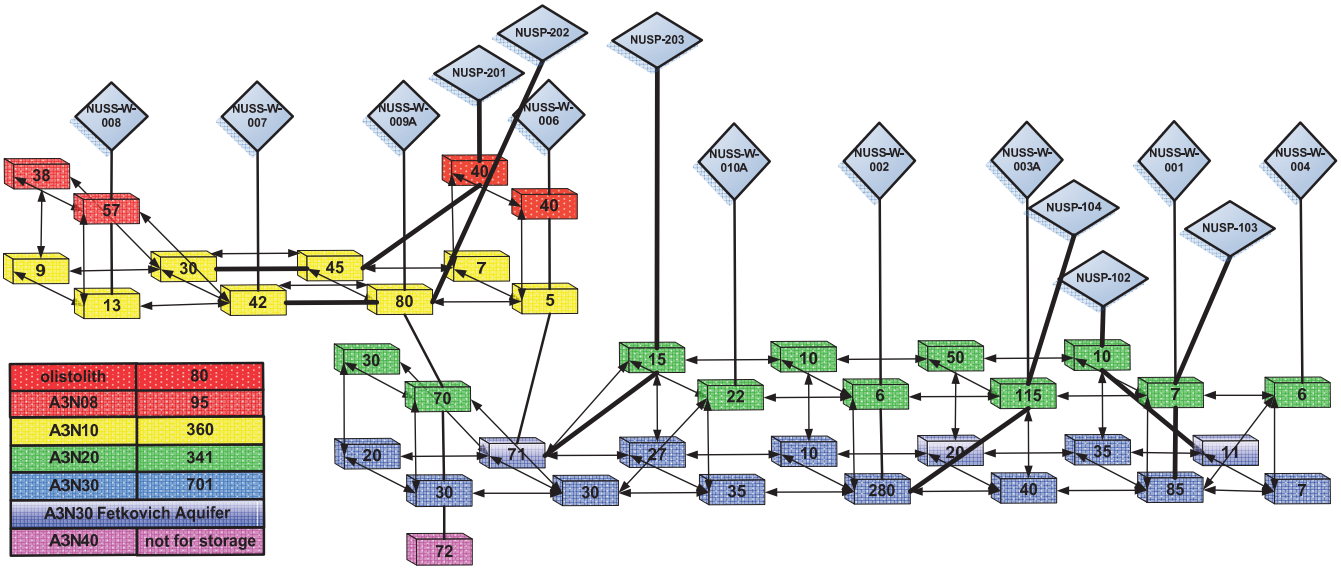

Figure 5.6 Set up multi-tank system in MBAL® representing all important reservoir layers of Nußdorf. A colour code helps to identify the 5 different horizons. The trajectories of the production wells are pictured with thin black lines. The well paths of the storage wells are labelled with thick lines. Within the A3N30 horizon an aquifer is encountered. Three Fetkovich aquifer tank models are implemented to simulate the water influx along the water gas contact.

The multi-tank model of UGS Nußdorf contains 37 tanks with a total amount of 1448 MMSm³, which are connected to each other. Three tanks of the A3N30 horizon are containing Fetkovich aquifer models. It is assumed that due to the big dimensions of the encountered aquifer small water inflow occurs, even if the material balance plot is only showing depletion drive (Rohöl Aufsuchungs AG, 2009). The production history of the wells and the quality of the history match in the particular tanks are mentioned in Appendix C.

The properties of the linear Fetkovich aquifer models are:

Tank	k_a	L_a	J
	[md]	[m]	[m³/d bar]
NW3a-A3N30	27	500	1.4
NW4-A3N30	2.5	250	0.008
NW6A3N20-30	19.5	750	1

Table 5.1: properties of the applied aquifer models in the particular tank

5.4. Nußdorf UGS Wells

The Nußdorf UGS will be drilled from two cluster sites. NUSP 102, -103, 104 are prospected from the northern site, intersecting the northern area of the A3N20 and A3N30 horizon near the producers NW-003a, NW-002 and NW-001. NUSP 201, -202 and 203 are drilled from the southern site. NUSP 201 and NUSP 202 are penetrating the horizons A3N08 and A3N10 in the near area of the producers NW-007, NW-009a and NW-006. NUSP 203 is prospected to encounter the A3N20 and A3N30 horizons in the area of NW-010 and NW -006.

UGS well NUSP-102

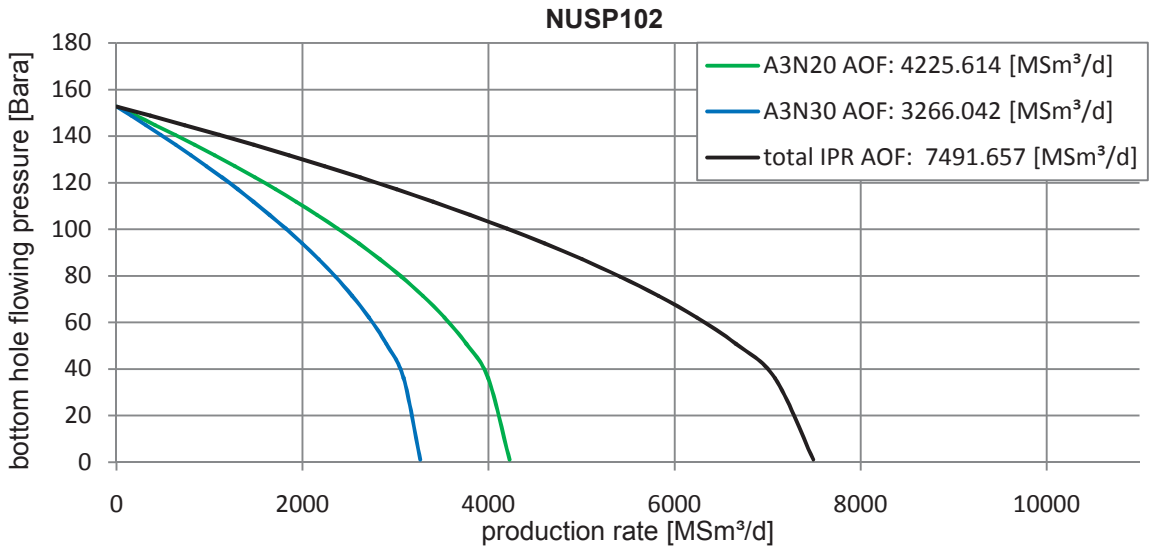

Figure 5.7 IPRs of well NUSP 102, calculated with multi-lateral and Babu-Odeh inflow model plotted bottom hole flowing pressure versus production rate.

UGS well NUSP-103

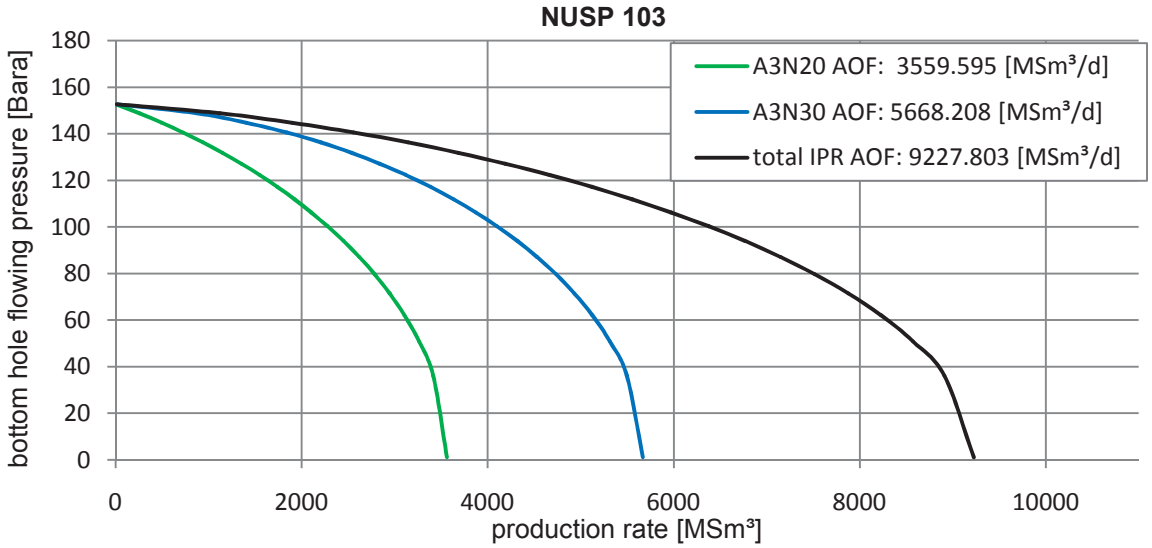

Figure 5.8: IPRs of well NUSP 103, calculated with multi-lateral and Babu-Odeh inflow model plotted bottom hole flowing pressure versus production rate.

UGS well NUSP-104

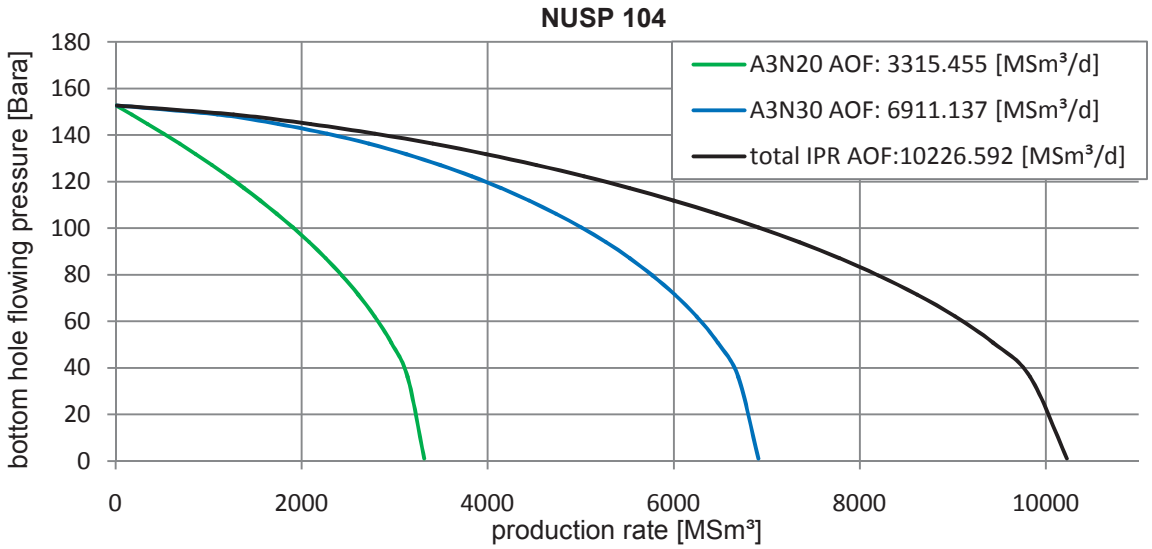

Figure 5.9: IPRs of well NUSP 104, calculated with multi-lateral and Babu-Odeh inflow model plotted bottom hole flowing pressure versus production rate.

UGS well NUSP-201

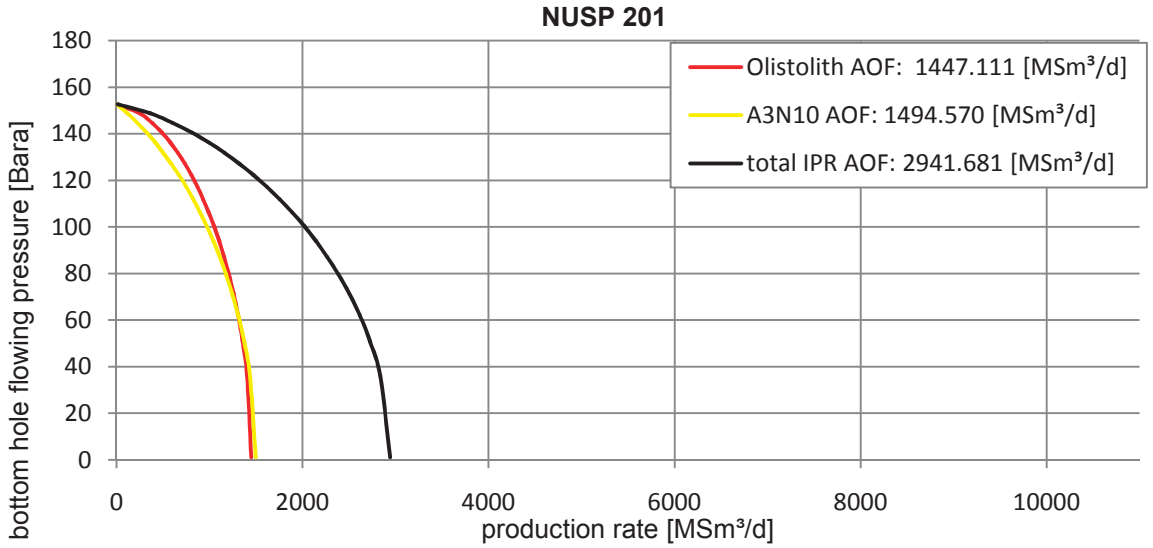

Figure 5.10: IPRs of well NUSP 201, calculated with multi-lateral and Babu-Odeh inflow model plotted bottom hole flowing pressure versus production rate.

UGS well NUSP-202

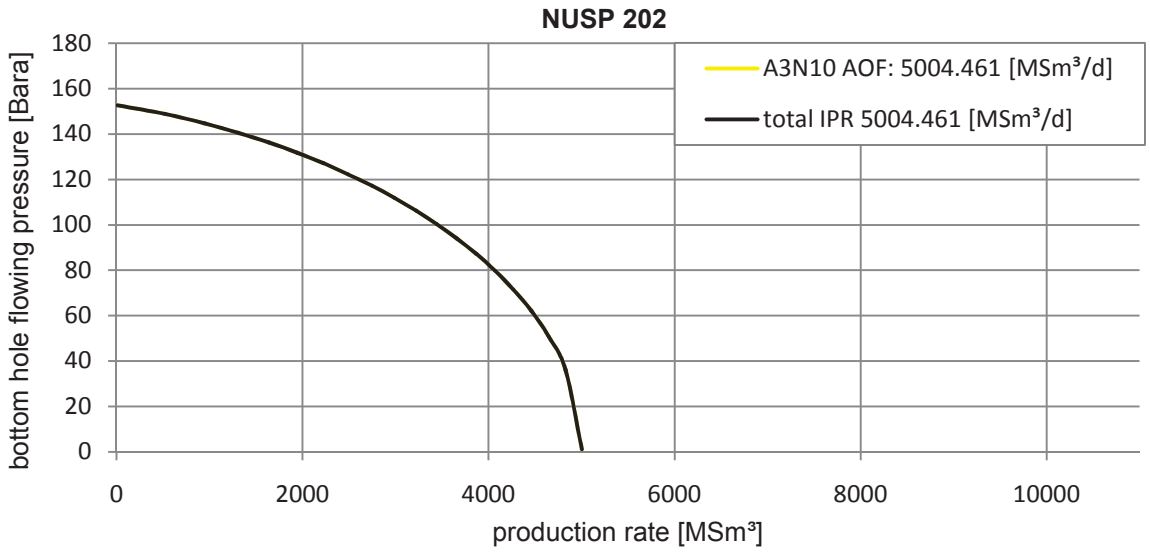

Figure 5.11: IPRs of well NUSP 202, calculated with multi-lateral and Babu-Odeh inflow model plotted bottom hole flowing pressure versus production rate.

UGS well NUSP-203

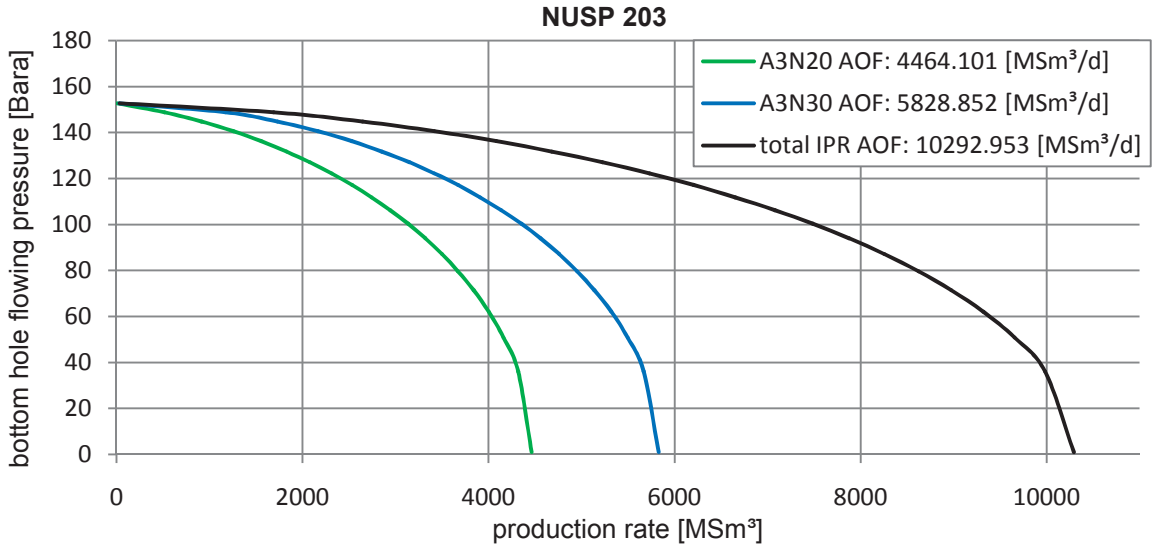

Figure 5.12: IPRs of well NUSP 203, calculated with multi-lateral and Babu-Odeh inflow model plotted bottom hole flowing pressure versus production rate.

6. Results

6.1. Results for UGS Zagling

Estimation of maximum turnover volume and comparison of original and alternative trajectory development scenario

Due to experiences during operation of the underground gas storage installation Haidach it is assumed that a production scenario of a skin value of 30 is most probable.

summary of prediction cases 1 and 2											
case	wells	path	skin	THP	profile	start rate	end rate	TOV		cushion gas	
				[bara]		[1000Sm³/d]	[1000Sm³/d]	[MMSm³]	[MMNm³]	[MMSm³]	[MMNm³]
1	ZASP1-a		30	30.02	25%	6085.31	1521.33	**486.8**	**461.5**	**226.2**	**214.5**
	ZASP2	orig.									
	ZASP3	orig.									
	ZASP4	orig.									
2	ZASP1-a		30	30.04	25%	6046.68	1511.67	**483.7**	**458.6**	**229.3**	**217.4**
	ZASP2	alt.									
	ZASP3	alt.									
	ZASP4	alt.									

Table 6.1: Results of MBAL® prediction runs case 1 and case 2, with the posterior modified well path of ZASP1-a, comparing the development scenarios original and alternative.

summary of prediction cases 3 and 4											
case	wells	path	skin	THP	profile	start rate	end rate	TOV		cushion gas	
				[bara]		[1000Sm³/d]	[1000Sm³/d]	[MMSm³]	[MMNm³]	[MMSm³]	[MMNm³]
3	ZASP1		30	30,05	25%	6237.18	1559,33	**498,0**	**472,2**	**215,0**	**203,8**
	ZASP2	orig.									
	ZASP3	orig.									
	ZASP4	orig.									
4	ZASP1		30	30,02	25%	6150,68	1537,67	**492,0**	**466,5**	**221,0**	**209,5**
	ZASP2	alt.									
	ZASP3	alt.									
	ZASP4	alt.									

Table 6.2: Results of MBAL® prediction runs case 3 and case 4, with the already modified well path of ZASP1, comparing the development scenarios original and alternative. Case 3 is showing the highest calculated TOV.

Estimation of the best-performing production schedule

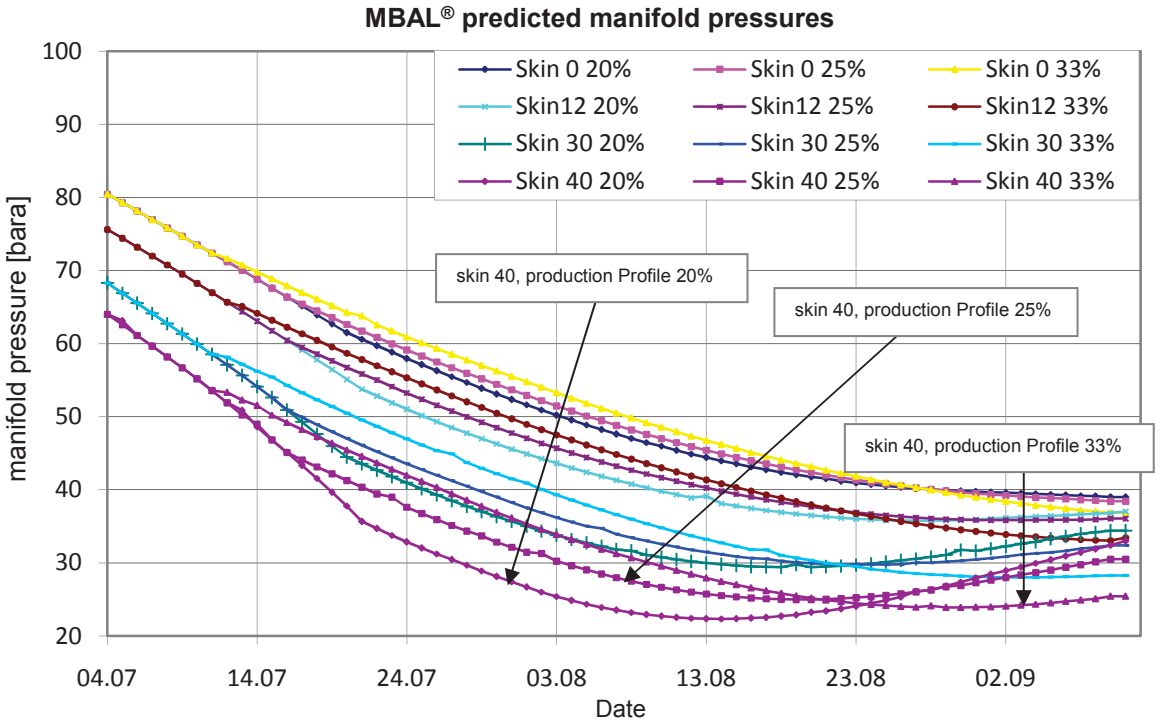

Figure 6.1: Zagling MBAL® predicted manifold pressures with equal initial field rates, plotted versus production time. The production schedules 20%, 25% and 33% are compared, regarding skin factors ranging from 0 to 40. The production case with skin factor 40 is pointed out for further discussion.

Sensitivity analyses on the parameter skin factor

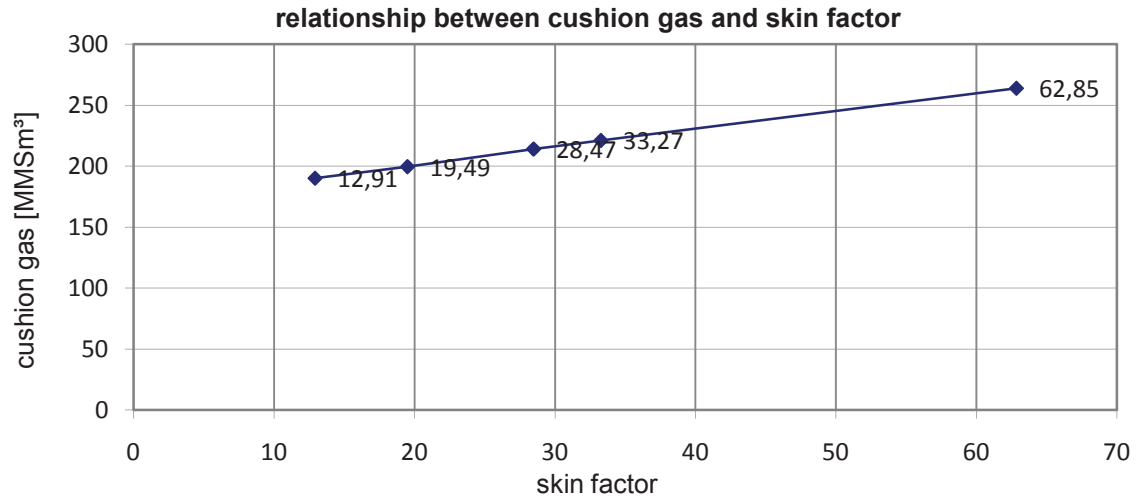

Figure 6.2: The amount of needed cushion gas, calculated by the MBAL® prediction model, is plotted versus skin factor. The calculated skin scenarios are labelled in the graph.

Comparison of the findings of this thesis with the results of the ECLIPSE 100® reservoir simulator

summary of prediction cases 1 and 2											
case	wells	path	skin	THP	profile	start rate	end rate	TOV		cushion gas	
				[bara]		[1000Sm³/d]	[1000Sm³/d]	[MMSm³]	[MMNm³]	[MMSm³]	[MMNm³]
1	ZASP1-a		30	30.02	25%	6085.31	1521.33	486.8	**461.5**	226.2	**214.5**
	ZASP2	orig.									
	ZASP3	orig.									
	ZASP4	orig.									
2	ZASP1-a		30	30.04	25%	6046.68	1511.67	483.7	**458.6**	229.3	**217.4**
	ZASP2	alt.									
	ZASP3	alt.									
	ZASP4	alt.									

Table 6.3: Results of MBAL® prediction runs case 1 and case 2, with the posterior modified well path of ZASP1-a, comparing the development scenarios original and alternative.

summary of prediction cases calculated by ECLIPSE 100®							
case	storage wells	minimum THP	TOV	cushion gas		cushion / TOV	remarks
				volume	pressure		
		[bara]	million Nm³	million Nm³	[bara]		
1	4 horizontal	30	486.6	185.8	39	0.38	reduced PI
1a	4 horizontal	30	498.6	174.3	36	0.35	
2	4 horizontal	30	478.5	193.7	40	0.40	reduced PI
3	4 deviated	30	**451.0**	**219.1**	46	0.49	
3a	4 deviated	30	433.5	240.1	49	0.55	

Table 6.4: Results of different development scenarios of the ECLIPSE100® simulation. Case 3 is comparable with case 1 of the MBAL® prediction runs. (HOT Engineering, 2007)

6.2. Results for UGS Berndorf

Estimation of the turn over volume and best-performing production schedule

Due to experiences during operation of the underground gas storage installation Puchkirchen it is assumed that a production scenario of a skin value of 10 is most probable.

Summary of prediction case Berndorf											
Case	Wells	Effective well length	Skin	THP [Bara]	Profile	initial rate [1000Sm³/d]	fina rate [1000Sm³/d]	TOV [MMSm³]	TOV [MMNm³]	Cushion Gas [MMSm³]	Cushion Gas [MMNm³]
1	BESP1	1	10	30,025	**25%**	1395,21	348,8	**111,9**	**105,9**	**79,5**	**75,2**
	BESP2	1									
	BESP3	1									

Table 6.5: Results of the MBAL® prediction run, showing the highest estimated TOV and best-performing production scenario for Berndorf reservoir with the most probable skin situation.

Sensitivity analyses on the parameter skin and effective well length and estimation of its influences on turnover volume

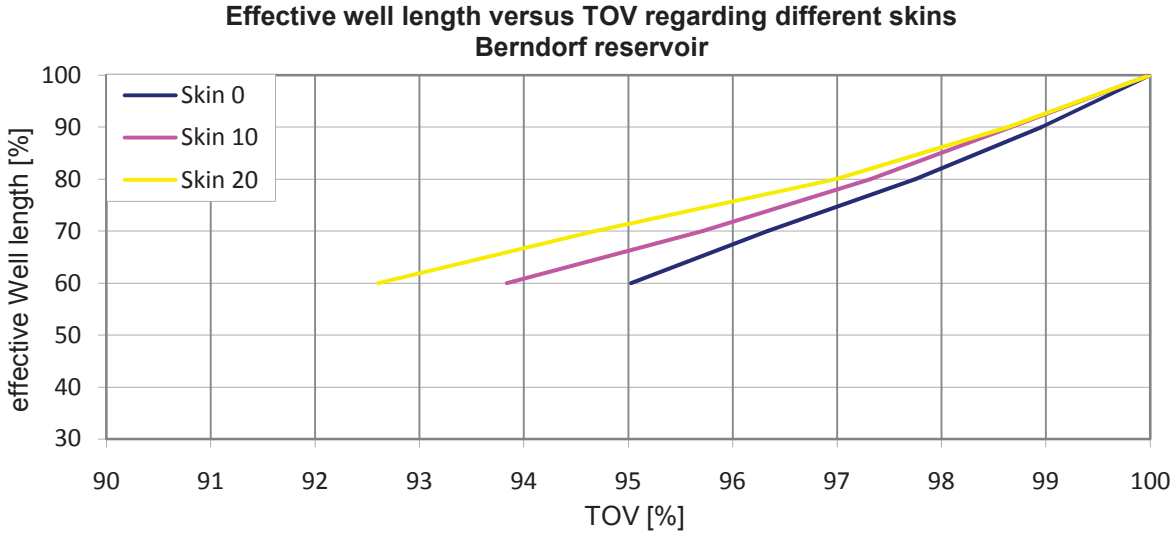

Figure 6.3: The effective well length is plotted versus percentage of reduced turnover volume, starting form base case: TOV of Skin 0; effective well length 1 (upper right corner). Different skin situations are compared.

Comparison of the development scenarios 7 inch tubing and 5.5 tubing

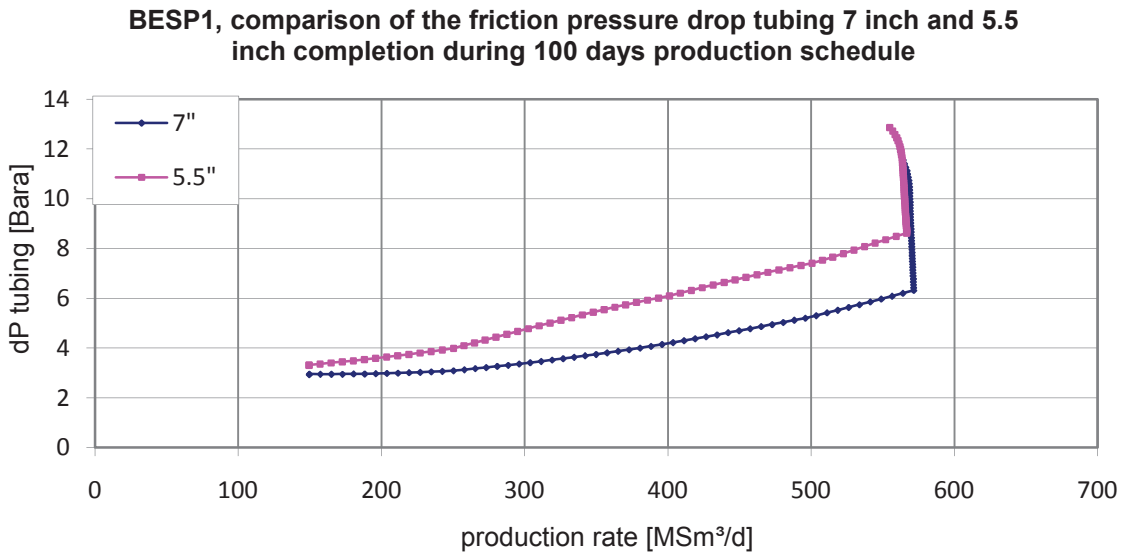

Figure 6.4: BESP 1; Comparison of the friction pressure drop between a 7 inch and 5.5 inch tubing during 100 days production. The tubing pressure drop is plotted versus well production rate.

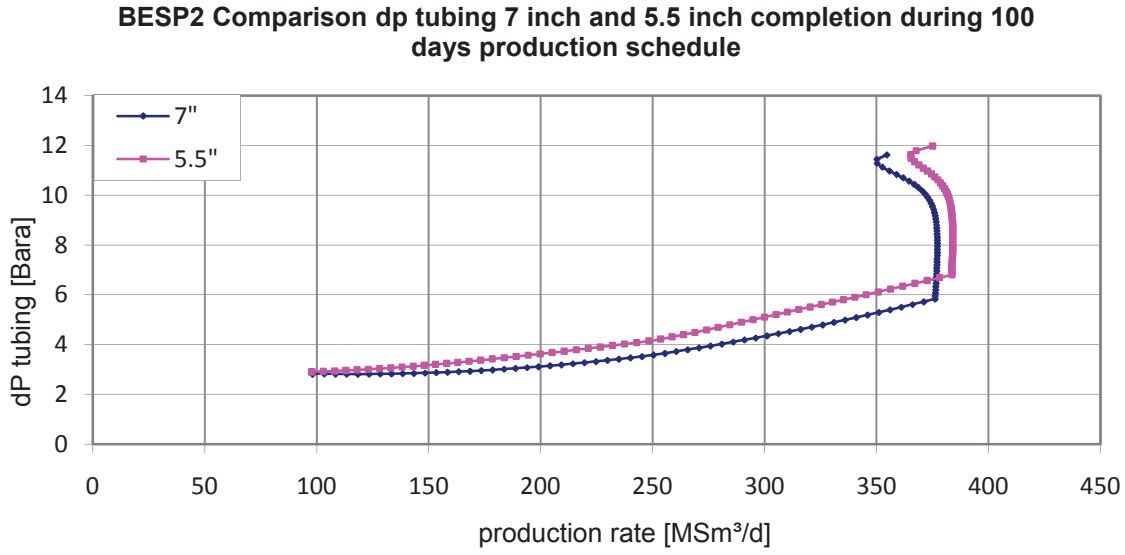

Figure 6.5: BESP 2; Comparison of the friction pressure drop between a 7 inch and 5.5 inch tubing during 100 days production. The tubing pressure drop is plotted versus well production rate.

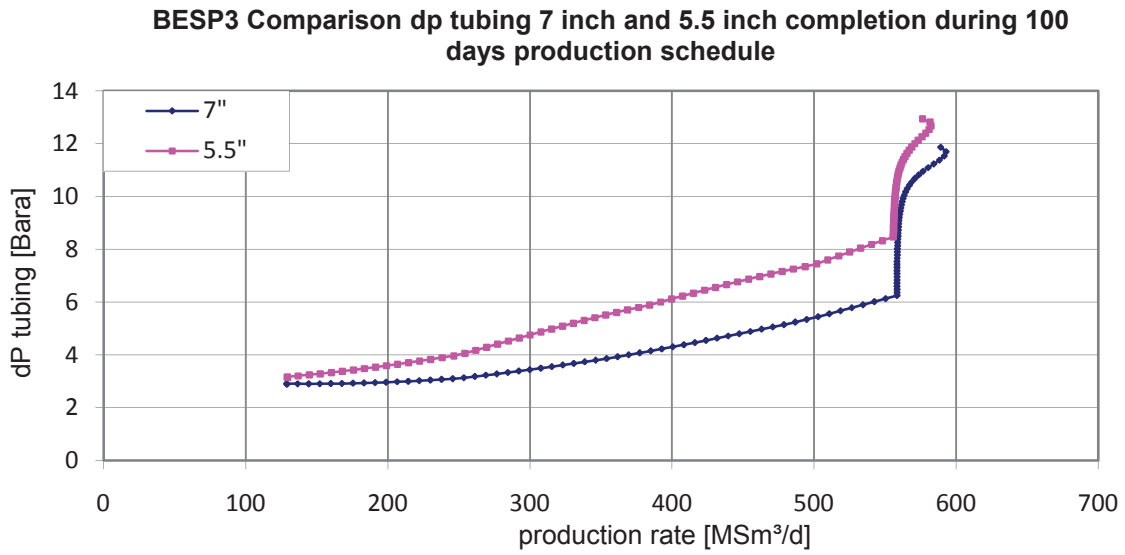

Figure 6.6: BESP 3; Comparison of the friction pressure drop between a 7 inch and 5.5 inch tubing during 100 days production. The tubing pressure drop is plotted versus well production rate.

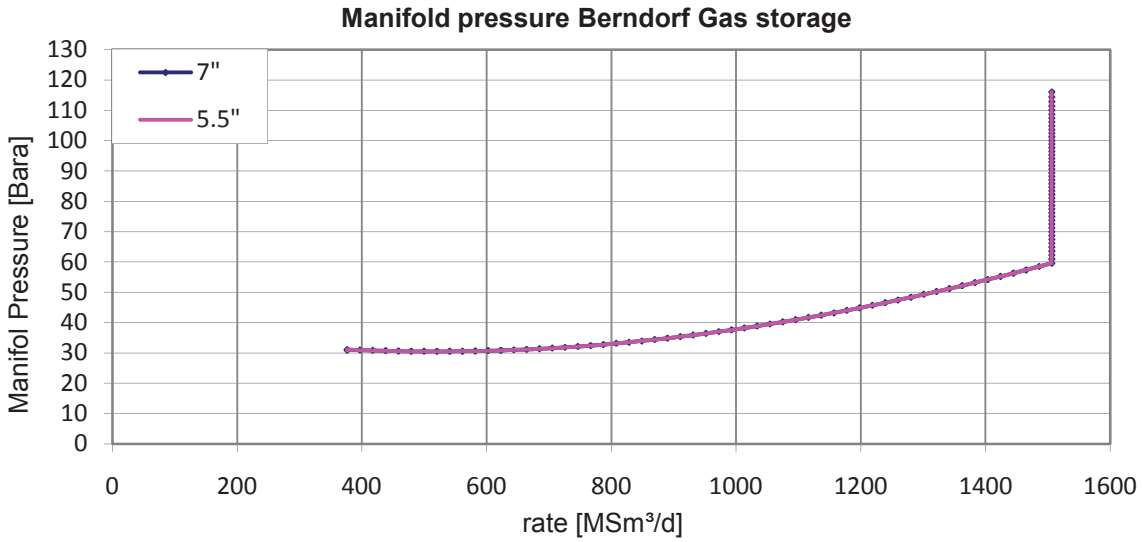

Figure 6.7: Comparison of the manifold pressures of 7 inch and 5.5 inch tubing, installed in all three wells, during 100 days production schedule. The manifold pressures are plotted versus total field production rate.

Comparison of the findings of this thesis with the results of the ECLIPSE 100® reservoir simulator

Summary of prediction case Berndorf											
Case	Wells	Effective well length	Skin	THP [Bara]	Profile	initial rate [1000Sm³/d]	fina rate [1000Sm³/d]	TOV [MMSm³]	TOV [MMNm³]	Cushion Gas [MMSm³]	Cushion Gas [MMNm³]
1	BESP1	1	10	30,025	25%	1395,21	348,8	111,9	**105,9**	79,5	**75,2**
	BESP2	1									
	BESP3	1									

Table 6.6: Results of the MBAL® prediction run, showing the highest estimated TOV for Berndorf reservoir with the most probable skin situation.

Summary of prediction cases Berndorf calculated by ECLIPSE 100®					
Case	Plateau Rate	TOV	Injected Cushion Gas	Wells	Remarks
	[Nm³/d]	[MMNm³]	[MMNm³]		
2	1.433.000	**114,6**	**65,5**	BESP-001, -002 & -003	Skin=10
3	1.492.000	119,4	63,8	BESP-001, -002 & -004	Skin=10
4	1.285.000	102,8	78,3	BESP-001& -003	Skin=10

Table 6.7: Results of different development scenarios of the ECLIPSE100® simulation. Case 2 is comparable with case 1 of the MBAL® prediction runs. (HOT Engineering, 2007)

6.3. Results for UGS Nußdorf

Turn over volume and best-performing production schedule

Result summary for UGS Nußdorf										
case	wells	skin	THP [bara]	profile	start rate [1000Sm³/d]	end rate [1000Sm³/d]	TOV [MMSm³]	TOV [MMNm³]	cushion gas [MMSm³]	cushion gas [MMNm³]
1	NUSP 102	0	30.73	30%	8360.00	2508.00	629.49	664.06	818.51	863.46
	NUSP 103									
	NUSP 104									
	NUSP 201									
	NUSP 202									
	NUSP 203									

Table 6.8: Results of the MBAL® prediction runs for the prospected Underground gas storage Nußdorf.

7. Discussion

7.1. Interpretation of the results for UGS Zagling

Estimation of maximum turnover volume and comparison of original and alternative trajectory development scenario

The statistical investigation of the already drilled wells of underground gas storage Haidach shows a skin value of 30 as the most probable upcoming situation. Therefore the maximum turnover volume is estimated for this scenario. A production profile with a linear decline, after passing the initial production field rate, and an ending rate of 25% of the initial rate, delivers the highest turnover volume for the calculated cases.

The production scenario with the improved well path of ZASP 1, which is planned to intersect the reservoir in the near ZAG-001 drainage area, is most promising. The improvement of the inflow situation of this well brings an increase of about 11 MMNm³ in turnover volume.

Drilling wells with steeper trajectories, which are intersecting the Zagling reservoir at the same spots like the originally planned wells is decreasing the turnover volume in the range of 3MMNm³ to 5 MMNm³. But due to the total saved well path of about 280m this alternative is recommended.

Estimation of the best-performing production schedule

To estimate the best-performing production schedule all three predefined production scenarios (P_{init}= 20%, 25% or 33%) are combined with 4 investigated skin situations (Skin =0, 12, 30, 40). The pictured cases in Figure 6.1 are calculated with a total initial rate of 6237.18 MSm³/d, which is equal for the different scenarios. During production time, the reservoir pressure is declining and the boundary condition of 30 Bara manifold pressure is either reached or undercut. The pressure decline curve with the highest produced volume and the best characteristics is best-performing.

The 20% profile undercuts the 30 Bara limit line way before the end of production. A build up can be observed during the last days, which indicates an excessive field production at the middle of the production period. The 33% profile falls below the manifold pressure limitation

shortly before end of production, indicating a high end rate. The 25% end rate profile is best-performing, because it produces the highest volume without undercutting the 30 Bara manifold limitations. The other two profiles are too demanding either in the earlier production period, or shortly before end of production.

As the plot shows, the design of the production schedule during the last 60 production days has a major influence on performance and storable turnover volume. In Figure 6.1 the inflow scenario with skin factor 40 is pointed out, because an additional effect can be observed: The worse the inflow situation, the more important is the choice of the production profile.

Sensitivity analyses on the parameter skin factor

To assess the influence of skin effect on inflow and reservoir performance several prediction runs are carried out in PROSPER® and MBAL®. For this calculation the original, more deviated well paths are chosen. The parameter skin effect is changed and new turnover volumes are calculated by iteration runs, maintaining the limitations of UGS Zagling. So a linear relationship between reduced inflow conditions and TOV is observed (Figure 6.2).

Comparison of the findings of this thesis with the results of the ECLIPSE 100® reservoir simulator

The result of the MBAL® prediction case 1 is comparable with the calculated ECLIPSE100® scenario 3. For UGS Zagling the results of this thesis do not deviate more than 4% from the findings of the ECLIPSE100® simulation runs (Table 6.3 and Table 6.4).

7.2. Interpretation of the results for UGS Berndorf

Estimation of the turn over volume and best-performing production schedule

For UGS Berndorf a production profile with a final rate of 25 % leads to the highest reservoir performance. Due to the similarity to the Puchkirchen sands, an inflow situation with a skin factor of 10 represents the most probable upcoming inflow situation.

Sensitivity analyses on the parameter skin and effective well length and estimation of its influences on turnover volume

Several prediction runs with different skin factors and reduced well length are performed. The base case (TOV 100%) was calculated with several skin factors and an effective well length factor of 1 (Figure 6.3). The result for UGS Berndorf was a reduced turnover volume of only 7-10 % in case of 60% effective well length reduction for all three UGS wells. This indicates that the UGS performance is relatively less influenced by shorter or partially off target drilled wells.

Comparison of the development scenarios 7 inch tubing and 5.5 tubing

The 5.5 inch completion produces a slightly higher pressure drop during production (Figure 6.4, Figure 6.5, Figure 6.6), but due to the relatively small rates the smaller size has no significant disadvantage compared to the 7 inch completion. Neither manifold pressure, nor TOV is responding on the changed parameters. My recommendation is, to install a 5.5 inch completion instead of a previously planned 7 inch completion to save investment costs.

Comparison of the findings of this thesis with the results of the ECLIPSE 100® reservoir simulator

The simulated MBAL® production scenario is comparable with ECLIPSE100® case 2, calculated by HOT engineering. The calculated rate and turnover volumes differ less than 7%.

7.3. Interpretation of the results for UGS Nußdorf

Estimation of the turn over volume and best-performing production schedule

The calculated turnover volume of 629 MMSm³ is relatively small in relation to the needed amount of cushion gas. Thus the ratio of TOV/cushion gas is lower than in the other investigated UGS reservoirs. My recommendation is to drill more storage wells, to improve the storage capacity.

7.4. Review and application field of the devised model

The devised method is based on the combination of material balance, inflow performance calculation and tubing performance calculation. The method uses the commercial material balance modelling software MBAL®, version 8.0 and the commercial well modelling software PROSPER® version 9.0, which are part of the integrated production modelling software package IPM 5.0, developed by the company PETROLEUM EXPERTS®. The implemented visual Basic Excel Routine uses the OPENSERVER® command library, which is part of this software package as well.

Advantages

The advantages of this method are easy parameter changes and simple readout of the results into Excel tables or graphs, by using the OPENSERVER® commands. The implemented routine is Open Source and can be easily modified according to the requirements of the user.

Disadvantages

The multi-lateral model of the newer version of PROSPER® (version 10.0) computes different results, although using same values, than version 9.0. The multi-lateral model is an in-house developed model of the company PETROLEUM EXPERTS® and is not released for publication. It is not fully clear which calculation steps are applied for IPR calculation. The main reasons for the choice of this model are program engineering issues.

Field of application

Thus the material balance is a zero dimensional calculation method, the model is very abstract and the relation to real reservoir compartments is difficult to imagine. It is not a full reservoir simulation study and should not be the only tool of planning UGS wells or estimating storage capacities. The devised method is supposed to assess the sensitivity parameter in the preliminary phase, or it should be applied for quality control of a more detailed reservoir simulation study.

Extension of the devised model

Due to the command library of the OPENSERVER® package, the devised model could be extended by implementing automated calculations of additional sensitivity parameters like well survey, completion selection or VLP calculation. Even the implementation of a fully automated probability based iterative method is possible to carry out risk analyses.

Bibliography

A. B. Zolotukhin, J.-R. Ursin. 2000. *Introduction to Petroleum Reservoir Engineering.* Kristiansand : Norwegian Academic Press, 2000. ISBN 82-7634-065-2.

Alan C. Gringarten, Henry J. Ramey, Jr. 1973. *The use of Source and Green's functions in solving Unsteady-flow Problems in Reservoirs.* s.l. : Society of Petroleum Engineers Journal, 1973. SPE 3818.

Bartsch, Hans-Jochen. 1999. *Taschenbuch Mathematischer Formeln.* München : Fachbuchverlag Leipzig, 1999. pp. 571-576. ISBN: 3-446-21048-2.

D. K. Babu, A. S. Odeh, A. J. Al-Kalifa, R. C. McCann:. 1991. *The Relation between Wellblock and Wellbore Pressures in Numerical Simulation of Horizontal Wells.* 1991. SPE 20161.

D.A. McVay, J.P. Spivey. 1994. *Optimizing Gas Storage Reservoir Performance.* New Orleans, L.A. : s.n., 1994. SPE 28639 presented at the SPE 69th Annual Technical Conference 1994, New Orleans, L.A., U.S.A. 25-28 September.

D.K.Babu, Aziz S. Odeh. 1989. *Productivity of a Horizontal Well.* 1989. SPE18334, First presented at Annual technical conference 2-5 October 1988 , Houston, Texas .

Dake, L. P. 1978. *Fundamentals of Reservoir Engineering.* Amsterdam : Elsevier Science BV, 1978. ISBN:0-444-41830-X.

Duane, John W. 1967. *Gas Storage Field Development Optimization.* s.l. : JPT (Volume 19, Number 3), 1967. pp. 323-330. SPE 1503-PA.

Earlougher, R.C. 1977. *Advances in well test analysis.* Dallas : Society of Petroleum Engineers, 1977. ISBN-10: 0895202042.

Economides, Michael J., Hill, A. Daniel and Ehlig-Economides, Christine. 1994. *Petroleum Production Systems.* New Jersey : Prentice-Hall PTR, 1994. ISBN: 0-13-658683.

Gould, T. L.,Tek, M.R., Katz D. L. 1974. Two-Phase flow through Vertical, Inclined, or Curved Pipe. *Journal of Petroleum Technology.* 1974, Vol. 26, Number 8, pp. 915-926.

Gouynes, J., Squire, K., Blauch, W., Yeager, V., Yater, J.,Wallace, R., Frame, R., and Clark, R.: 2000. *Optimizing Deliverability in Five Gas-Storage Reservoirs-Case Study.* 2000. SPE 65636, presented at the 2000 SPE Eastern Regional Meeting, Morgantown, October 17-19.

H. Duns, Jr., N.C.J. Ros. 1963. *Vertical flow of gas and liguid mixtures in wells.* Frankfurt : Proc. Sixth World Petroleum Congress, 1963. Section II, Paper 22-PD6.

Heber Cinco-Ley, H. J. Ramey, Jr., Frank G. Miller. 1975. *Pseudo-Skin factors for partially - penetrating directionally - drilled wells.* 1975. SPE 5589, prepared for presentation at the 50 th annual Fall meeting of AIME, to held in Dallas, sept. 28. - oct. 1.1975.

Henderson, James H., Dempsey John R., Tyler James C. 1968. *" Use of Numerical Models to Develop and Operate Gas Storage Reservoirs".* s.l. : JPT (Volume 20, Number 11), 1968. pp. 1239-1246. SPE 2009-PA.

HOT Engineering. 2007. *Draft Report Zagling.* Leoben : s.n., 2007.

—. 2007. *UGS Berndorf draft report.* Leoben : s.n., 2007.

Jing Wan, V.R.Penmatcha, Sepher Arabi, Khalid Aziz. 2000. *Effects of Grid Systems on predicting Horizontal - Well productivity.* s.l. : SPE Journal, Vol. 5, No.3, September, 2000. SPE 65683.

Kewen Li, Roland N. Horne. 2002. *Calculation of Steam-Water Relative Permeability using Capillary Pressure Data.* Stanford University : SGP-TR-171, 2002.

Muskat, M. 1973. *Flow of Homogenous Fluids in Porous Media.* New York : Mc Graw-Hill, 1973. ISBN: 0-934634-16-5.

Omer Inanc Tureyen, SPE, Hulya Karaalioglu, SPE, Abdurrahman Satman, SPE, Istanbul University. 2000. *Effect of the Wellbore Conditions on the Performance of Underground Gas-Storage Reservoirs.* 2000. SPE 59737 presented at the 2000SPE/CERI Gas technology Symposium, Calgary, Alberta CA 3-5 April 2000.

Petroleum Experts Ltd. 2005. *Mbal Technical Description, Appendix C, Mbal Equations.* [ed.] Petroleum Experts, 10 Logie Mill, Edinburgh, EH7 4HG, Scotland, UK Ltd. 2005. pp. 2-3.

—. 2005. *Mbal Technical Description, Chapter 8, The Material Balance Tool.* [ed.] Petroleum Experts, 10 Logie Mill, Edinburgh, EH7 4HG, Scotland, UK Ltd. Edinburgh : s.n., 2005. p. 22.

—. 2005. *Mbal Technical Description, Chapter 8, The Material Balance Tool.* [ed.] Petroleum Experts, 10 Logie Mill, Edinburgh, EH7 4HG, Scotland, UK Ltd. 2005. pp. 36-39.

—. 2005. *Mbal Technical Description, Chapter 8, The Material Balance Tool.* [ed.] Petroleum Experts, 10 Logie Mill, Edinburgh, EH7 4HG, Scotland, UK Ltd. 2005. p. 88.

—. 2005. *Mbal Technical Description, Chapter 8, The Material Balance Tool.* [ed.] Petroleum Experts, 10 Logie Mill, Edinburgh, EH7 4HG, Scotland, UK Ltd. 2005. pp. 29-31.

—. 2005. *Prosper Technical Description, Chapter 9, Matching Menu.* [ed.] Petroleum Experts, 10 Logie Mill, Edinburgh, EH7 4HG, Scotland, UK Ltd. 2005. p. 3.

Rohöl Aufsuchungs AG. 2009. *Geological description of Nußdorf reservoir.* Vienna : s.n., 2009.

—. 2009. *Geological description of Berndorf reservoir.* Vienna : s.n., 2009.

—. 2007. *Geological description of Zagling reservoir.* Vienna : s.n., 2007.

Rungtip Kamkom, Ding Zhu, Texas A&M University. 2006. *Generalized Horizontal Well Inflow Relationships for Liquid, Gas or Two-Phase Flow.* 2006. SPE 99712, This paper was prepared for presentation at the 2006 SPE/DOE Symposium on Improved Oil Recovery held in Tulsa, Oklahoma, U.S.A., 22–26 April 2006.

Schlumberger. 2004. Eclipse Technical Description. *Chapter 64, Well Inflow Performance.* 2004, pp. 963-971.

van Horn, H. Glen and Wienecke, Donald R. 1970. *A Method for Optimizing the Design of Gas Storage Systems.* 1970. SPE 2966 presented at the 1970 Annual Fall Meeting, Houston, October 4-7.

A) Appendix A

MD	TVD	Equipment	MD	tubing diameter
[m]	[m]		[m]	[inch]
0.00	0.00	Xmas Tree	0.00	
252.00	251.99	Tubing	68.50	3.958
465.00	464.98	SSSV	69.00	3.813
696.00	695.44	Tubing	1337.00	3.958
796.00	794.75	Landing Nipple	1337.50	3.813
892.00	889.87	Tubing	1349.00	3.958
922.00	919.52	7 " Casing	1448.00	
996.00	992.98			
1043.00	1039.73			
1090.00	1086.54			
1137.00	1133.43			
1193.00	1189.36			
1248.00	1244.31			
1296.00	1292.26			
1341.00	1337.23			
1448.00	1444.10			

Table A.1: Trajectory and completion data of ZAG-001

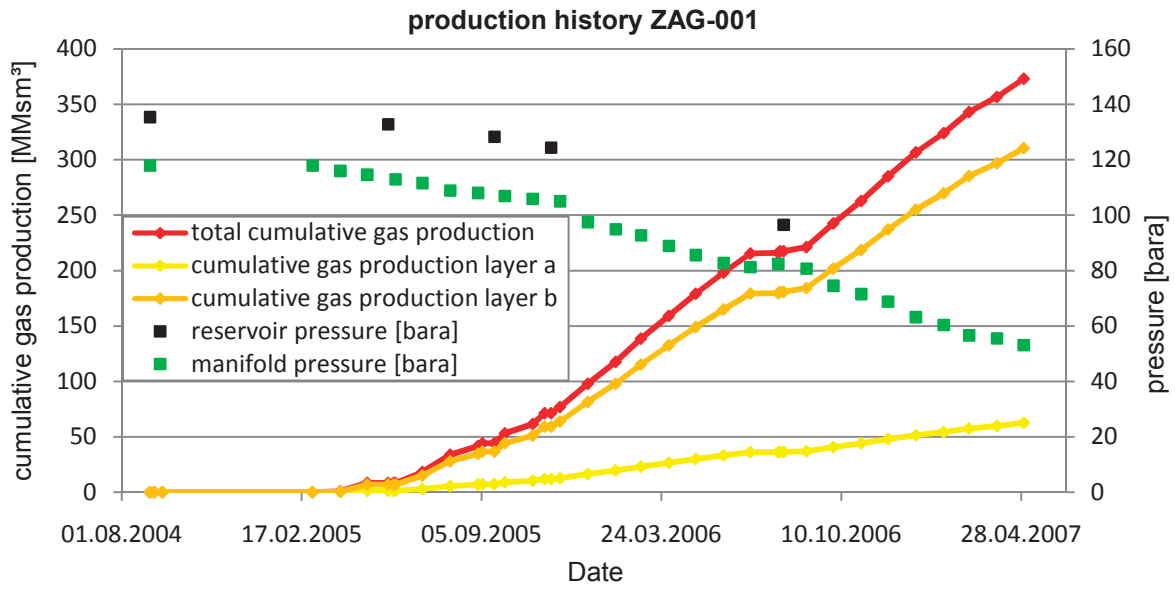

Figure A.1 Manifold pressure, reservoir pressure, total cumulative gas production and the particular gas production of the perforated layers is plotted versus production time.

Tank Volumes of the Zagling MBAL ® model

Tank	Volume	Tank	Volume	Tank	Volume
	[MMSm³]		[MMSm³]		[MMSm³]
SP1A2Z50-a	12.90	SP2A2Z50-a	8.60	ZA1A2Z50-a	8.60
SP1A2Z50-b	76.79	SP2A2Z50-b	75.82	ZA1A2Z50-b	51.19
SP1A2Z50-c	36.95	SP2A2Z50-d	9.72	ZA1A2Z50-c	24.63
SP1A2Z50-d	14.58	SP2A2Z50-e	32.95	ZA1A2Z50-d	9.72
				ZA1A2Z50-e	32.95
Total	141.21		127.09		127.09
Tank	Volume	Tank	Volume		
	[MMSm³]		[MMSm³]		
SP3A2Z50-a	8.60	SP4A2Z50-a	12.90		
SP3A2Z50-b	51.19	SP4A2Z50-b	76.79		
SP3A2Z50-c	24.63	SP4A2Z50-c	36.95		
SP3A2Z50-d	9.72	SP4A2Z50-d	14.58		
SP3A2Z50-e	32.95	SP4A2Z50-e	49.42		
Total	127.09		190.64		

Table A.2: Tank volume distribution with an overall Tank Volume of 713.12 MMSm³

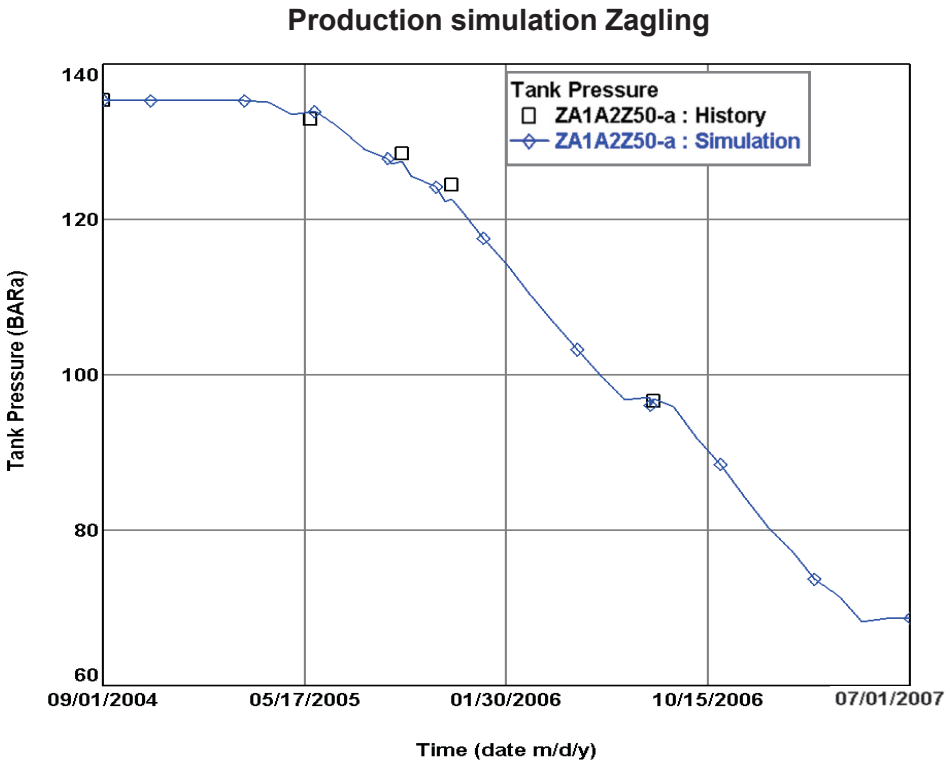

Figure A.2: History match of tank ZA1A2z50-a. The pressure and the cumulative production are plotted versus time. The historical measured pressure points, marked by the black squares, are tried to be matched by a production simulation, labelled by the blue curve.

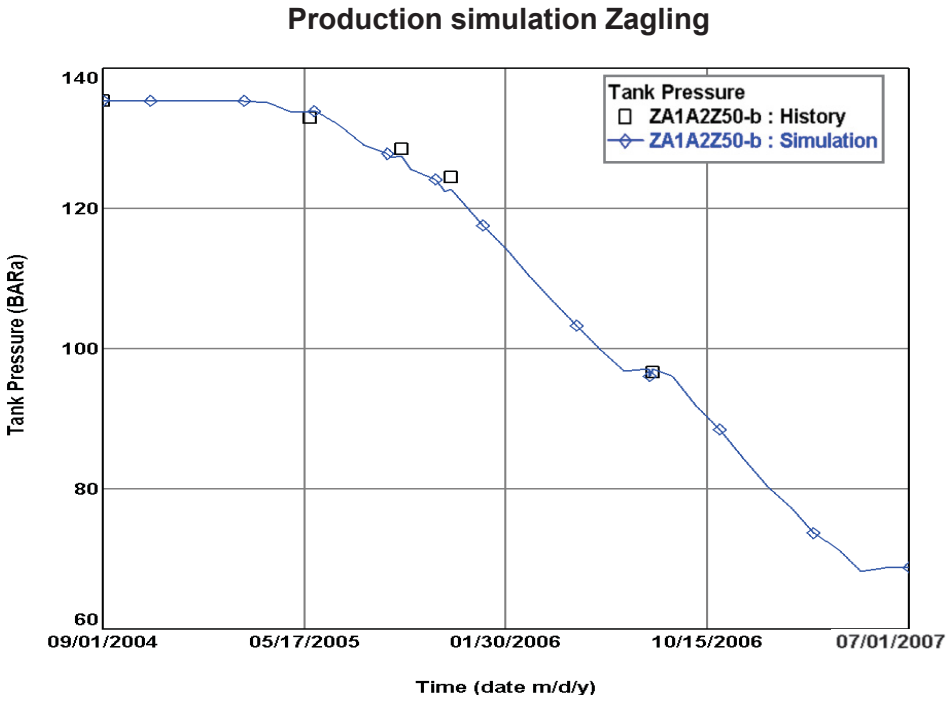

Figure A.3: History match of tank ZA1A2z50-b. The pressure and the cumulative production are plotted versus time. The historical measured pressure points, marked by the black squares, are tried to be matched by a production simulation, labelled by the blue curve.

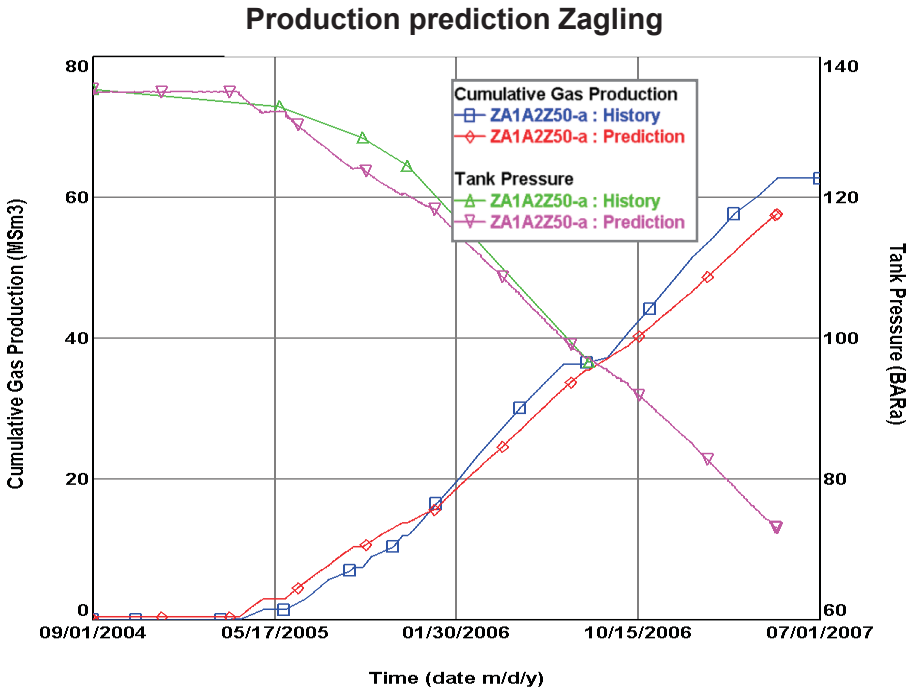

Figure A.4: Prediction simulation of tank ZA1A2z50-a. The historical measured gas production and the pressure points, marked by the blue and respectively by the green curve, are tried to be matched by a production simulation, labelled by the red and respectively the purple curve.

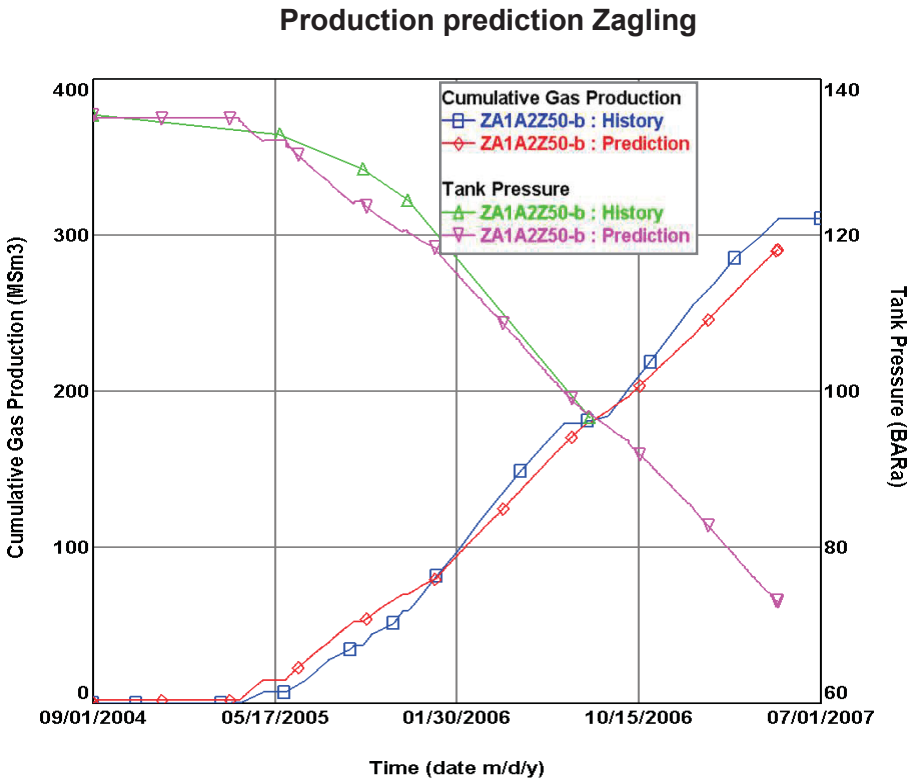

Figure A.5: Prediction simulation of tank ZA1A2z50-b. The historical measured gas production and the pressure points, marked by the blue and respectively by the green curve, are tried to be matched by a production simulation, labelled by the red and respectively the purple curve.

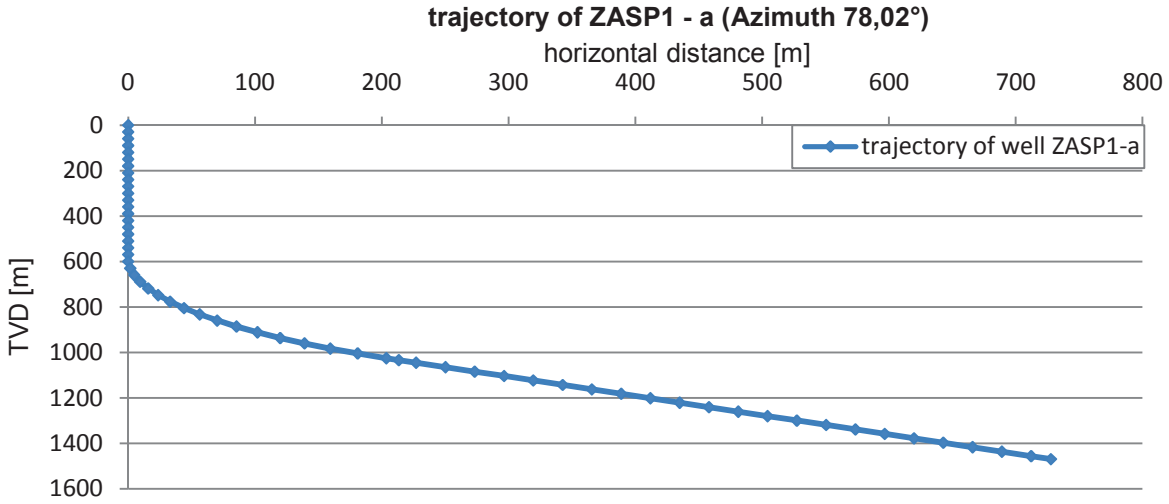

Figure A.6: well path of UGS ZASP1-a. The true vertical depth [m] is plotted versus the horizontal distance [m]. Surface coordinates Northing: 531371600; Easting: 1898

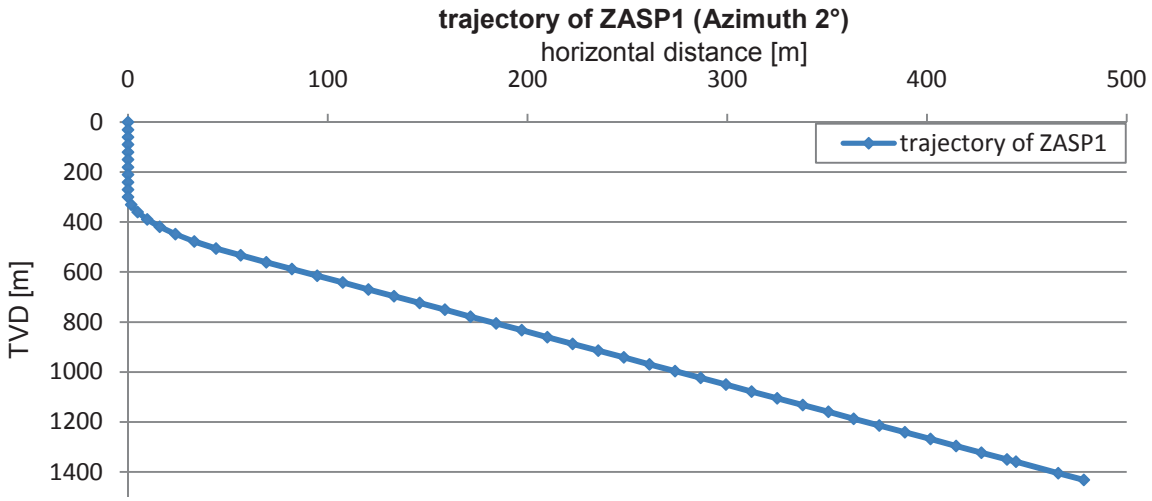

Figure A.7: Well path of UGS ZASP1. The true vertical depth [m] is plotted versus the horizontal distance [m]. Surface coordinates Northing: 531371600; Easting: 1898

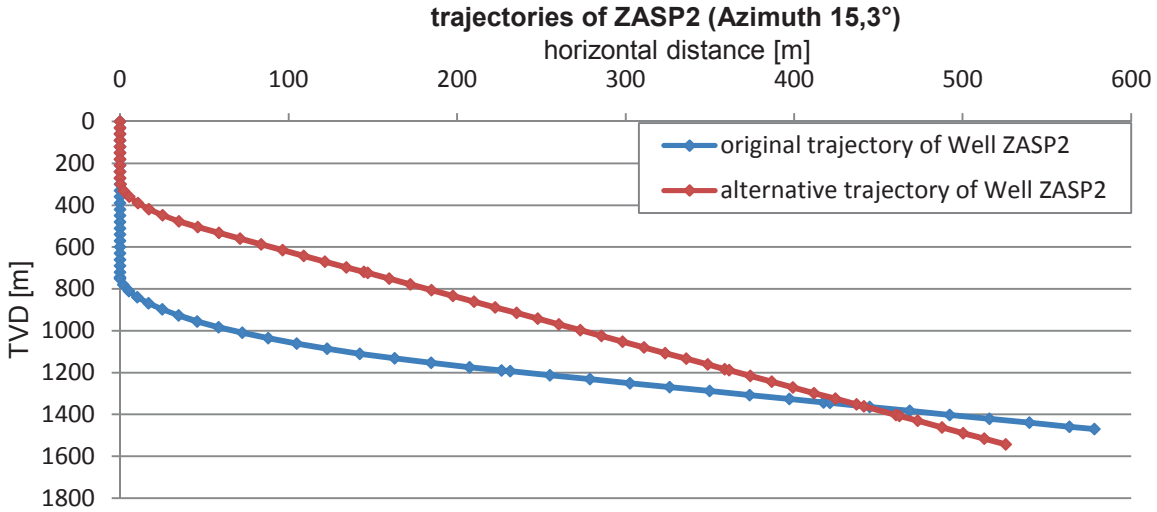

Figure A.8: Well path of UGS ZASP2. The blue line marks the originally planned trajectory and the red line labels the alternative trajectory. The true vertical depth [m] is plotted versus the horizontal distance [m]. Surface coordinates Northing: 531371600; Easting: 1898

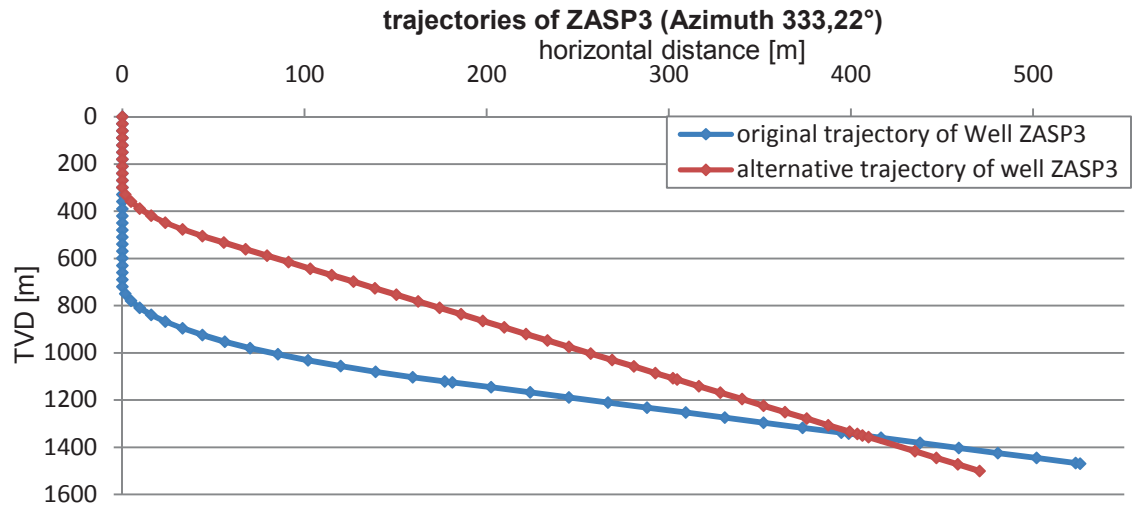

Figure A.9: Well path of UGS ZASP3. The blue line marks the originally planned trajectory and the red line labels the alternative trajectory. The true vertical depth [m] is plotted versus the horizontal distance [m]. Surface coordinates Northing: 531371600; Easting: 1898

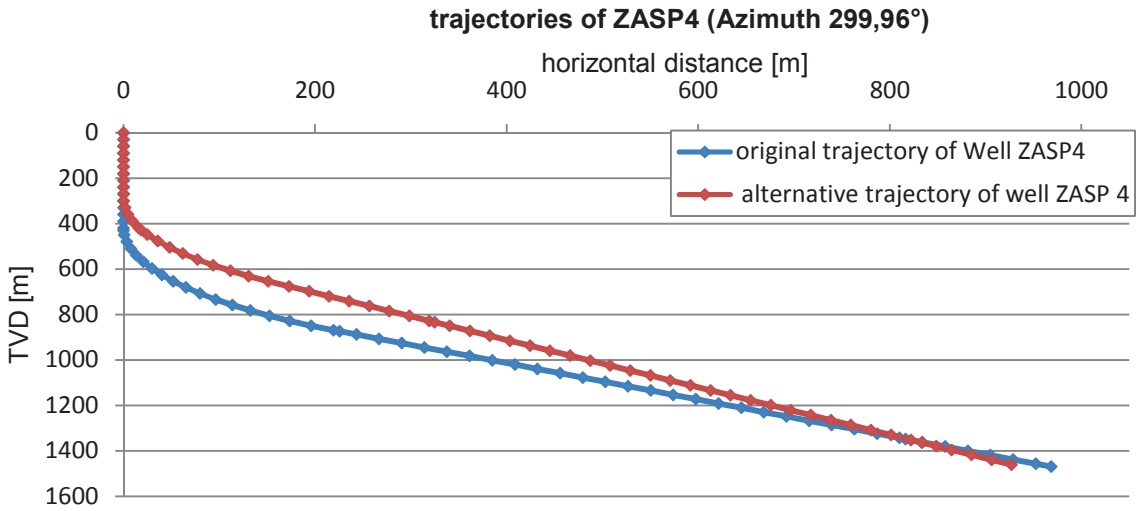

Figure A.10: Well path of UGS ZASP2. The blue line marks the originally planned trajectory and the red line labels the alternative trajectory. The true vertical depth [m] is plotted versus the horizontal distance [m]. Surface coordinates Northing: 531371600; Easting: 1898

Completion of ZASP 1-a

Equipment	MD	inside diameter
	[m]	[inch]
Xmas Tree	0.00	
7" Tubing	72.13	6.184
Flow Coupling	72.80	6.200
SSSV	87.00	5.960
7" Tubing	1450.00	6.184
Flow Coupling	1452.70	6.200
Landing Nipple	1455.09	5.840
Flow Coupling	1458.00	6.200
7" Liner	1760.00	6.276

Table A.3: Completion data, ZASP 1-a

Equipment	MD	inside diameter
Xmas Tree	0,00	
7" Tubing	72,13	6,184
Flow Coupling	72,80	6,200
7 "Tubing	83,45	6,184
SSSV	87,00	5,960
7" Tubing	1400	6,184
flow coupling	1401	6,2
7" Liner	1530	6,276

Table A.4: Completion data of ZASP 1

Completion of ZASP 2

Equipment	MD	inside diameter
	[m]	[inch]
Xmas Tree	0.00	
7" Tubing	72.13	6.184
Flow Coupling	72.80	6.200
7 "Tubing	83.45	6.184
SSSV	87.00	5.960
7" Tubing	1410.00	6.184
Flow Coupling	1448.00	6.200
Landing Nipple	1455.09	5.840
Flow Coupling	1458.00	6.200
7" Tubing	1460.00	6.184
7" Liner	1698.50	6.276

Equipment	MD	inside diameter
	[m]	[inch]
Xmas Tree	0.00	
7" Tubing	72.13	6.184
Flow Coupling	72.80	6.200
7 "Tubing	83.45	6.184
SSSV	87.00	5.960
7" Tubing	1350.00	6.184
Flow Coupling	1352.00	6.200
Landing Nipple	1355.09	5.840
Flow Coupling	1356.20	6.200
7" Tubing	1400.00	6.184
7" Liner	1653.00	6.276

Table A.5: Completion data of original and alternative trajectory, ZASP 2

Completion of ZASP 3

Equipment	MD	inside diameter
	[m]	[inch]
Xmas Tree	0.00	
7" Tubing	72.13	6.184
Flow Coupling	72.80	6.200
7 "Tubing	83.45	6.184
SSSV	87.00	5.960
7" Tubing	1400.00	6.184
Flow Coupling	1403.00	6.200
Landing Nipple	1406.30	5.840
Flow Coupling	1408.00	6.200
7" Tubing	1450.00	6.184
7" Liner	1653.00	6.276

Equipment	MD	inside diameter
	[m]	[inch]
Xmas Tree	0.00	
7" Tubing	72.13	6.184
Flow Coupling	72.80	6.200
7 "Tubing	83.45	6.184
SSSV	87.00	5.960
7" Tubing	1350.00	6.184
Flow Coupling	1352.00	6.200
Landing Nipple	1355.09	5.840
Flow Coupling	1356.20	6.200
7" Tubing	1400.00	6.184
7" Liner	1570.00	6.276

Table A.6: Completion data of original and alternative trajectory, ZASP 3

Completion of ZASP 4

Equipment	MD	inside diameter
	[m]	[inch]
Xmas Tree	0.00	
7" Tubing	72.13	6.184
Flow Coupling	72.80	6.200
7 "Tubing	83.45	6.184
SSSV	87.00	5.960
7" Tubing	1601.00	6.184
Flow Coupling	1603.00	6.200
Landing Nipple	1604.80	5.840
Flow Coupling	1607.90	6.200
7" Tubing	1625.00	6.184
7" Liner	1880.00	6.276

Equipment	MD	inside diameter
	[m]	[inch]
Xmas Tree	0.00	
7" Tubing	72.13	6.184
Flow Coupling	72.80	6.200
7 "Tubing	83.45	6.184
SSSV	87.00	5.960
Tubing3	1560.00	6.184
Flow Coupling	1562.00	6.200
Landing Nipple	1564.00	5.840
Flow Coupling	1566.00	6.200
7" Tubing	1610.00	6.184
7" Liner	1798.00	6.276

Table A.7: Completion data of original and alternative trajectory, ZASP 4

Artificial log data with permeability values and perforated zones for Zagling UGS wells

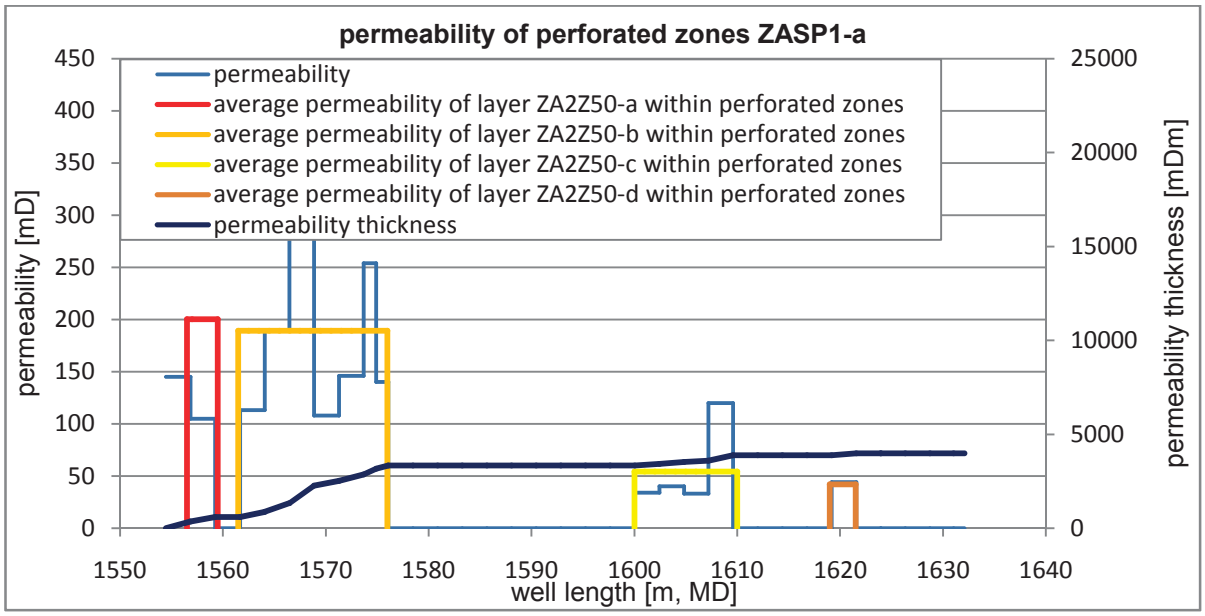

Figure A.11: The well perforates several layers, which are shown in different colours. The permeability along the well path and the permeability thickness product is pictured. The artificial permeability log was created out of the petrel static reservoir model.

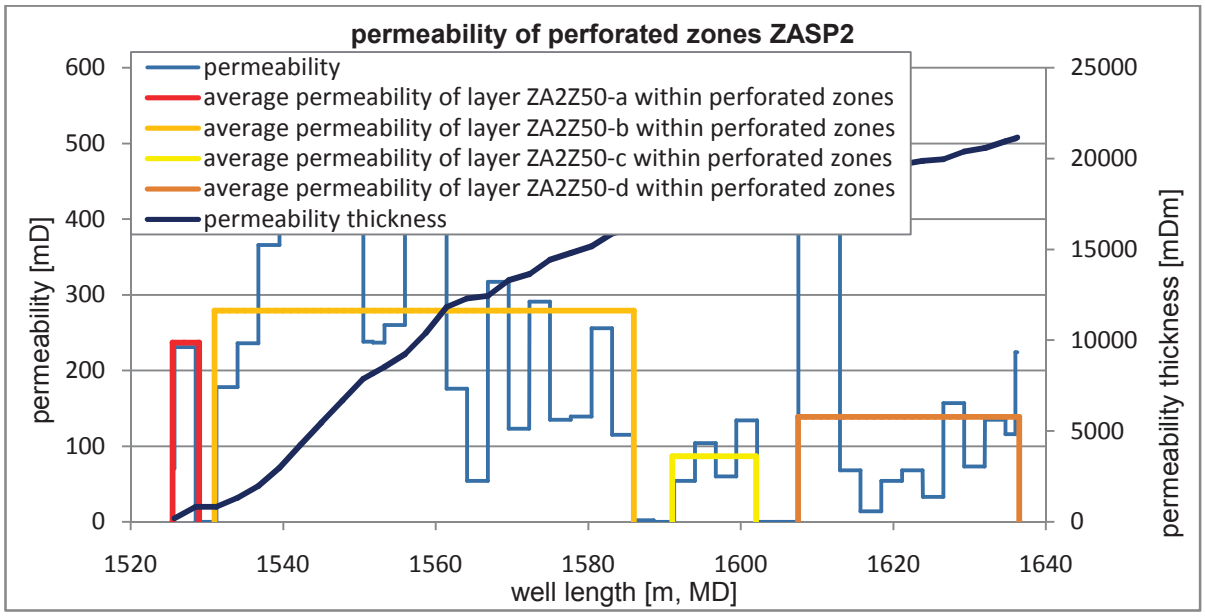

Figure A.12: The well perforates several layers, which are shown in different colours. The permeability along the well path and the permeability thickness product is pictured. The artificial permeability log was created out of the petrel static reservoir model.

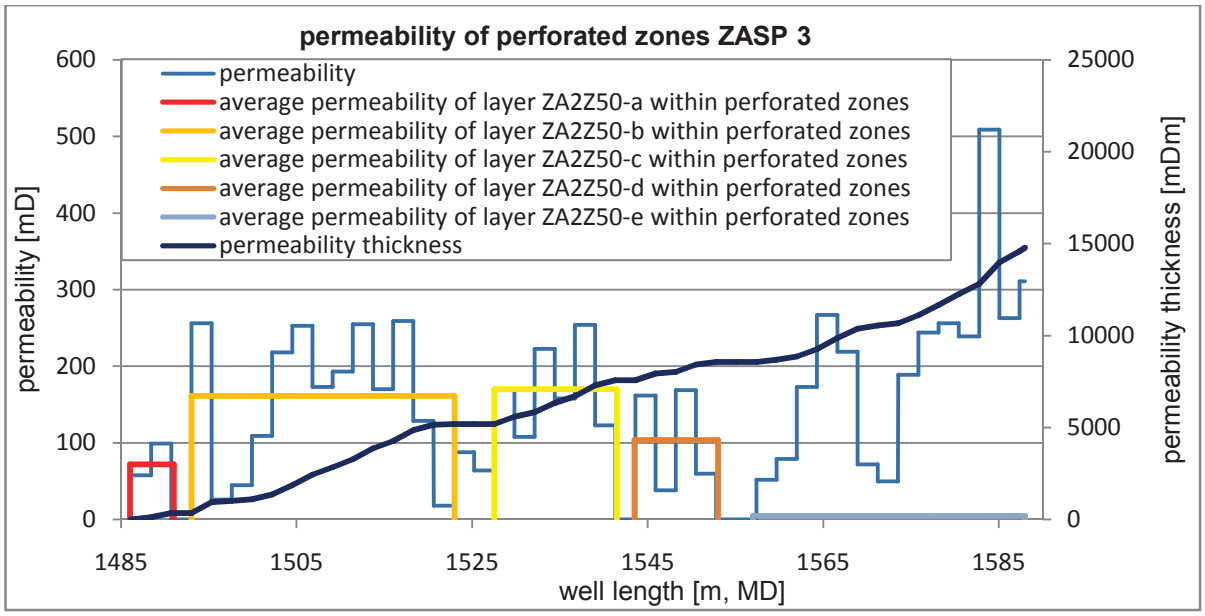

Figure A.13: The well perforates several layers, which are shown in different colours. The permeability along the well path and the permeability thickness product is pictured. The artificial permeability log was created out of the petrel static reservoir model.

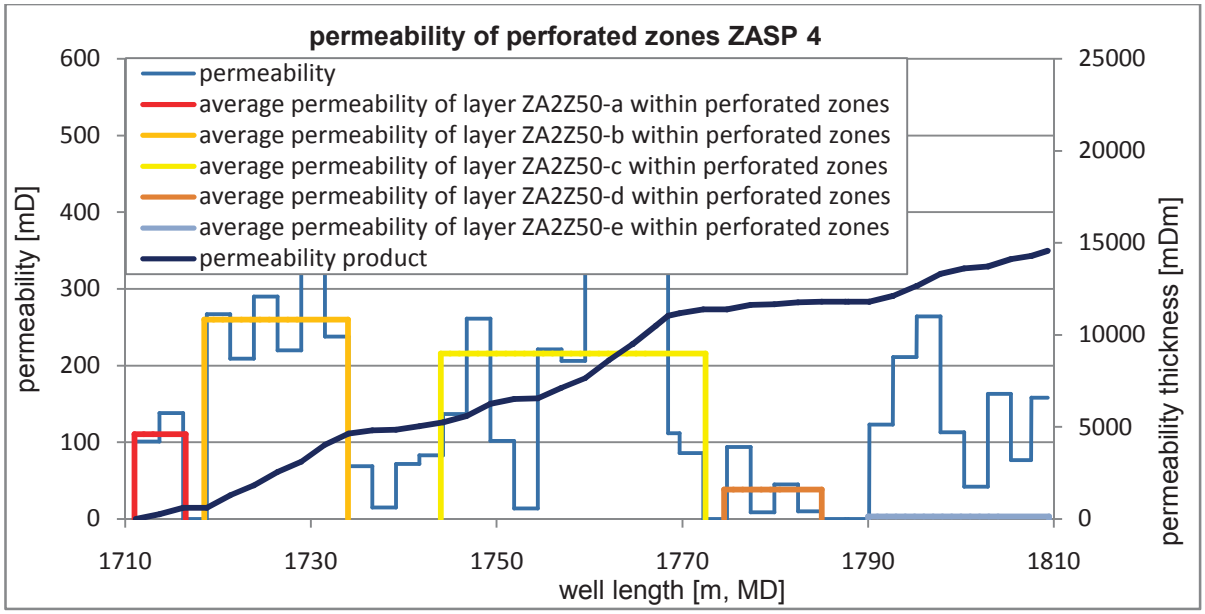

Figure A.14: The well perforates several layers, which are shown in different colours. The permeability along the well path and the permeability thickness product is pictured. The artificial permeability log was created out of the petrel static reservoir model.

B) Appendix B

Production History BERN-001

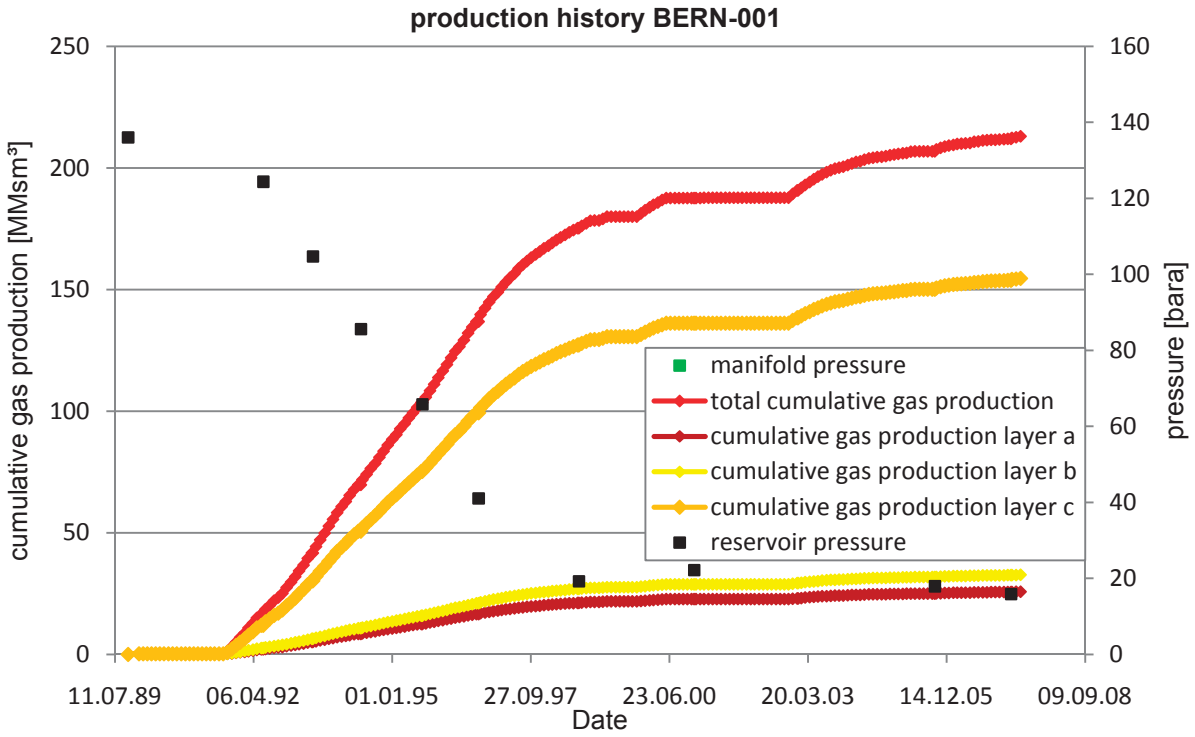

Figure B.1: The production history, including the gas production of the three different Berndorf layers, the reservoir pressure history and the manifold pressure history are plotted versus production time.

Berndorf tank volume distribution

Tank	Volume [MMSm³]	Tank	Volume [MMSm³]	Tank	Volume [MMSm³]	Tank	Volume [MMSm³]
BESP 3-a	4.60	BESP 3-a-a	4.80	BESP 2-a	2.62	BE001-a	8.05
BESP 3-b	9.26	BESP 3-b-a	5.00	BESP 2-b	6.82	BE001-b	3.42
BESP 3-c	37.34	BESP 3-c-a	21.50	BESP 2-c	33.00	BE001-c	17.50
Total	51.20		31.30		42.44		28.97

Tank	Volume [MMSm³]	Tank	Volume [MMSm³]	Tank	Volume [MMSm³]
BESP 1-a	5.70	BESP 1-a-a	4.80	A3L55-60	15.40
BESP 1-b	7.16	BESP 1-b-a	5.00	A3L55-65	5.90
BESP 1-c	38.19	BESP 1-c-a	21.00		
Total	51.05		30.80		21.30

Table B.1: MBAL tank volume distribution

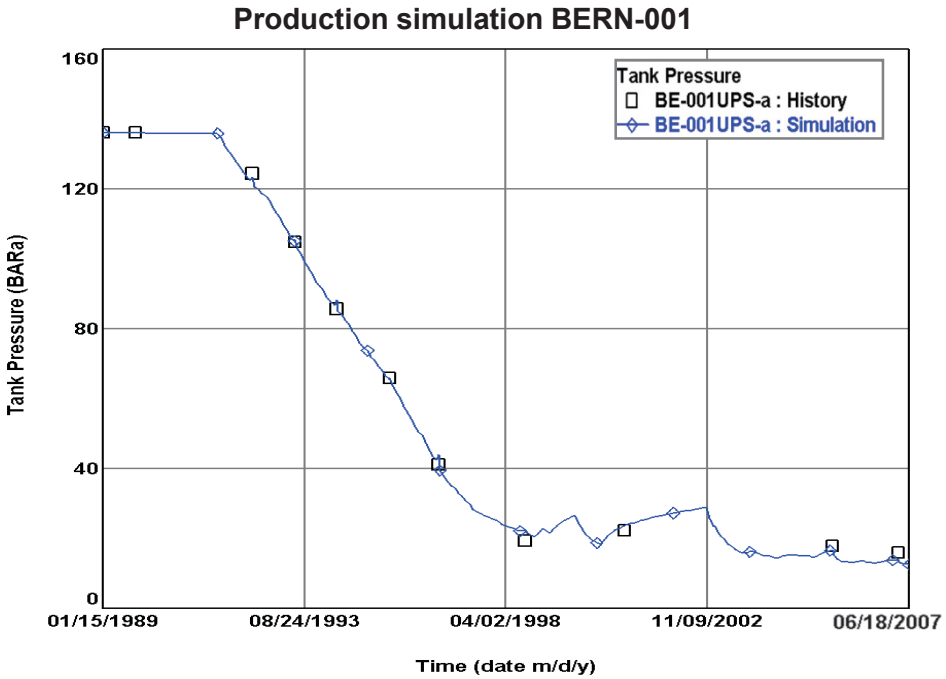

Figure B.2: History match of tank BE-001UPS-a. The pressure and the cumulative production are plotted versus time. The historical measured pressure points, marked by the black squares, are tried to be matched by a production simulation, labelled by the blue curve.

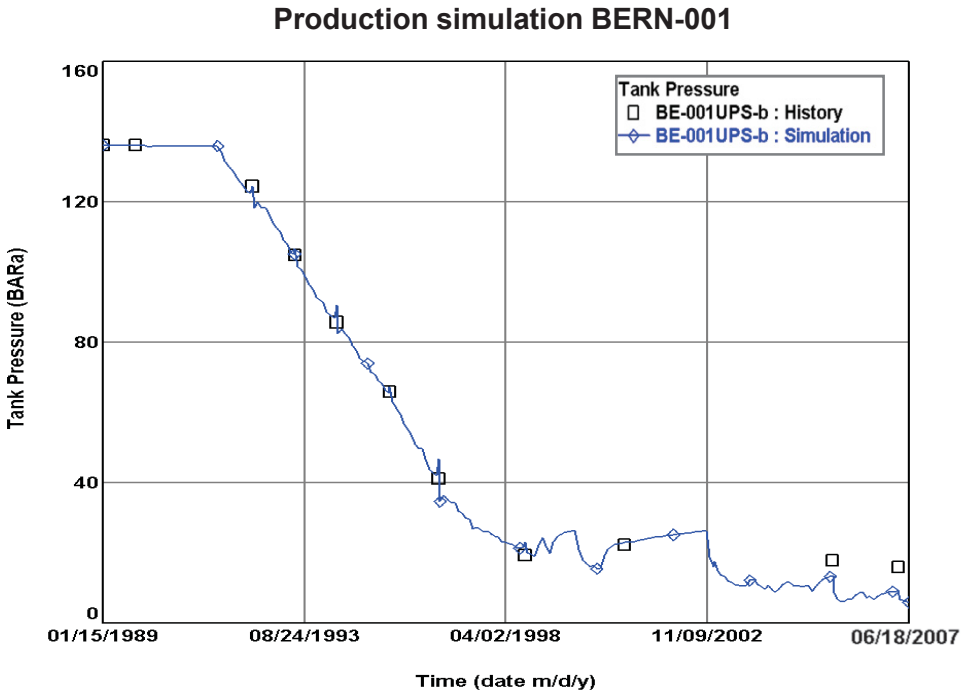

Figure B.3: History match of tank BE-001UPS-b. The pressure and the cumulative production are plotted versus time. The historical measured pressure points, marked by the black squares, are tried to be matched by a production simulation, labelled by the blue curve.

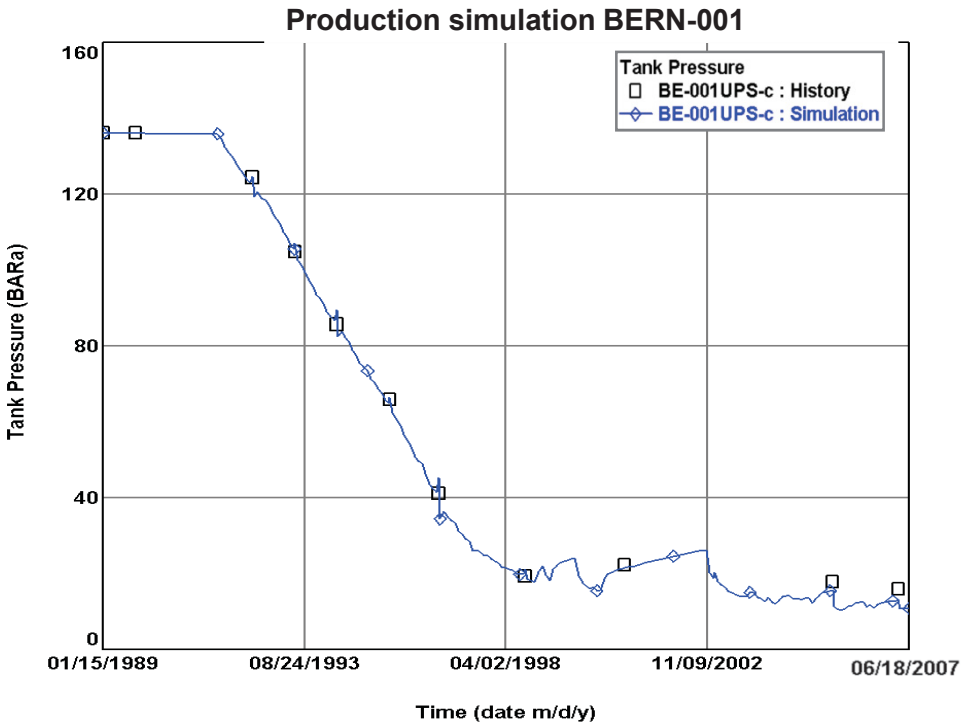

Figure B.4: History match of tank BE-001UPS-c. The pressure and the cumulative production are plotted versus time. The historical measured pressure points, marked by the black squares, are tried to be matched by a production simulation, labelled by the blue curve.

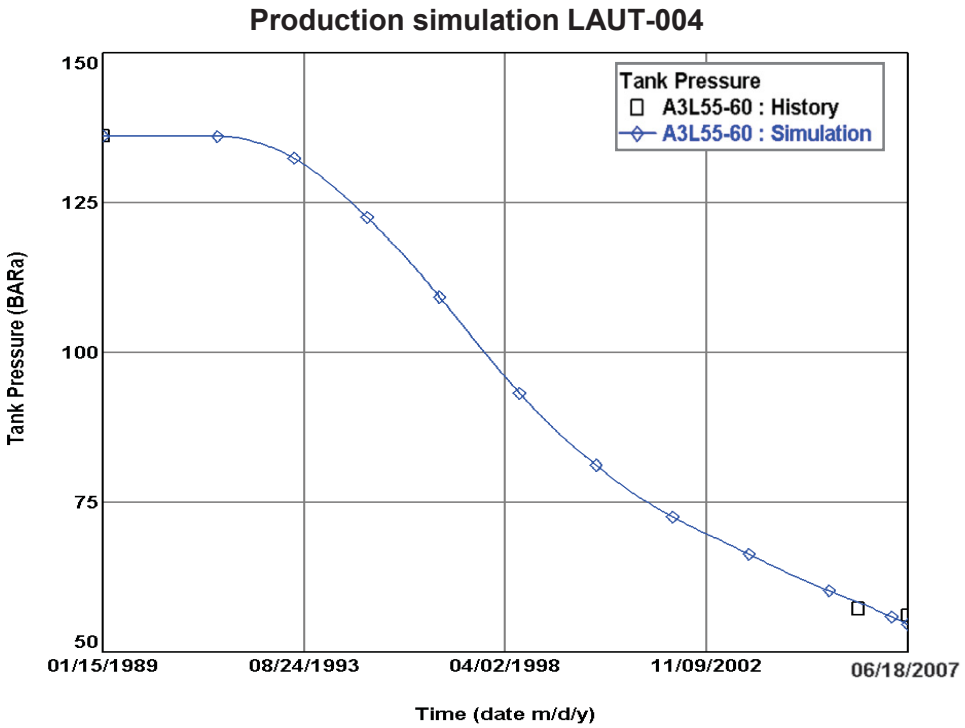

Figure B.5: History match of tank A3L55-60. The pressure and the cumulative production are plotted versus time. The historical measured pressure points, marked by the black squares, are tried to be matched by a production simulation, labelled by the blue curve.

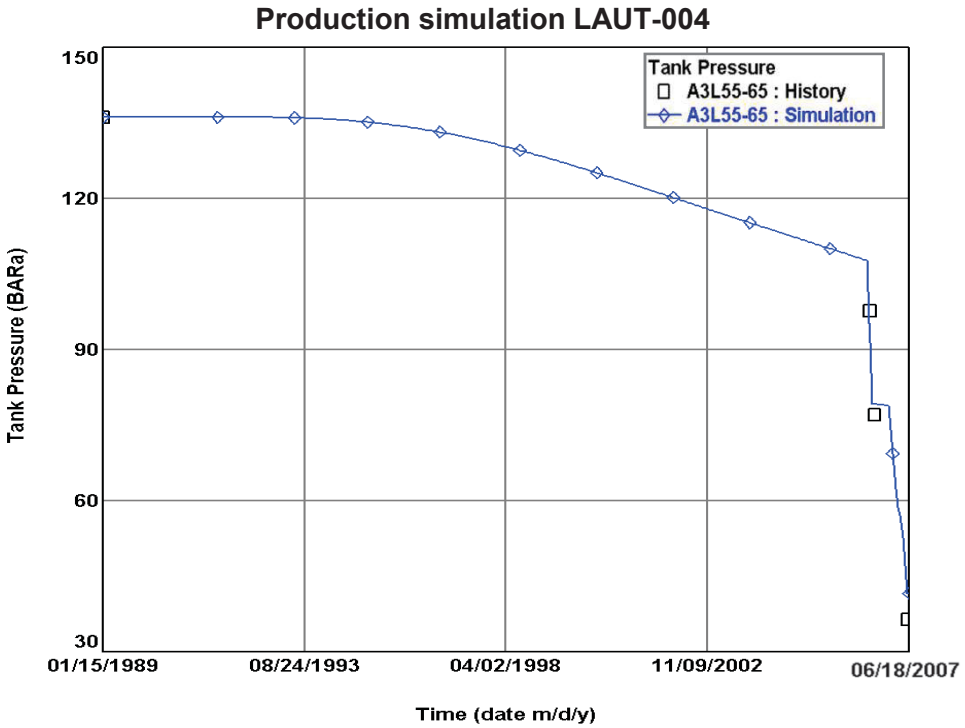

Figure B.6: History match of tank A3L55-65. The pressure and the cumulative production are plotted versus time. The historical measured pressure points, marked by the black squares, are tried to be matched by a production simulation, labelled by the blue curve.

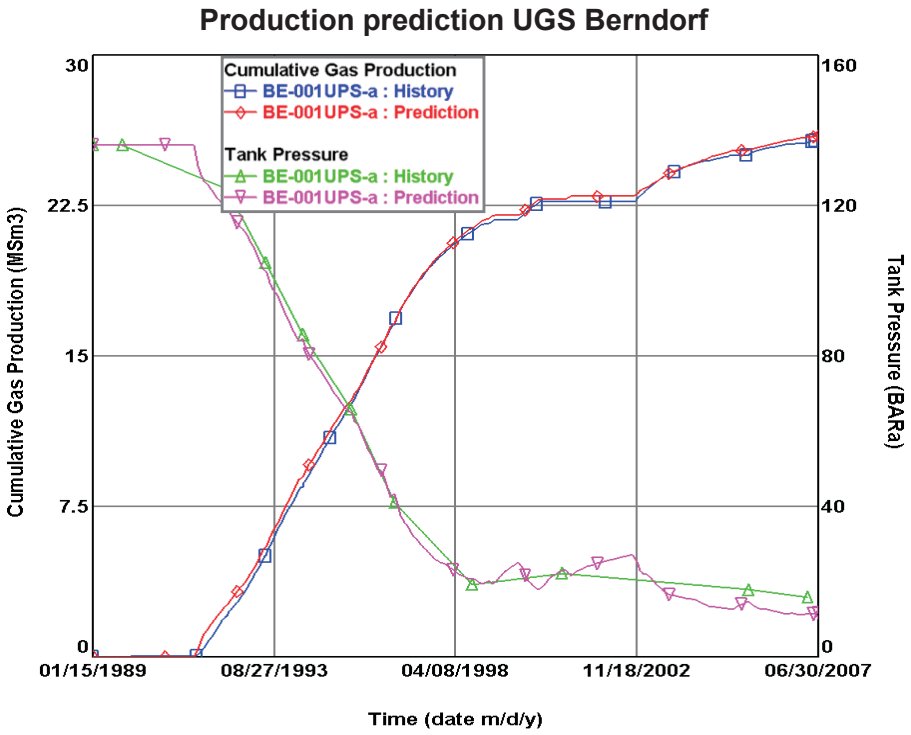

Figure B.7: Prediction simulation of tank BE-001UPS-a.The historical measured gas production and the pressure points, marked by the blue and respectively by the green curve, are tried to be matched by a production simulation, labelled by the red and respectively the purple curve.

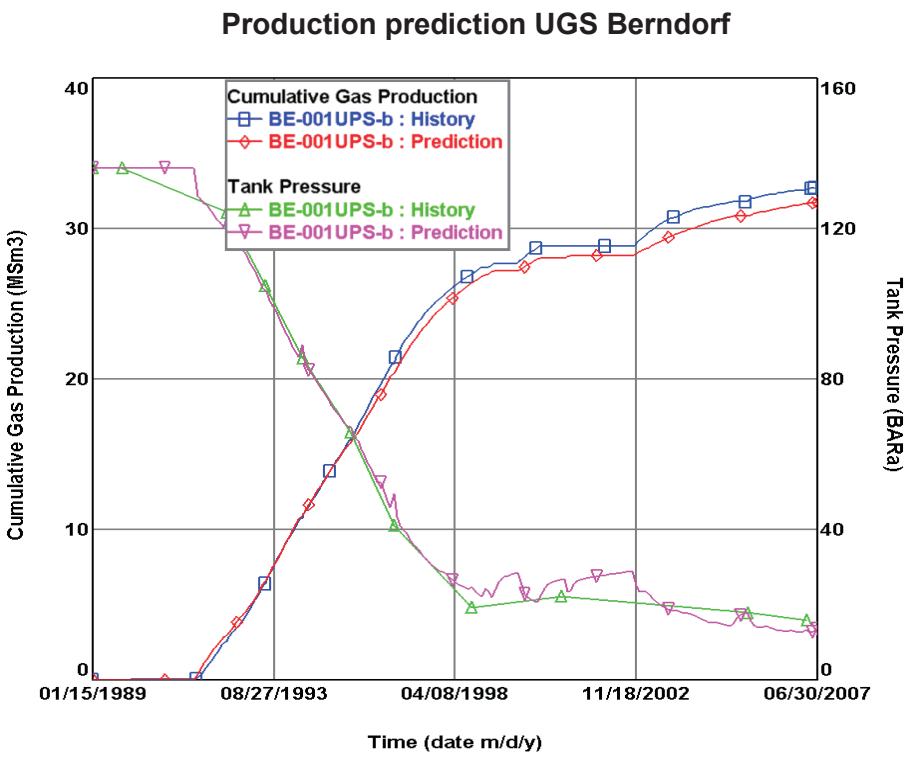

Figure B.8: Prediction simulation of tank BE-001UPS-b. The historical measured gas production and the pressure points, marked by the blue and respectively by the green curve, are tried to be matched by a production simulation, labelled by the red and respectively the purple curve.

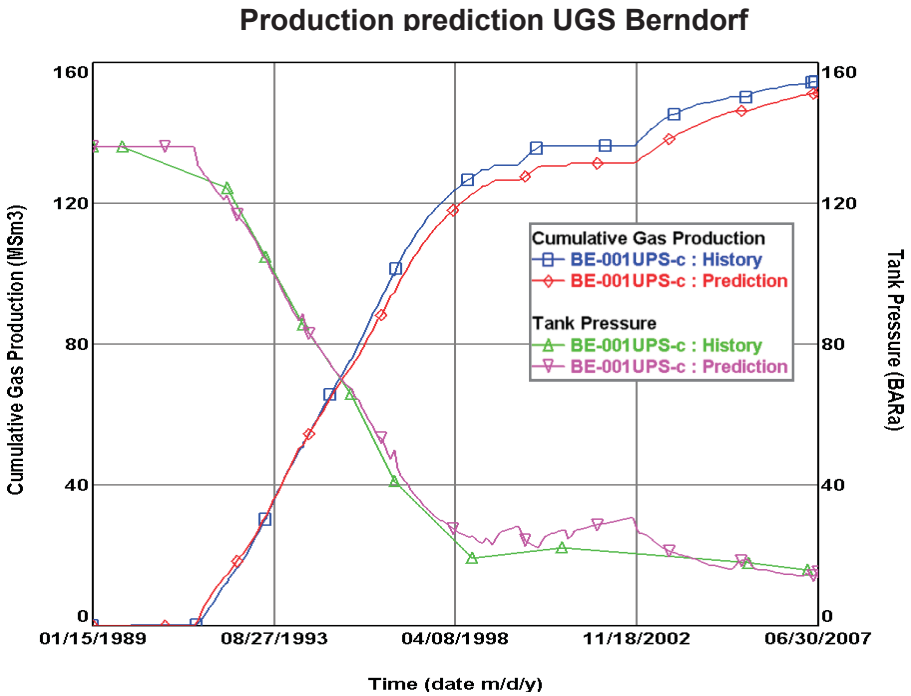

Figure B.9: Prediction simulation of tank BE-001UPS-c.The historical measured gas production and the pressure points, marked by the blue and respectively by the green curve, are tried to be matched by a production simulation, labelled by the red and respectively the purple curve.

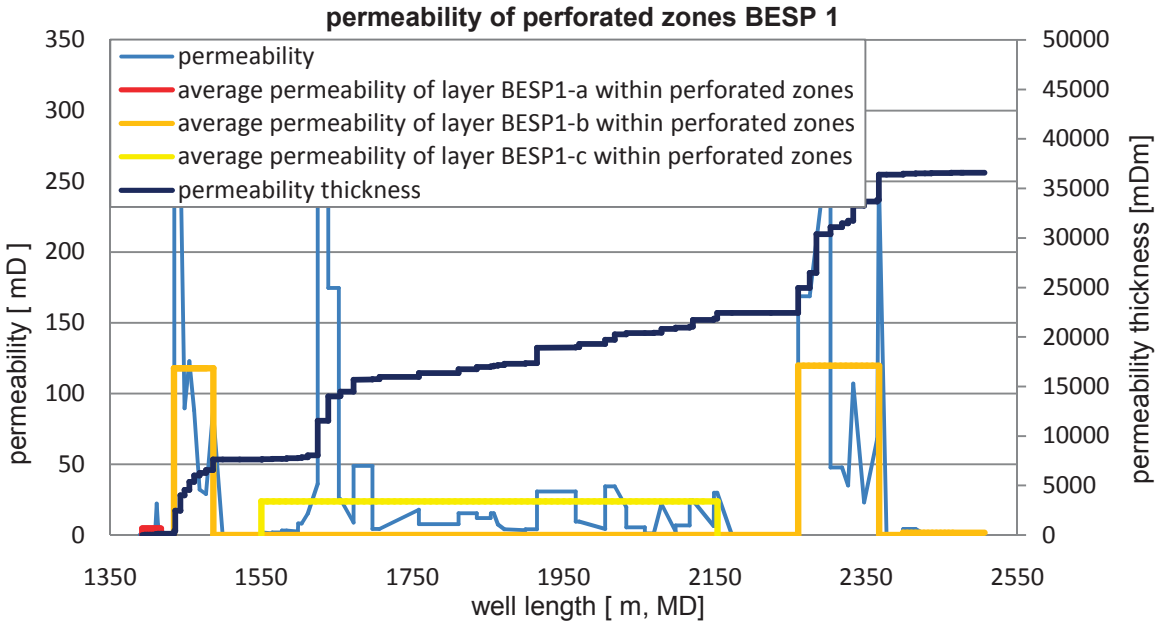

Figure B.10: The well intersects several layers, which are shown in different colours. The permeability along the well path and the permeability thickness product is pictured. The artificial permeability log was created out of the petrel static reservoir model.

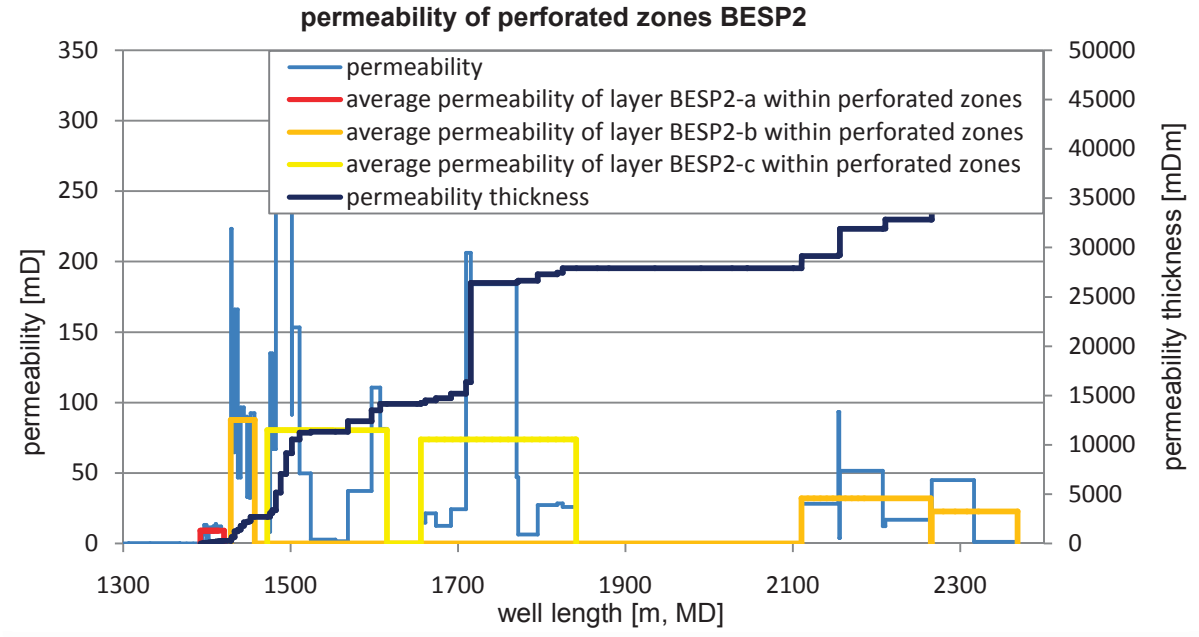

Figure B.11: The well intersects several layers, which are shown in different colours. The permeability along the well path and the permeability thickness product is pictured. The artificial permeability log was created out of the petrel static reservoir model.

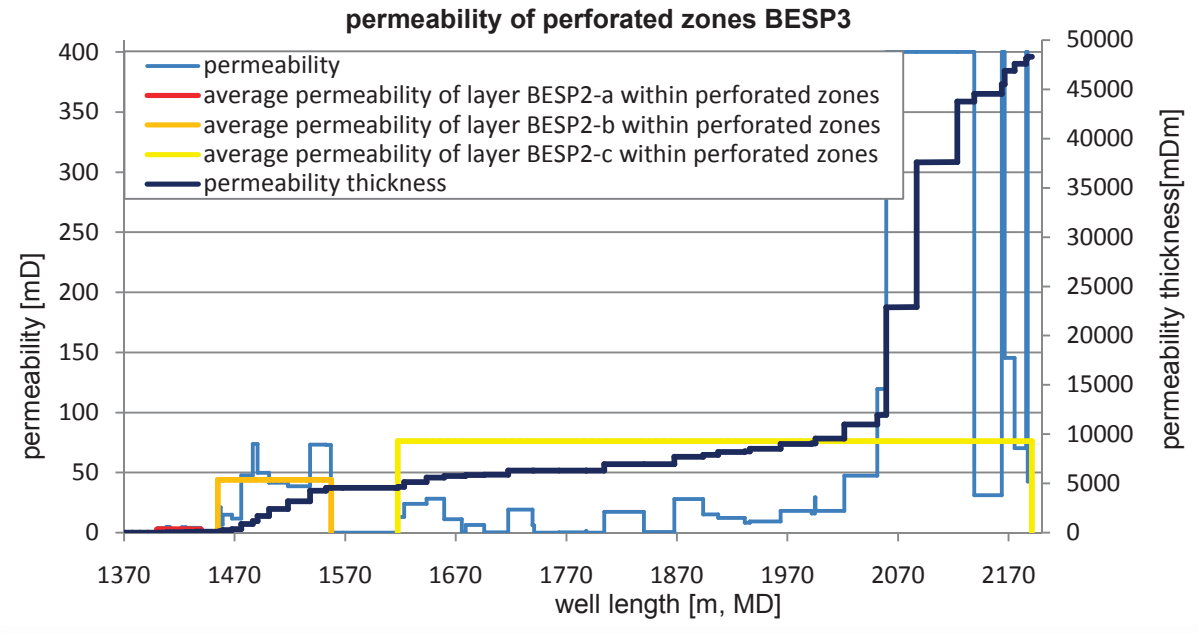

Figure B.12: The well intersects several layers, which are shown in different colours. The permeability along the well path and the permeability thickness product is pictured. The artificial permeability log was created out of the petrel static reservoir model.

Completion data of BESP 1

5.5 inch completion		
Equipment	MD	inside diameter
	[m]	[inch]
Xmas Tree	0.00	
7" Tubing	72.13	4.670
Flow Coupling	72.80	4.700
SSSV	83.45	4.500
Flow Coupling	87.00	4.700
7" Tubing	1230.00	4.670
Flow Coupling	1230.50	4.700
Landing Nipple	1231.00	4.500
Flow Coupling	1231.50	4.700
7" Liner	2506.00	4.670

7 inch completion		
Equipment	MD	inside diameter
	[m]	[inch]
Xmas Tree	0.00	
7" Tubing	72.13	6.184
Flow Coupling	72.80	6.200
SSSV	83.45	6.184
Flow Coupling	87.00	5.960
7" Tubing	1230.00	6.184
Flow Coupling	1230.50	6.200
Landing Nipple	1231.00	5.840
Flow Coupling	1231.50	6.200
7" Liner	2506.00	6.276

Table B.2: Completion data of BESP 1

Completion data of BESP 2

5.5 inch completion		
Equipment	MD	inside diameter
	[m]	[inch]
Xmas Tree	0.00	
7" Tubing	72.13	4.670
Flow Coupling	72.80	4.700
SSSV	83.45	4.500
Flow Coupling	87.00	4.700
7" Tubing	1330.00	4.670
Flow Coupling	1330.50	4.700
Landing Nipple	1331.00	4.500
Flow Coupling	1231.50	4.700
7" Liner	2368.00	4.670

7 inch completion		
Equipment	MD	inside diameter
	[m]	[inch]
Xmas Tree	0.00	
7" Tubing	72.13	6.184
Flow Coupling	72.80	6.200
SSSV	83.45	6.184
Flow Coupling	87.00	5.960
7" Tubing	1330.00	6.184
Flow Coupling	1330.50	6.200
Landing Nipple	1331.00	5.840
Flow Coupling	1331.50	6.200
7" Liner	2368.00	6.276

Table B.3: Completion Data of BESP 2

Completion data of BESP 3

5.5 inch completion		
Equipment	MD	inside diameter
	[m]	[inch]
Xmas Tree	0.00	
7" Tubing	72.13	4.670
Flow Coupling	72.80	4.700
SSSV	83.45	4.500
Flow Coupling	87.00	4.700
7" Tubing	1330.00	4.670
Flow Coupling	1330.50	4.700
Landing Nipple	1331.00	4.500
Flow Coupling	1331.50	4.700
7" Liner	2190.00	4.670

7 inch completion		
Equipment	MD	inside diameter
	[m]	[inch]
Xmas Tree	0.00	
7" Tubing	72.13	6.184
Flow Coupling	72.80	6.200
SSSV	83.45	6.184
Flow Coupling	87.00	5.960
7" Tubing	1330.00	6.184
Flow Coupling	1330.50	6.200
Landing Nipple	1331.00	5.840
Flow Coupling	1331.50	6.200
7" Liner	2190.00	6.276

Table B.4: Completion data of BESP 3

C) Appendix C

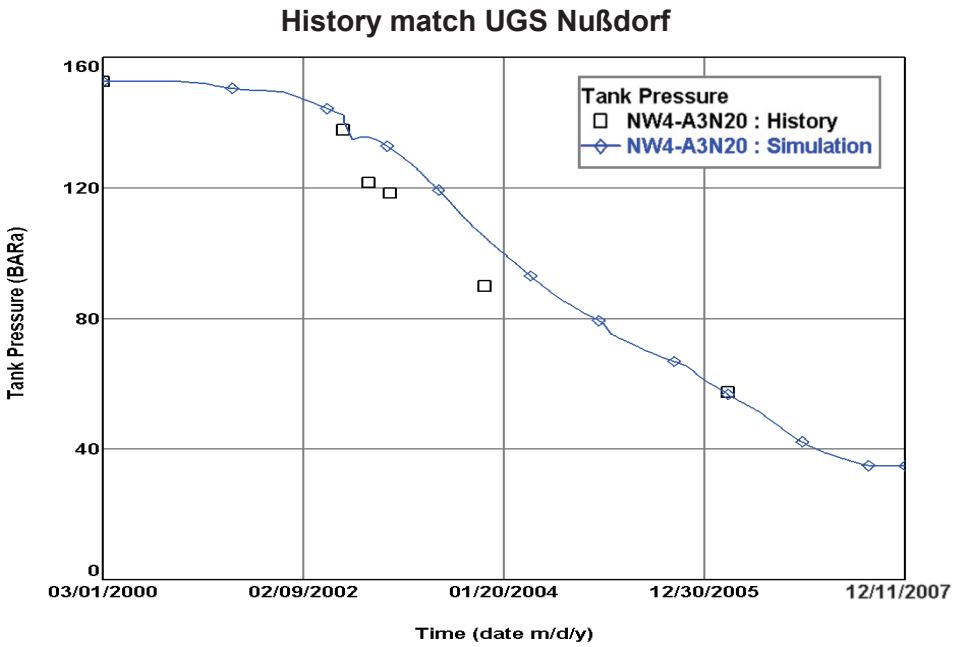

Figure C.1: History match of tank NW4-A3N20. The pressure and the cumulative production are plotted versus time. The historical measured pressure points, marked by the black squares, are tried to be matched by a production simulation, labelled by the blue curve.

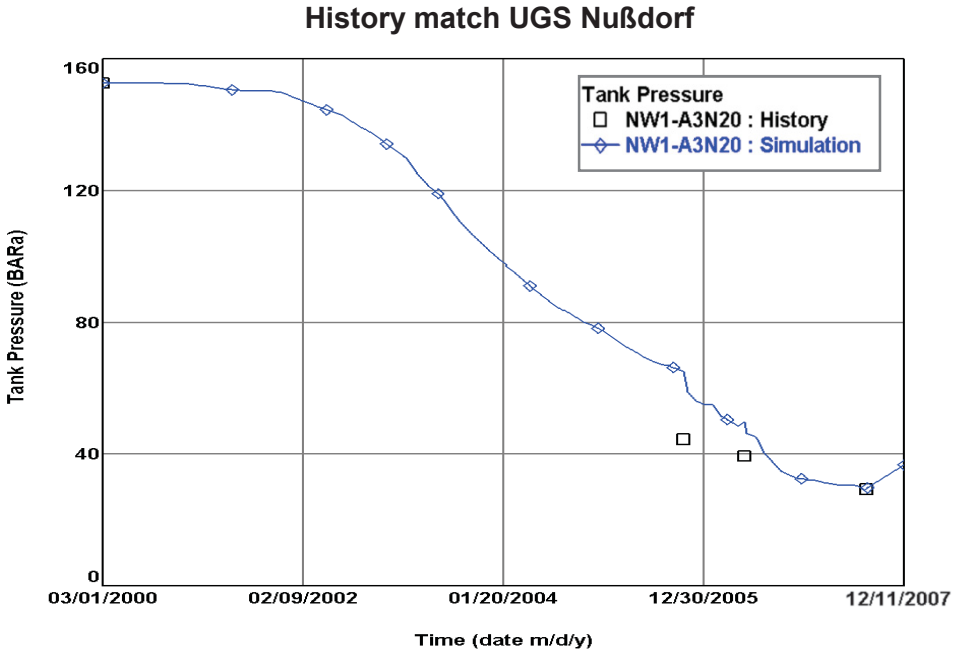

Figure C.2: History match of tank NW1-A3N20. The pressure and the cumulative production are plotted versus time. The historical measured pressure points, marked by the black squares, are tried to be matched by a production simulation, labelled by the blue curve.

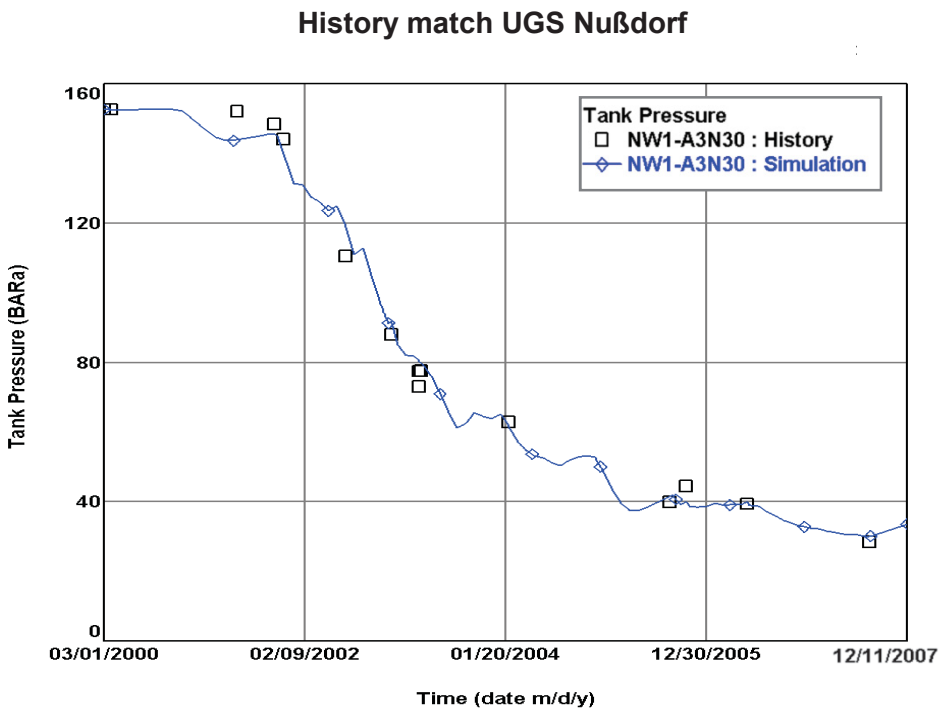

Figure C.3: History match of tank NW1-A3N30. The pressure and the cumulative production are plotted versus time. The historical measured pressure points, marked by the black squares, are tried to be matched by a production simulation, labelled by the blue curve.

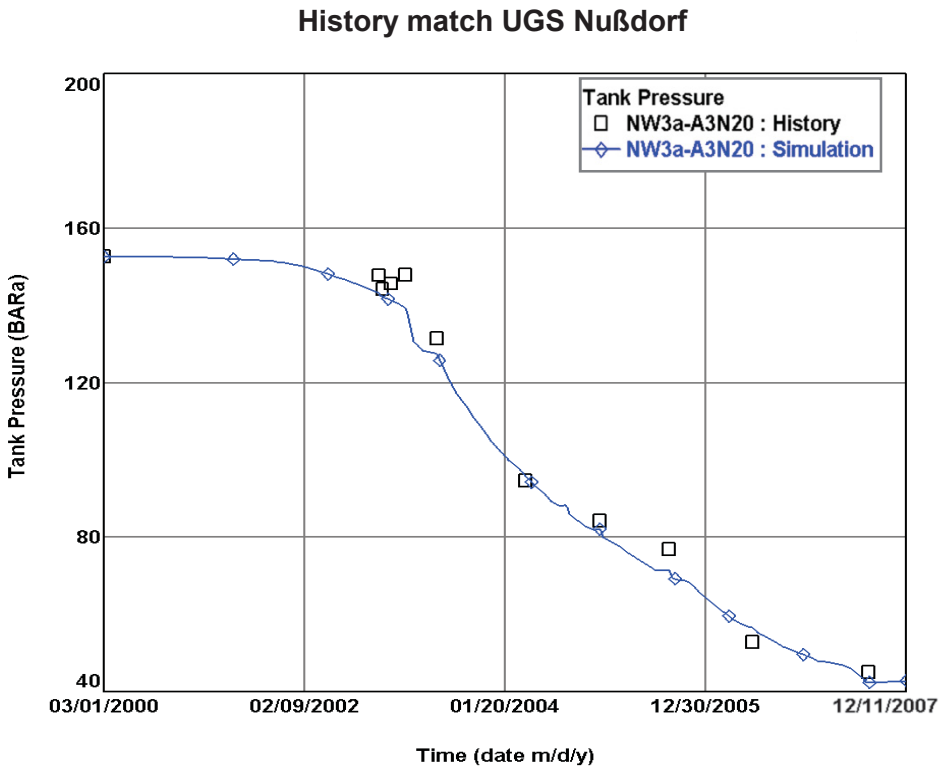

Figure C.4: History match of tank NW3a-A3N20. The pressure and the cumulative production are plotted versus time. The historical measured pressure points, marked by the black squares, are tried to be matched by a production simulation, labelled by the blue curve.

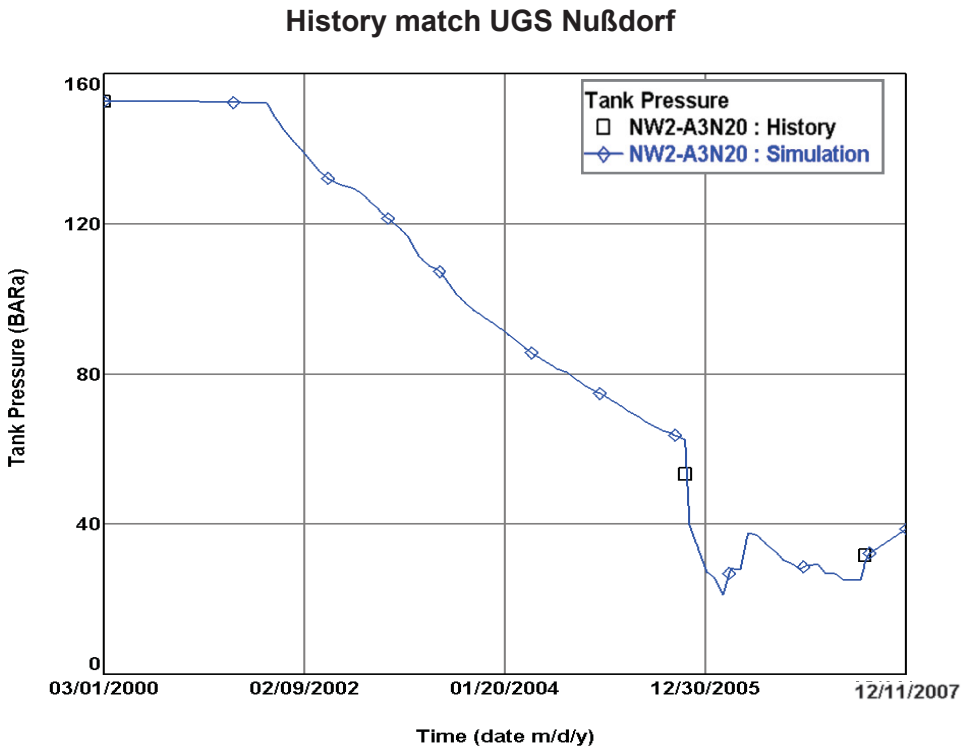

Figure C.5: History match of tank NW2-A3N20. The pressure and the cumulative production are plotted versus time. The historical measured pressure points, marked by the black squares, are tried to be matched by a production simulation, labelled by the blue curve.

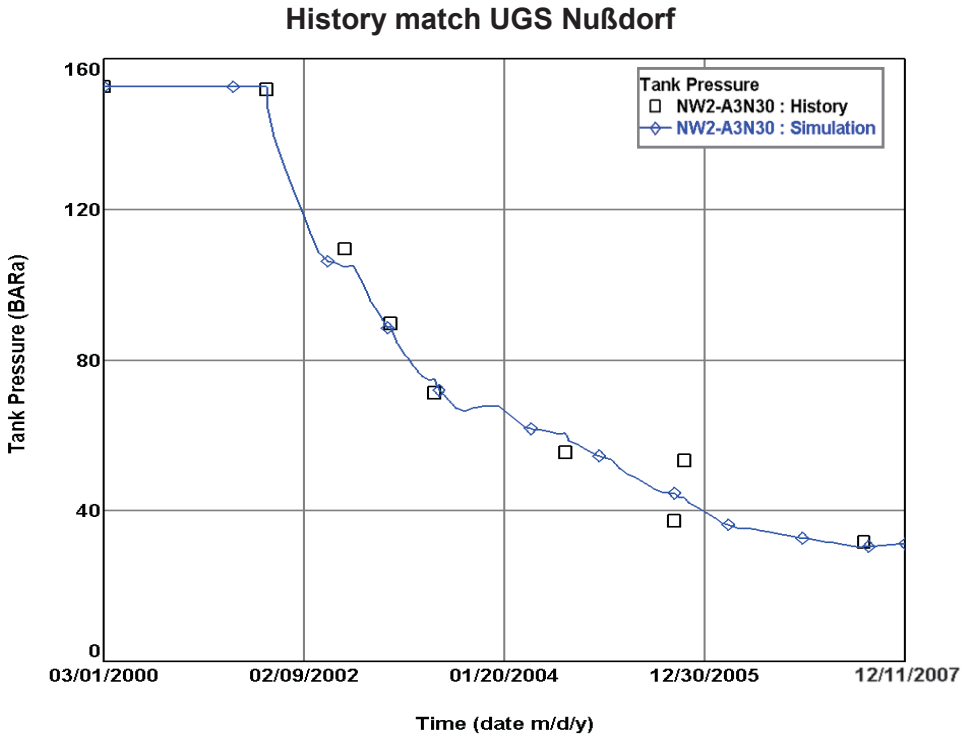

Figure C.6: History match of tank NW2-A3N30. The pressure and the cumulative production are plotted versus time. The historical measured pressure points, marked by the black squares, are tried to be matched by a production simulation, labelled by the blue curve.

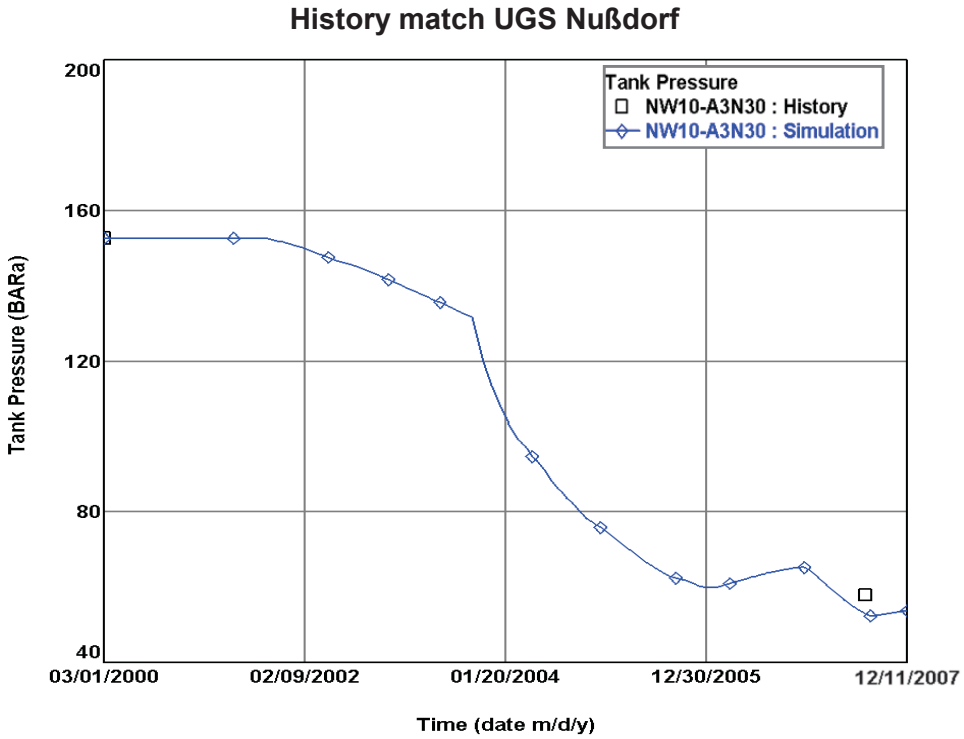

Figure C.7: History match of tank NW10-A3N30. The pressure and the cumulative production are plotted versus time. The historical measured pressure points, marked by the black squares, are tried to be matched by a production simulation, labelled by the blue curve.

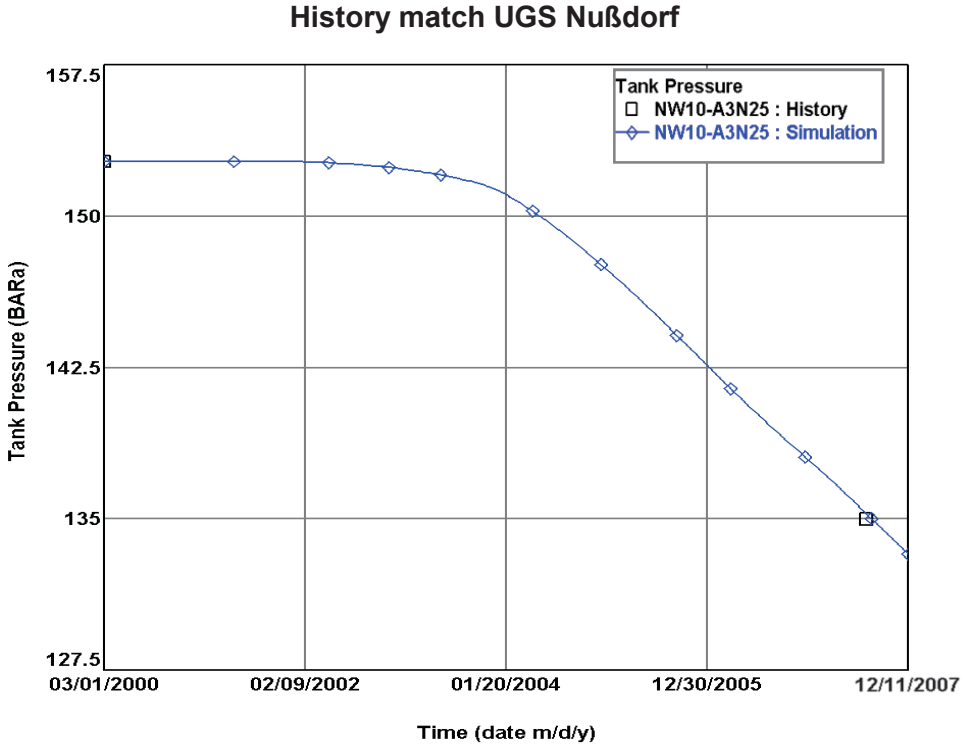

Figure C.8: History match of tank NW10-A3N25. The pressure and the cumulative production are plotted versus time. The historical measured pressure points, marked by the black squares, are tried to be matched by a production simulation, labelled by the blue curve.

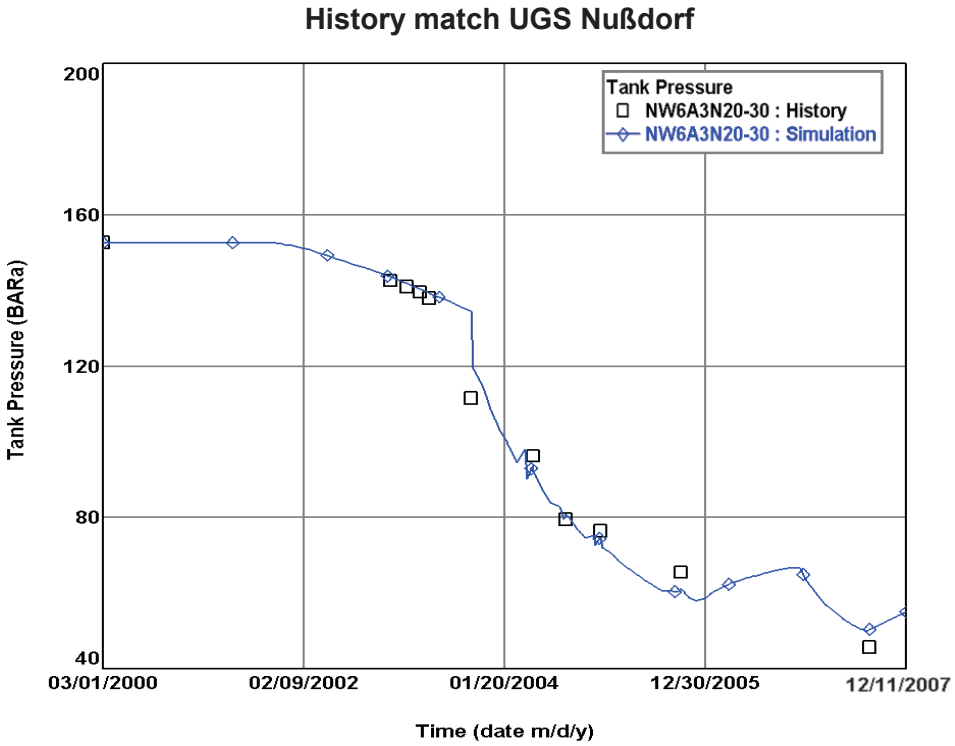

Figure C.9: History match of tank NW6-A3N20-30. The pressure and the cumulative production are plotted versus time. The historical measured pressure points, marked by the black squares, are tried to be matched by a production simulation, labelled by the blue curve.

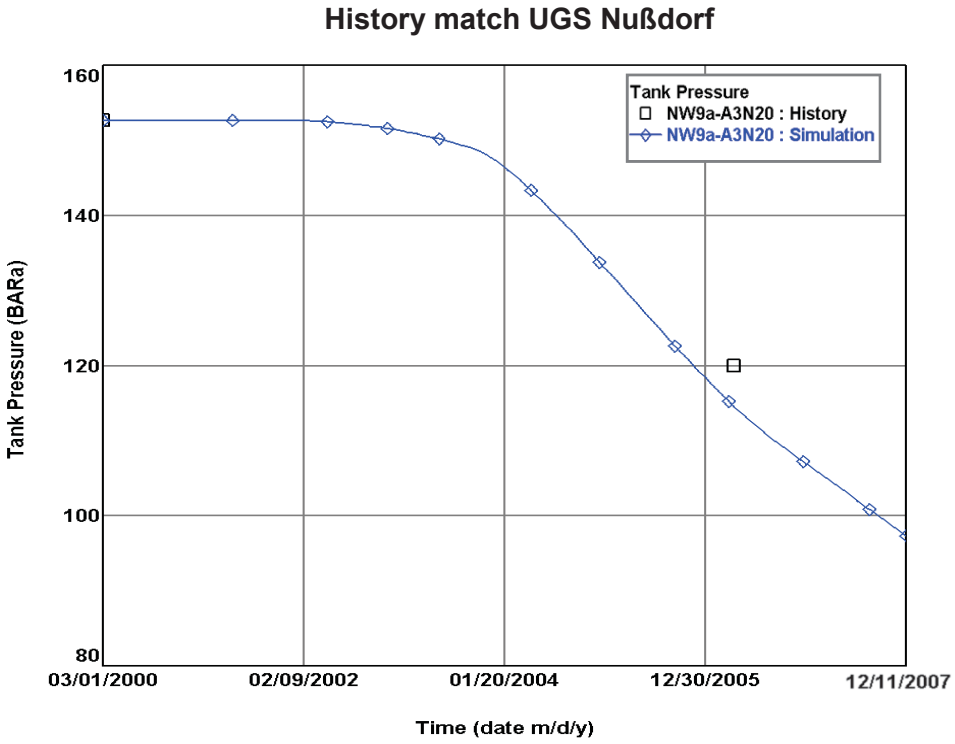

Figure C.10: History match of tank NW9a-A3N20. The pressure and the cumulative production are plotted versus time. The historical measured pressure points, marked by the black squares, are tried to be matched by a production simulation, labelled by the blue curve.

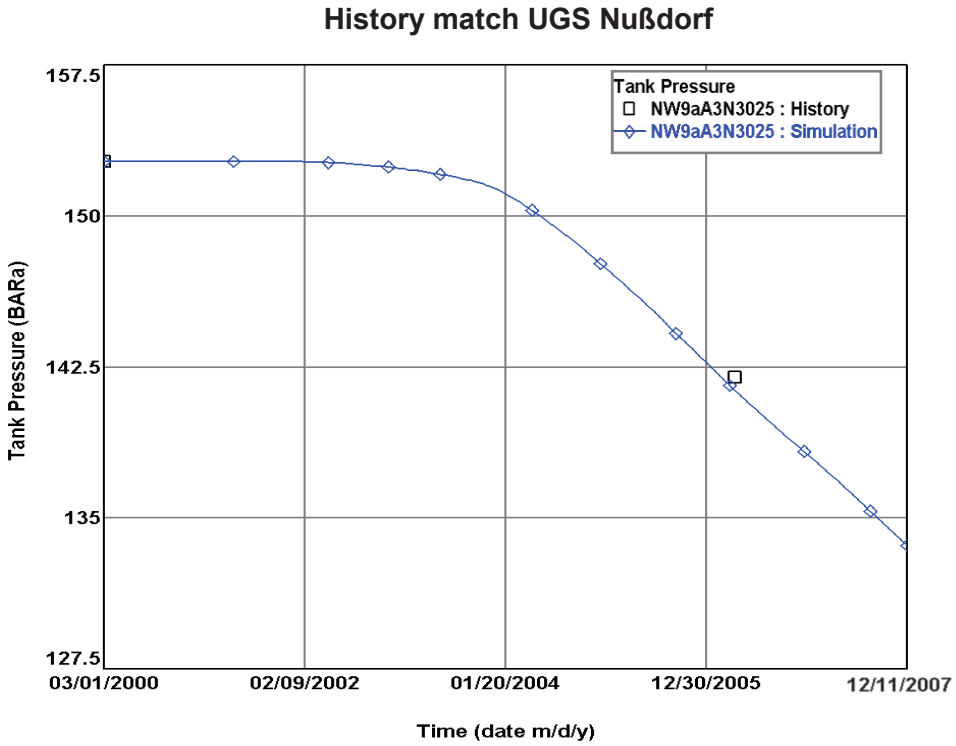

Figure C.11: History match of tank NW9a-A3N3025. The pressure and the cumulative production are plotted versus time. The historical measured pressure points, marked by the black squares, are tried to be matched by a production simulation, labelled by the blue curve.

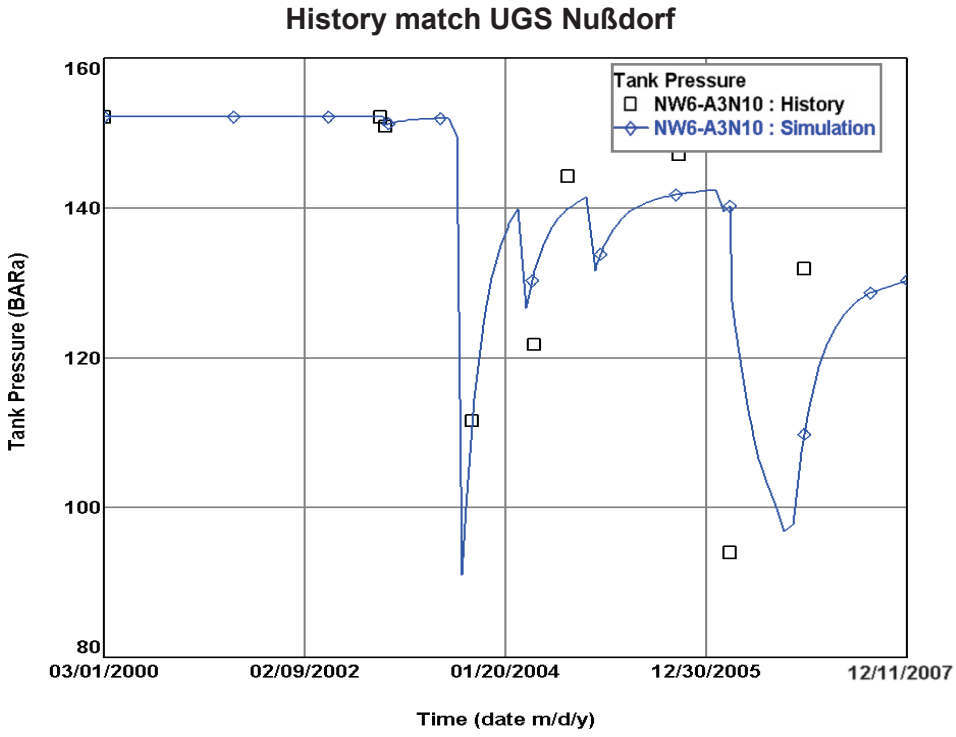

Figure C.12: History match of tank NW6-A3N10. The pressure and the cumulative production are plotted versus time. The historical measured pressure points, marked by the black squares, are tried to be matched by a production simulation, labelled by the blue curve.

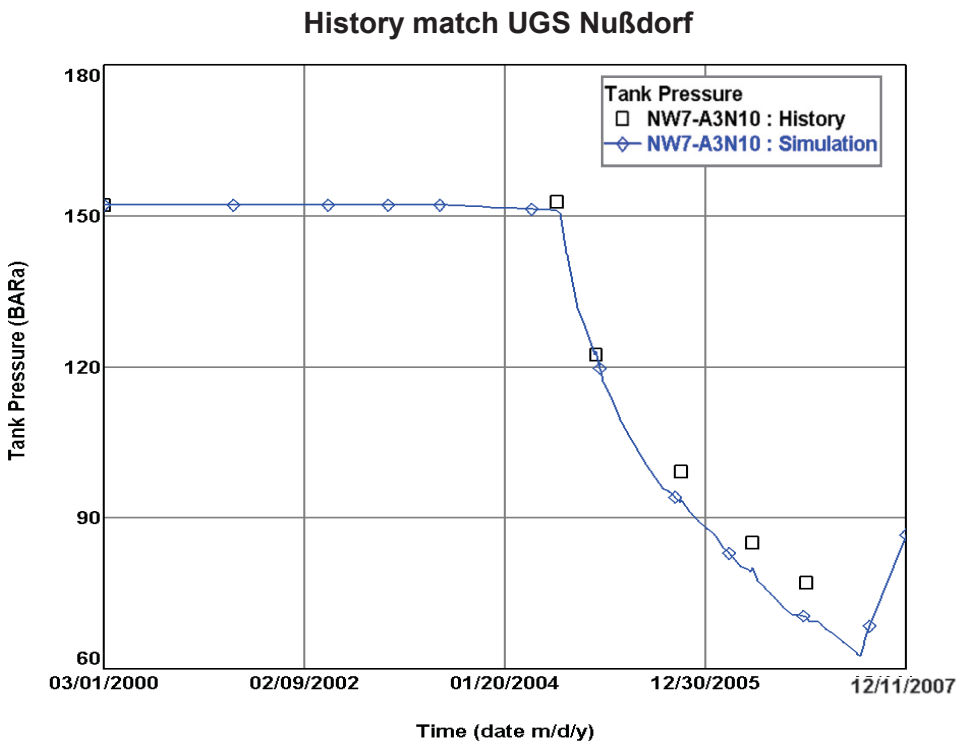

Figure C.13: History match of tank NW7-A3N10. The pressure and the cumulative production are plotted versus time. The historical measured pressure points, marked by the black squares, are tried to be matched by a production simulation, labelled by the blue curve.

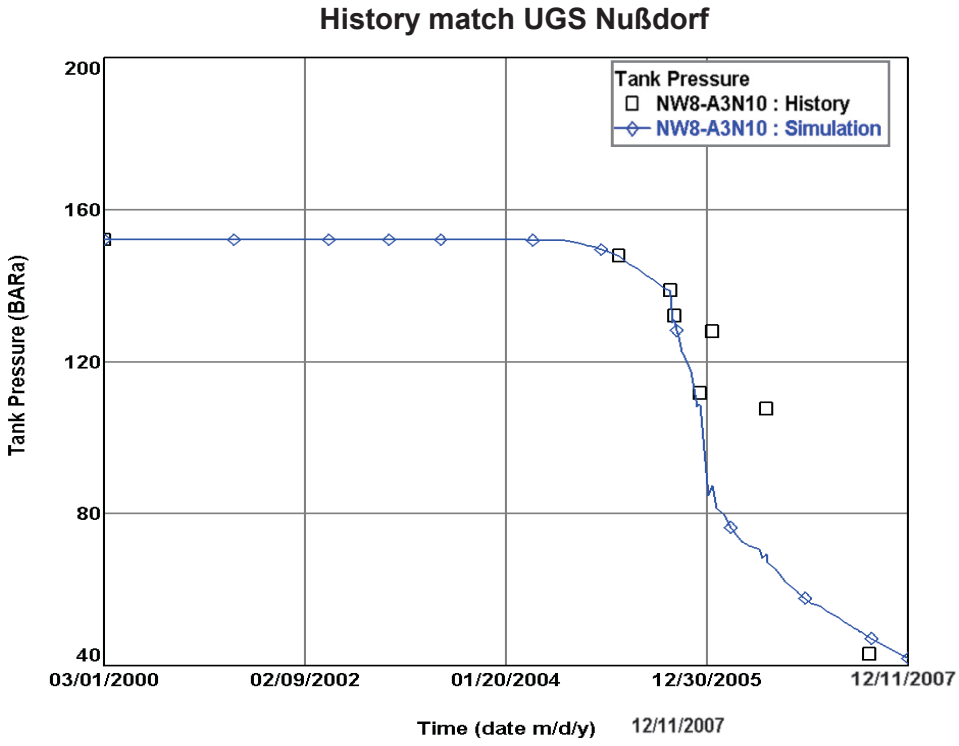

Figure C.14: History match of tank NW8-A3N10. The pressure and the cumulative production are plotted versus time. The historical measured pressure points, marked by the black squares, are tried to be matched by a production simulation, labelled by the blue curve.

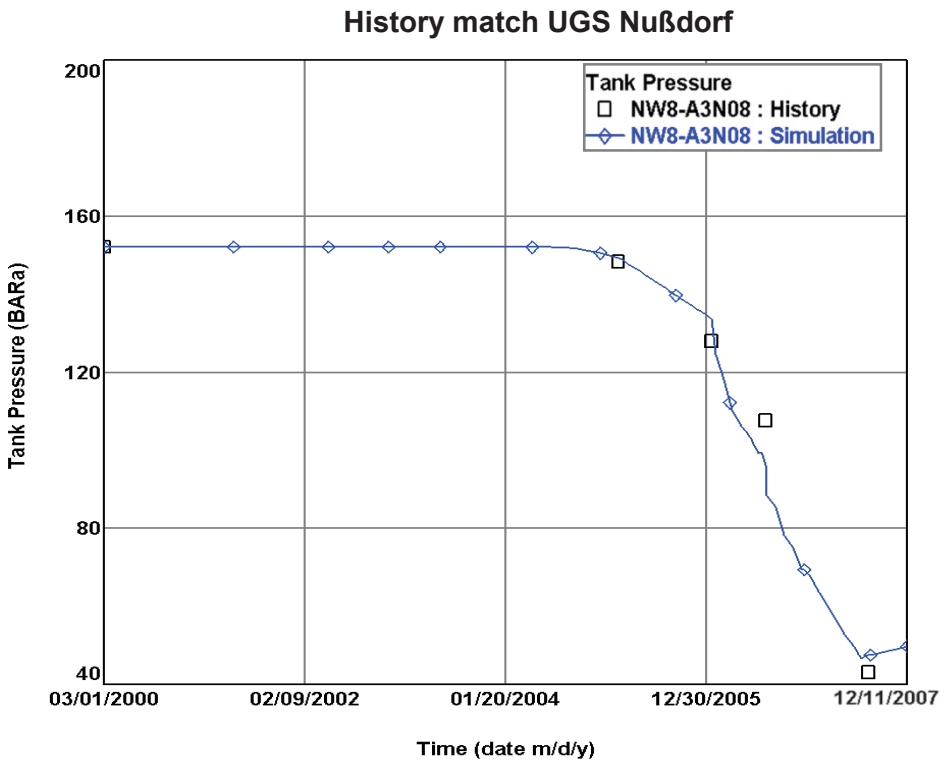

Figure C.15: History match of tank NW8-A3N08. The pressure and the cumulative production are plotted versus time. The historical measured pressure points, marked by the black squares, are tried to be matched by a production simulation, labelled by the blue curve.

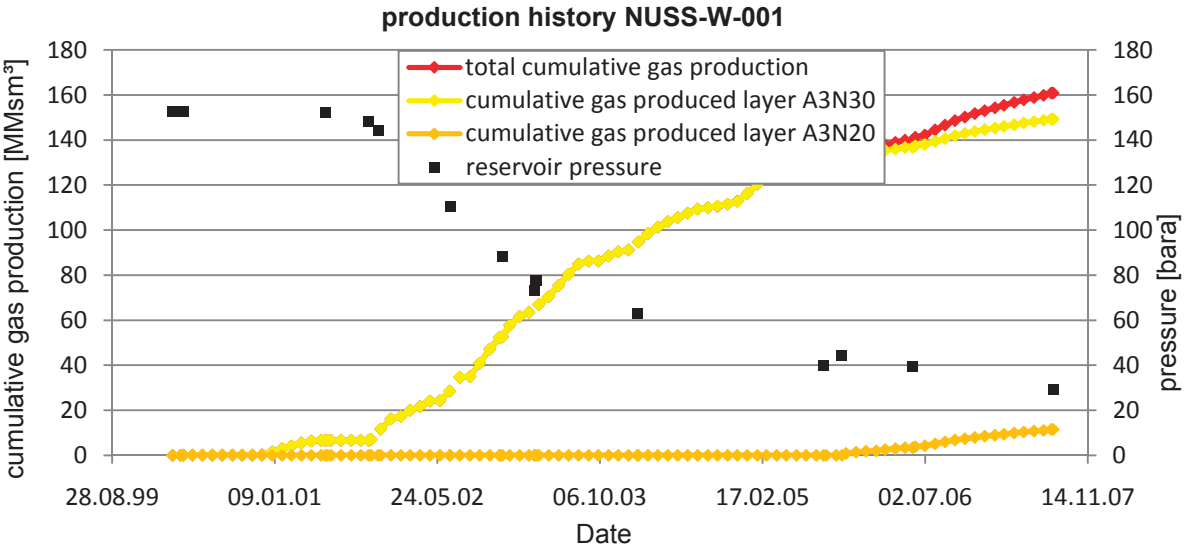

Figure C.16: The production history, including the gas production of the different productive layers and the reservoir pressure history are plotted versus production time.

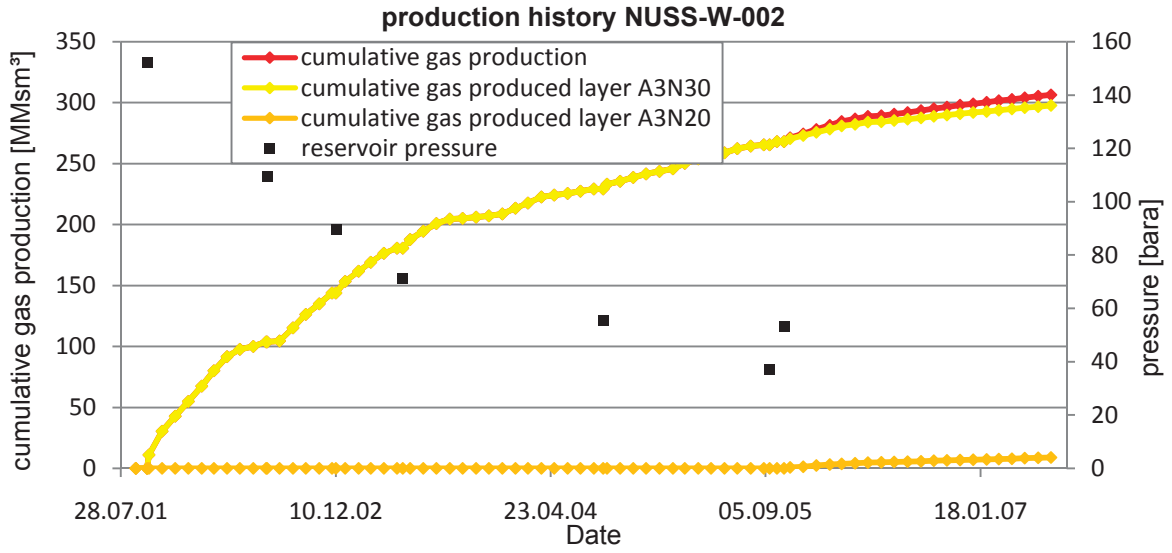

Figure C.17: The production history, including the gas production of the different productive layers and the reservoir pressure history are plotted versus production time.

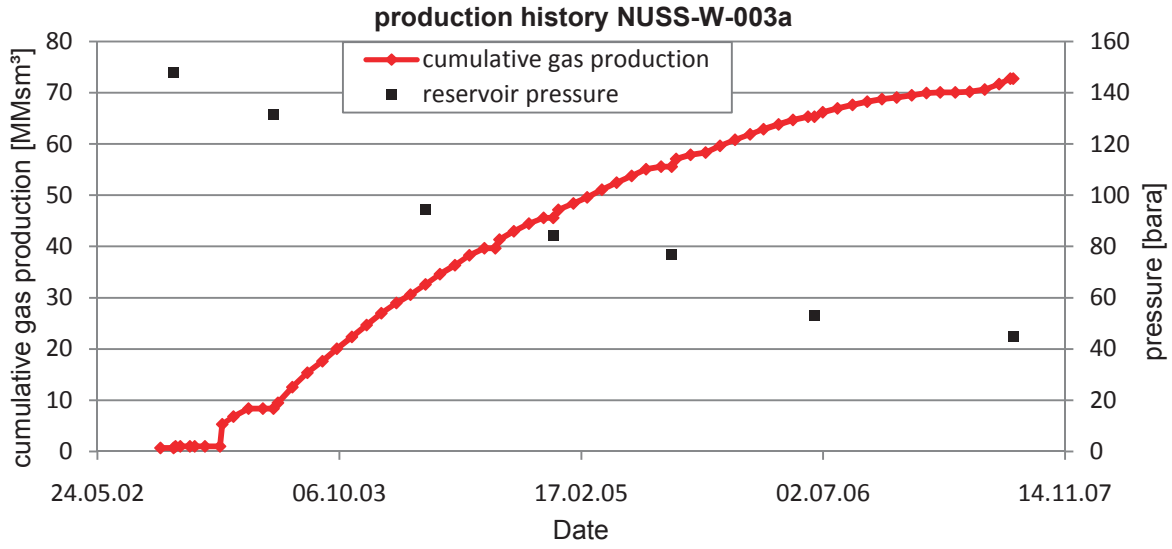

Figure C.18: The production history, including the gas production of the different productive layers and the reservoir pressure history are plotted versus production time.

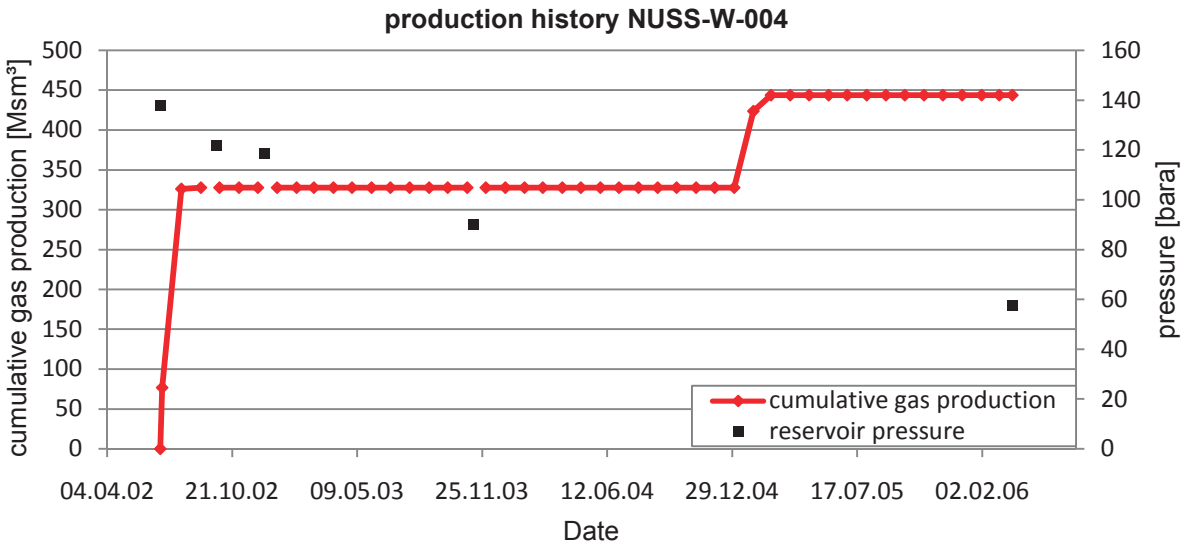

Figure C.19: The production history, including the gas production of the different productive layers and the reservoir pressure history are plotted versus production time.

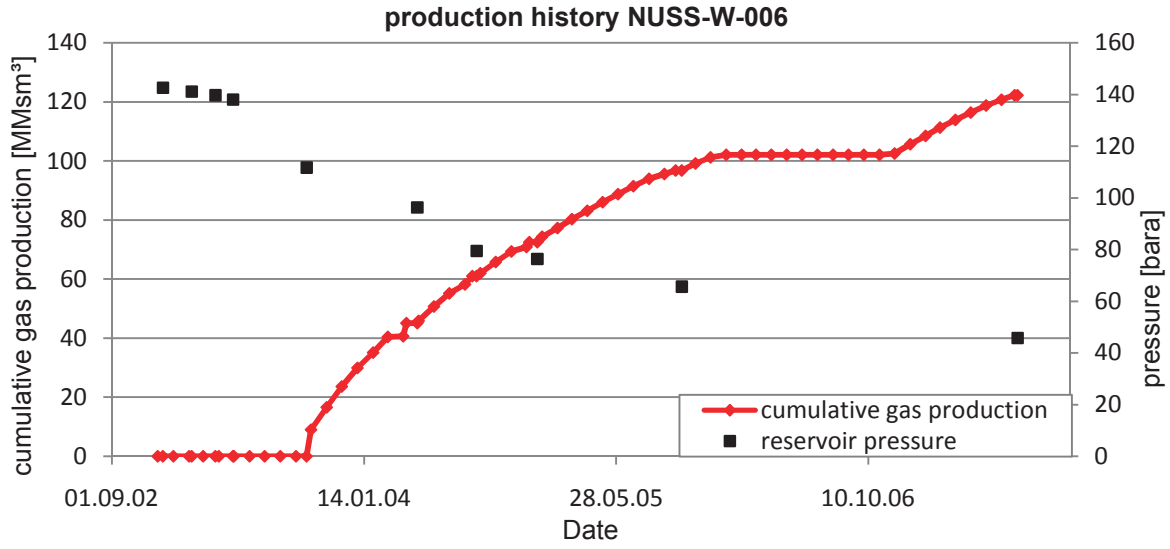

Figure C.20: The production history, including the gas production of the different productive layers and the reservoir pressure history are plotted versus production time.

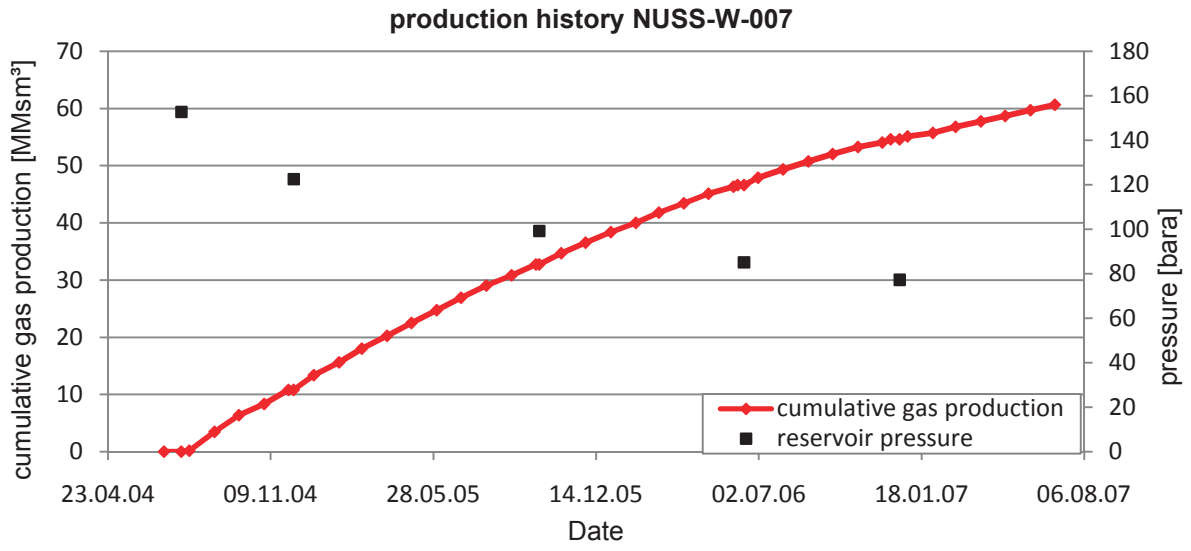

Figure C.21: The production history, including the gas production of the different productive layers and the reservoir pressure history are plotted versus production time.

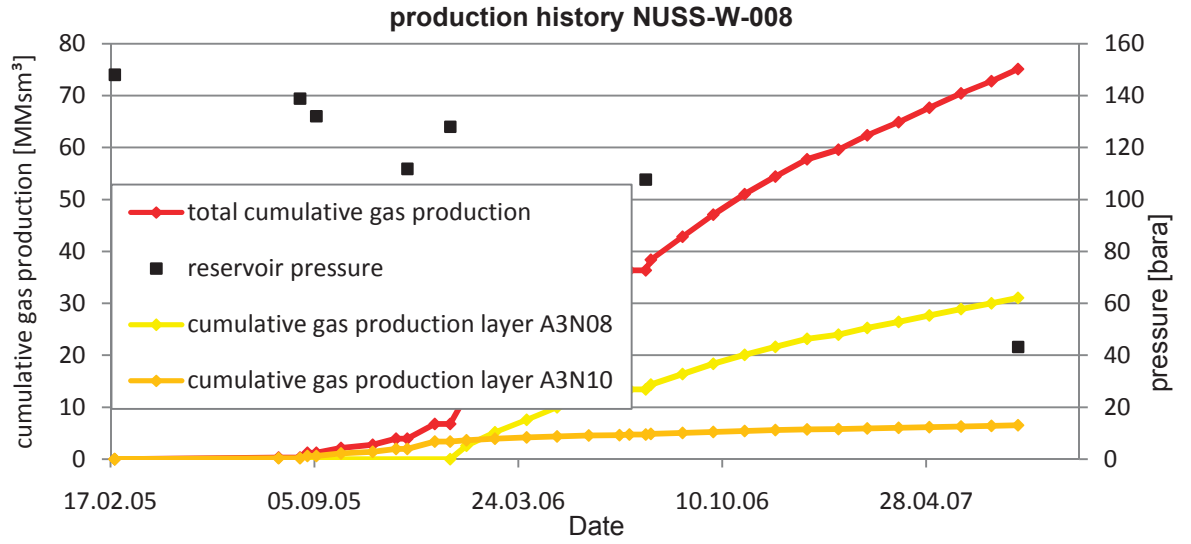

Figure C.22: The production history, including the gas production of the different productive layers and the reservoir pressure history are plotted versus production time.

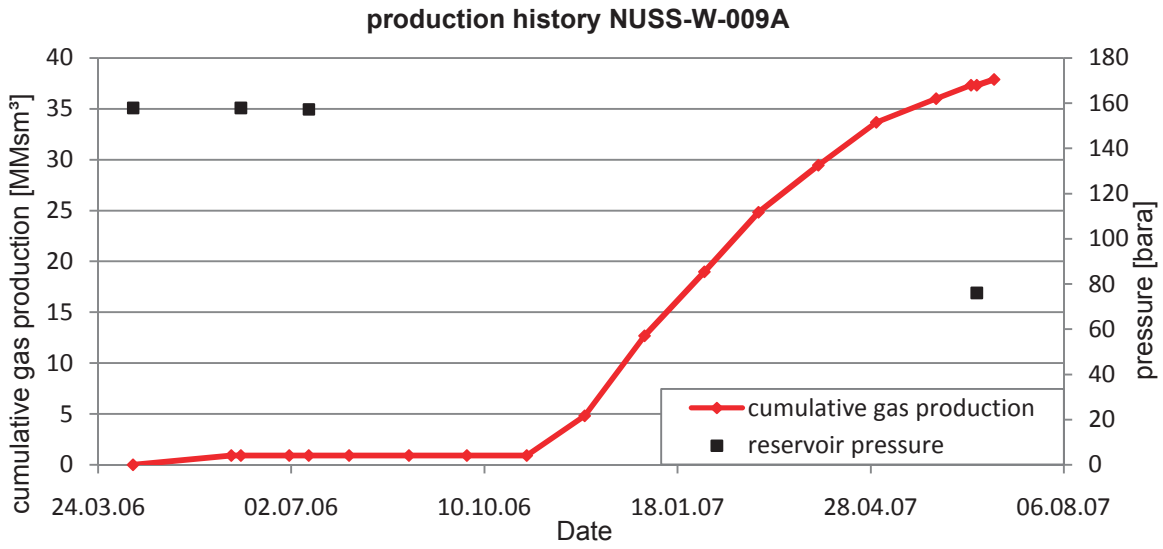

Figure C.23: The production history, including the gas production of the different productive layers and the reservoir pressure history are plotted versus production time.

Tank volume distribution Nußdorf

Horizon	Tank	Volume [MMSm³]	Horizon	Tank	Volume [MMSm³]
Olistolith	NW6-A3N08	40	A3N30	NW1-A3N30	85
	NW6-A3N08-a	40		NW1-A3N30-a	35
	total	**80**		NW2-A3N30	280
A3N08	NW8-A3N08	57		NW2-A3N30-a	10
	NW8-A3N08-a	38		NW3a-A3N30	40
	total	**95**		NW3a-A3N30-a	20
A3N10	NW6-A3N10	7		NW4-A3N30	11
	NW6-A3N10-a	5		NW4-A3N30-a	7
	NW7-A3N10	42		NW6A3N20-30	71
	NW7-A3N10-a	30		NW6-A3N20-30	30
	NW8-A3N10	13		NW9aA3N3025	30
	NW8-A3N10-a	9		NW9aA3N3025a	20
	NW9a-A3N10	80		NW10-A3N30	35
	NW9a-A3N10-a	45		NW10-A3N30-a	27
	total	**231**		**total**	**701**
A3N20-25	NW1-A3N20	7			
	NW1-A3N20-a	10			
	NW2-A3N20	6			
	NW2-A3N20-a	10			
	NW3a-A3N20	115			
	NW3a-A3N20-a	50			
	NW4-A3N20	6			
	NW9a-A3N20	70			
	NW9a-A3N20-a	30			
	NW10-A3N25	22			
	NW10-A3N25-a	15			
	total	**341**			

Table C.1: Tank volume distribution for Nußdorf MBAL® model

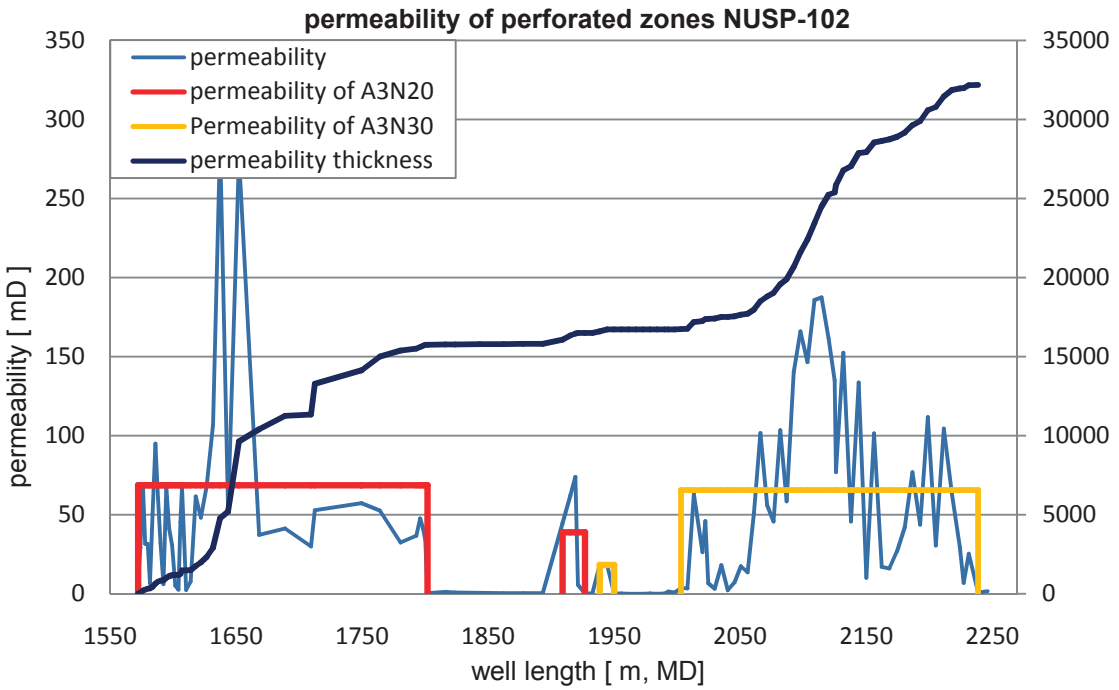

Figure C.24: The well intersects several layers, which are shown in different colours. The permeability along the well path and the permeability thickness product is pictured. The artificial permeability log was created out of the petrel static reservoir model.

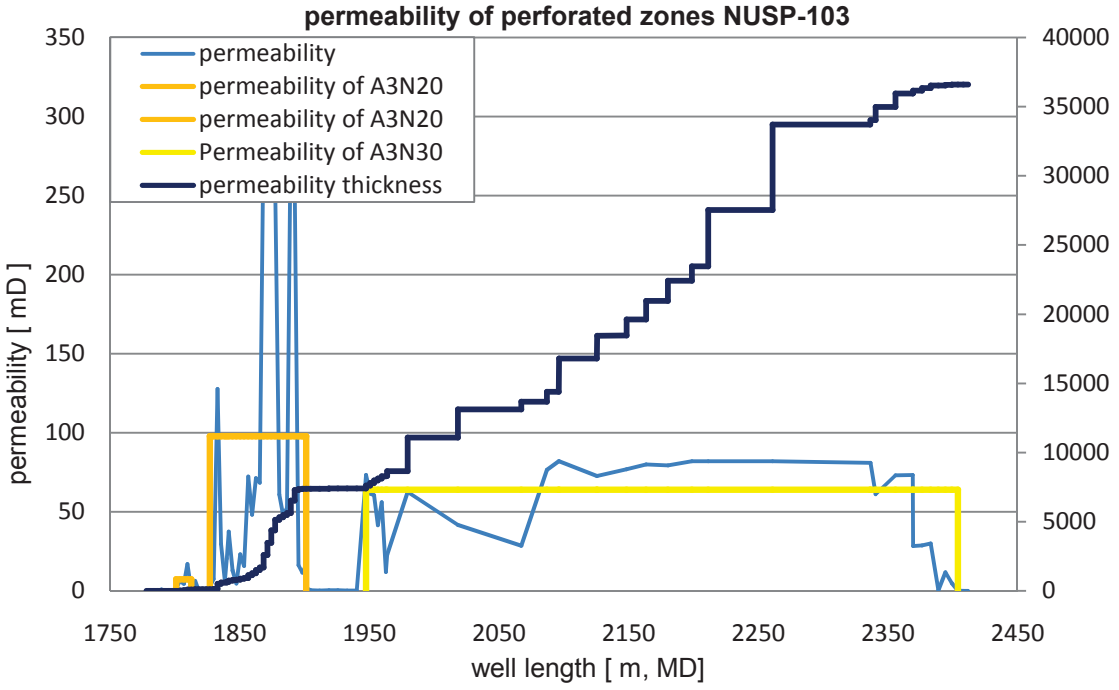

Figure C.25: The well intersects several layers, which are shown in different colours. The permeability along the well path and the permeability thickness product is pictured. The artificial permeability log was created out of the petrel static reservoir model.

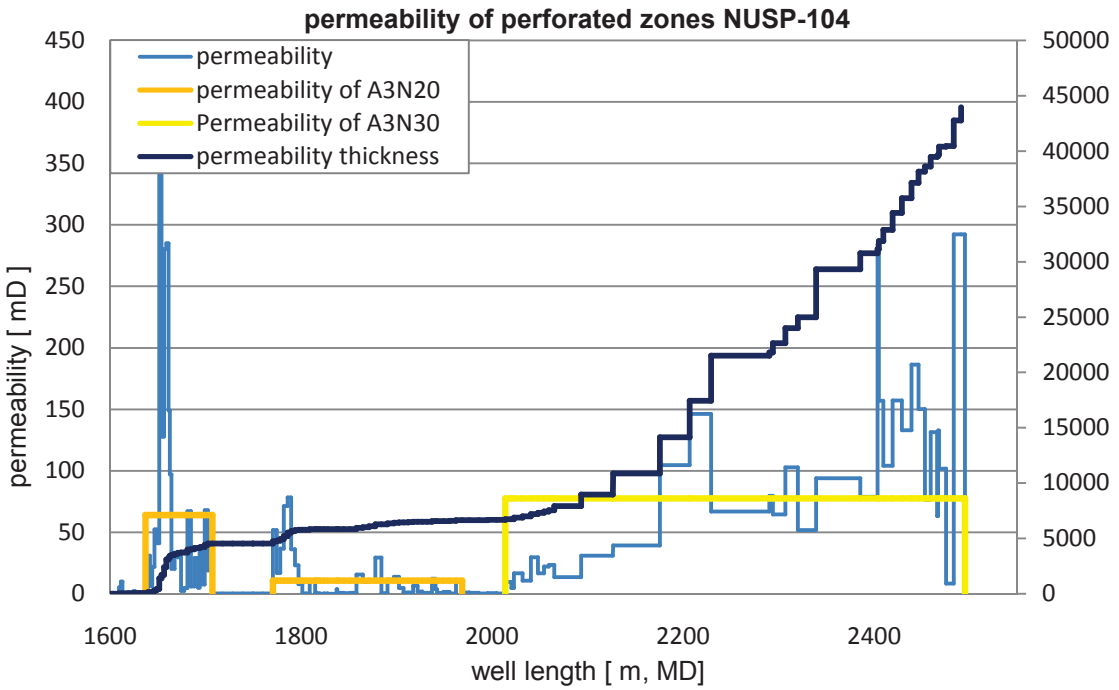

Figure C.26: The well intersects several layers, which are shown in different colours. The permeability along the well path and the permeability thickness product is pictured. The artificial permeability log was created out of the petrel static reservoir model.

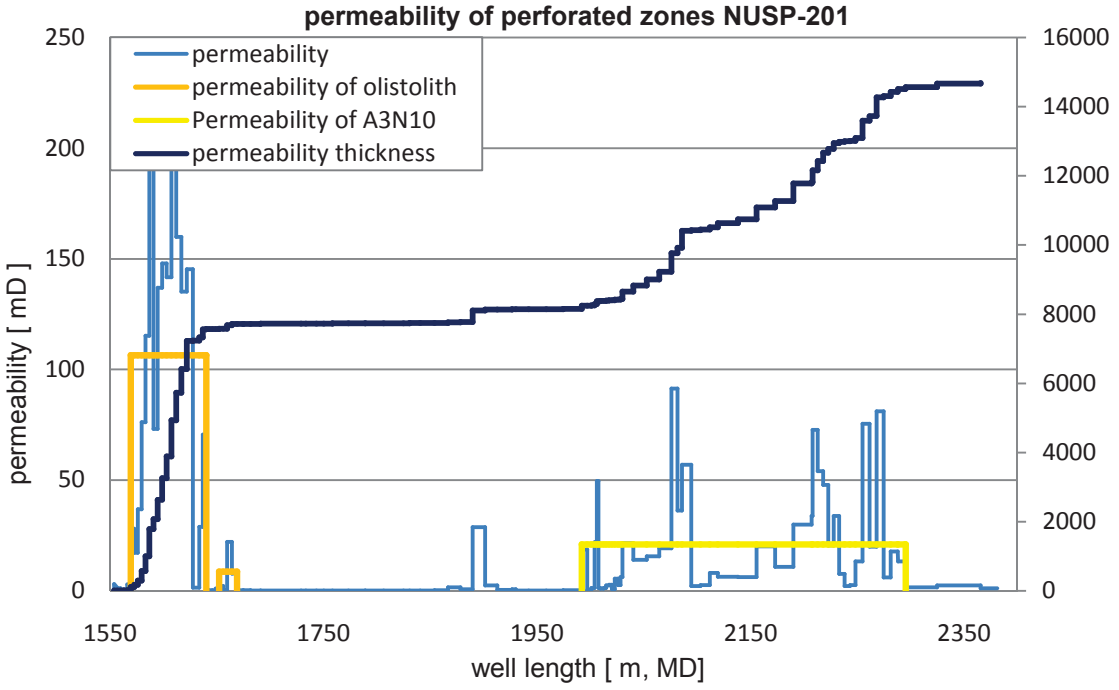

Figure C.27: The well intersects several layers, which are shown in different colours. The permeability along the well path and the permeability thickness product is pictured. The artificial permeability log was created out of the petrel static reservoir model.

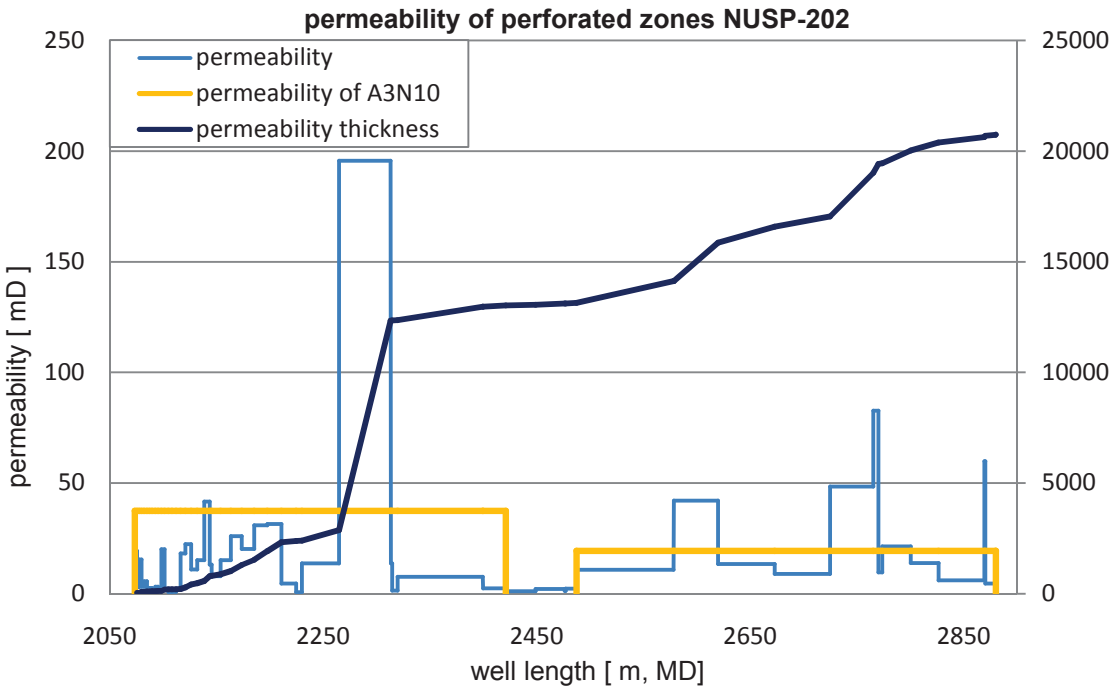

Figure C.28: The well intersects several layers, which are shown in different colours. The permeability along the well path and the permeability thickness product is pictured. The artificial permeability log was created out of the petrel static reservoir model.

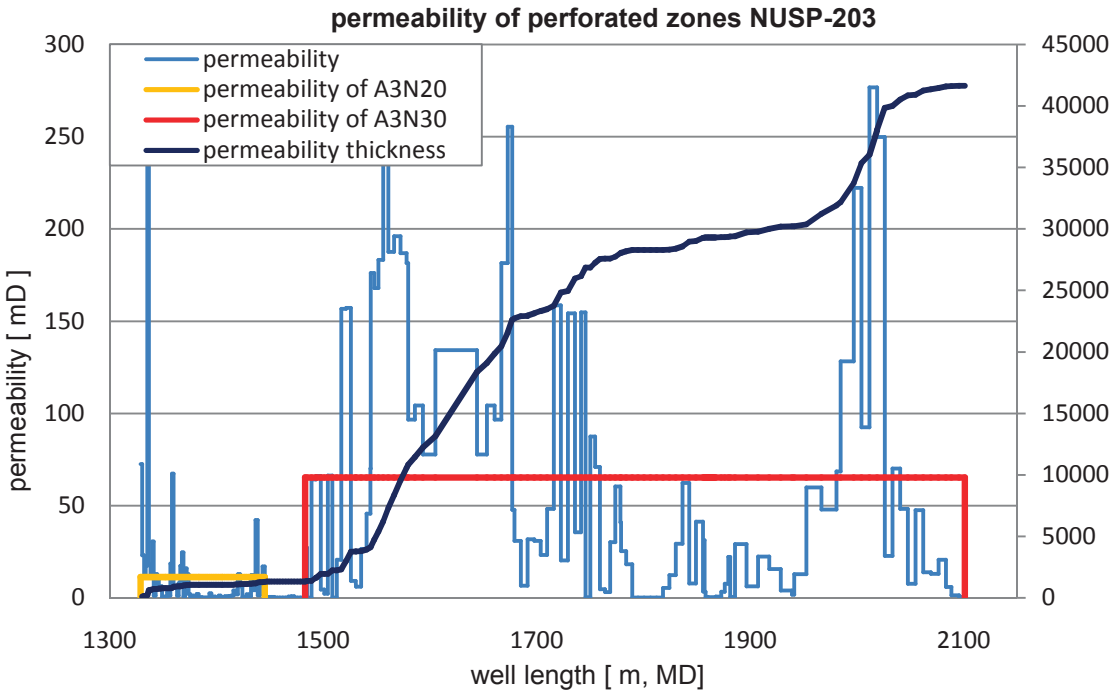

Figure C.29: The well intersects several layers, which are shown in different colours. The permeability along the well path and the permeability thickness product is pictured. The artificial permeability log was created out of the petrel static reservoir model.